PENSOFT

SENCKENBERG
world of biodiversity

Leibniz Association

A new massopodan sauropodomorph from Trossingen Formation (Germany) hidden as '*Plateosaurus*' for 100 years in the historical Tübingen collection

Festschrift in Honour of Professor Dr. Wolfgang Maier
Edited by Ingmar Werneburg & Irina Ruf

Omar Rafael Regalado Fernández[1], Ingmar Werneburg[1,2]

1 *Fachbereich Geowissenschaften an der Universität Tübingen, Hölderlinstraße 12, 72074 Tübingen, Germany*
2 *Senckenberg Centre for Human Evolution and Palaeoenvironment an der Universität Tübingen, Sigwartstraße 10, 72076 Tübingen, Germany*

http://zoobank.org/144C1C64-1A6A-43B7-B004-2F0D8888338E

Corresponding author: Omar Rafael Regalado Fernández (omar.fernandez.13@alumni.ucl.ac.uk)

Academic editor Irina Ruf | **Received** 9 May 2022 | **Accepted** 15 July 2022 | **Published** 8 September 2022

Citation: Regalado Fernández OR, Werneburg I (2022) A new massopodan sauropodomorph from Trossingen Formation (Germany) hidden as '*Plateosaurus*' for 100 years in the historical Tübingen collection. Vertebrate Zoology 72: 771–822. https://doi.org/10.3897/vz.72.e86348

Abstract

A literature review showed that there is not a defined consensus on what specimens belong to *Plateosaurus* in current phylogenetic analyses, and after the assignation of SMNS 13200 as the neotype for *Plateosaurus*, the specimen composition of *Plateosaurus* as an operational taxonomic unit (OTU) needs to be addressed in further iterations of phylogenetic analyses. At least one of the specimens used to illustrate plateosaurian anatomy contains several characters identified in more derived sauropodomorphs commonly referred to as massopodans. This partial skeleton, traditionally known as specimen 'GPIT IV', was found in the lower dinosaur bone bed of the Obere Mühle, a Trossingen Formation outcrop, during an excavation in 1922 near the city of Tübingen, Germany. The holotype of *Plateosaurus trossingensis* and several other specimens referred to as this species were found in this level, which was initially interpreted as a synchronic deposit of animals. However, the current understanding of the Trossingen Formation indicates that this bed was probably a constant accumulation of carcasses through miring and transport down a river for hundreds of years. In this work, a framework to compare phylogenetic signals with morphological and histological data is provided to help in the species delineation of *Plateosaurus*, and support is found to refer the historic specimen 'GPIT IV' as a new genus and a new species.

Keywords

Comparative anatomy, Late Triassic, Massopoda, phylogenetics, Sauropodomorpha

1. Introduction

The collection of sauropodomorph material housed in the Palaeontological Collection of the University of Tübingen (GPIT; acronym from former "Geologisch-Paläontologisches Institut Tübingen"; for further acronyms, see Materials and Methods) in Germany is one of Europe's largest, but one of the least studied. The material was col-

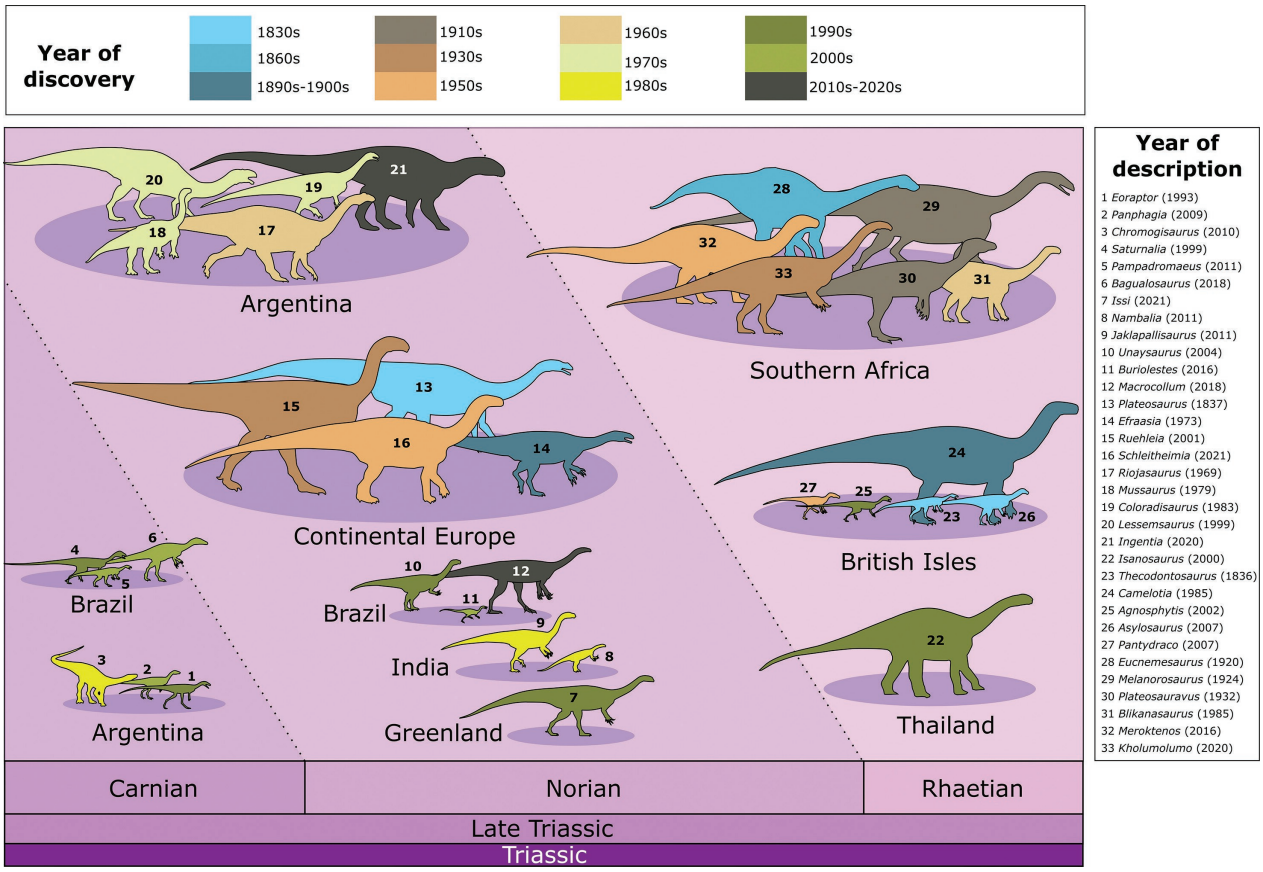

Figure 1. Summary of the taxonomic history of Late Triassic sauropodomorphs. The colour code corresponds to the decades in which the specimens used as holotypes for new genera were first collected, and, to the right, there is a list that indicates in which year a description of the specimen was first published, even if it was not a formal or detailed description. The taxa are grouped by regions, showing their alpha diversity. The time separating the discovery from the description does not mean that the specimen was not used as reference material in comparative anatomy. Although roughly half of the specimens used to erect the genera in this chart were discovered before or during the 1960s, only five genera were erected in the same interval. The infographic helps to illustrate that taxonomic revision of the material stored in collections around the world must be considered a constant work in progress.

lected from localities near Tübingen, namely Trossingen, Bebenhausen, Pfrondorf, Kreßbach, and Steinenberg, but also from the beds near Aixheim and Löwenstein (Hinz and Werneburg 2019). Based on the records published so far, the material comes from several sections of the Upper Keuper Marls (Hinz and Werneburg 2019). The material has been referred to as the genus *Plateosaurus* Meyer, 1837, of which only four out of about 20 species are treated as valid today, i.e., *P.* '*engelhardti*' Meyer, 1837, *P. longiceps* Jaekel, 1913, *P. ingens* (Rütimeyer, 1856) and *P. gracilis* (von Huene, 1905) (see Tables 1 and 2 for references).

Von Huene (1901, 1905a, b, 1907, 1915, 1926, 1932, 1956, 1959) recognised as many as 22 species in Europe, and eight were found in Trossingen alone. Galton (2001b) interpreted this as a "sort of microcosm for plateosaurids of Germany". After revising the material, Galton (2001b) reduced the number of species to four, considering many as *nomina dubia*. The assignation was a consequence of the definition of *Plateosaurus* at this time, which was based on cranial and femoral characters. Several specimens housed in the GPIT collection lack cranial and femoral material. However, the material quality is similar to the conservation of distinct taxa elsewhere in South America and South Africa. Following Galton's (2001a, 2001b) taxonomic revision, many specimens and their variation were interpreted as either individual variation or as evidence of phenotypic plasticity. The different morphological characteristics of femora, and the overall distinction between gracile and robust categories, were explained as evidence of sexual dimorphism (Galton 1999) or ontogenetic stages (Galton 1973, 1985c; Galton and Upchurch 2004). Although supported by morphometric analyses, the phenotypic plasticity is not consistent with endothermic animals (Weishampel and Chapman 1990); it was, therefore, suggested that the material from Trossingen corresponded to a transitional evolutionary stage towards dinosaurian endothermy (Sander and Klein 2005). Nevertheless, the histological evidence, namely the fibrolamellar complex in the long bones, corresponds to more endothermic animals (Ray et al. 2009).

The idea of ontogenetic changes has been supported by what has been found in other localities. For instance, in Argentina, several stages of *Mussaurus* Bonaparte and Vince, 1979, can be identified, showing a transition from biped to quadrupedality as they grew (Otero et al. 2019). On the other hand, in South Africa, *Massospondylus* Owen, 1854, also shows ontogenetic shifting, but, unlike *Mussaurus*, cranial evidence such as the inner ear anat-

Table 1. Specimen composition of the historical catalogue numbers "GPIT A-E" and "GPIT I-VII".

Historical catalogue number	New catalogue numbers	Locality	Details
GPIT A (Old numbers PV-10975, PV-10976 Nm. I–II, PV-10977 Nm. 1–2, PV 10977 Nm. 3)	GPIT-PV-60296 These specimens were referred to as GPIT A, and it is unclear if this is meant to be one individual, a composite mounted to illustrate one species or several specimens collected over time that tentatively belonged to the same species.	Found in 1864 in the localities of Jächklinge, near Pfrondorf (Quenstedt 1864: p. 308) found by Mr. Revierförster Pfizenmayer. The field designation "Gecht" could also mean "Gechtbach", which flows into "Tiefenbach" and most likely formed the Bradklinge.	Originally mounted (UAT 678/73, von Huene 1907: Foreword, p. III) and consisted of a complete pelvis with most of the fore- and hindlimbs, an articulated partial sacrum and the dorsal series with ribs, and as far as the eighth dorsal vertebra (Quenstedt 1867: pl. 9, fig. 4–12; Quenstedt,1882–85: 178–180, fig. 60, pl. 13, figs. 5–13). The specimen was later illustrated in detail (von Huene 1907: 29–42, figs. 17–28, pl. 10, figs. 1–5, 7, Pls. 11–16, 102).
	Taxonomic opinions	Quenstedt used the name *Zanclodon laevis* Plieninger, 1846, but was later referred to as a new species, *Zanclodon quenstedti* Seeley, 1892 (see Koken 1900), then referred to as *Plateosaurus quenstedti* von Huene, 1905. According to Galton (1999, 2001a), the lack of diagnostic characters in the sacrum and the skull material made this a *nomen dubium*. However, due to the uncertainty of its provenance, it is not clear whether this number refers to a specimen.	
GPIT B	GPIT-PV-60293	Found during a construction site at Roter Graben near Bebenhausen in 1870, when Forstrat Tscherning collected and sent them for study to Quenstedt (von Huene 1907: 127).	The material comprises several vertebrae, metacarpals, manual phalanges, a pelvis, a partial femur, a partial tibia, several metatarsals, and pedal phalanges. It was mounted as part of the same hindleg notwithstanding the correct anatomy (von Huene 1907: 127–140: figs. 120–139, pl. 53, pl. 54, fig. 4, pl. 55, pl. 56, fig. 2)
	Taxonomic opinions	Referred to as *Gresslyosaurus robustus* von Huene, 1907	
GPIT C = GPIT VII	GPIT-PV-30790	It was discovered in 1881 by Jacob Hildenbrand from Ohmen when doing topographic prospections in Wüstenroth, southeast from Löwenstein.	Quenstedt acquired it for the palaeontological collection in Tübingen; it was until 1901 that the material, which Hildebrand put inside a cement block (von Huene 1907: 138, pl. 56–59). Von Huene mounted it after he prepared and isolated the elements.
	Taxonomic opinions	von Huene (1905) made specimen GPIT C the holotype of *Pachysaurus ajax* von Huene, 1905.	
GPIT D (Old numbers: PV 11210–11212, 11297–11316)	GPIT-PV-60298 third sacral vertebra (= PV 11210). GPIT-PV-60173 to 60176 left metacarpals (= PV 11300) (von Huene 1907: pl. 61, fig. 2). GPIT-PV-60182 right humerus (= PV 11212) (von Huene 1907: pl. 63, fig. 1).	It was discovered in 1864 and given the old number PV 11297, collected from a deep rift in Brandklinge, near Jächklinge. However, von Huene (1907: p. 146) stated this finding was done in the "late 1870s". Currently, in the collection, it is difficult to determine which material belongs to GPIT D and which belongs to GPIT A, both obtained from similar localities.	It consists of a third sacral vertebra, ribs (old number PV 11211, lost), both pectoral girdles and humeri, parts of the radius, left metacarpus and a fragment of an ilium and a tibia (von Huene 1907: 146–153, figs. 155–159, pl. 59, fig. 7, Pls. 60–63; Galton 1999). It is impossible to distinguish between the collection sites of Brandklinge and Jächklinge, and every collection element now has independent numbers. Von Huene (1907: p. 146) described them as "a large number of worthless fragments".
	Taxonomic opinions	Von Huene (1905) made specimen GPIT C the holotype of *Pachysaurus magnus* von Huene, 1905.	
GPIT E	GPIT-PV-60234–60236	It was collected from the upper bone bed from the Obere Mühle, an outcrop of the Trossingen Formation, where von Huene organised an expedition in 1921–1923.	Three metatarsals (von Huene 1932: pl. 12, fig. 11). GPIT E was found as a block, catalogued as "Block 98", and consisted of three large metatarsal bones in a relatively poor preservation state (von Huene 1932). This includes a lost bone (block 98/4) that von Huene (1932, p. 111) interpreted as a phalanx, and Galton (2001b, p. 446, fig. 4f) interpreted as a calcaneum.
	Taxonomic opinions	The large size of the metatarsals (mt. II being 52 cm long) was used as a condition to erect the species *Pachysaurus giganteus* von Huene, 1932.	
GPIT I (mounted individual)	GPIT-PV-30784	Collected from the lower dinosaur bed, Obere Mühle.	Complete skeleton with few elements missing (von Huene 1926: pl. 5, fig. 9, text-fig. 4; von Huene 1928: pl. 10, von Huene 1932: 141–160, pl. 24, fig. 1, 2, text-fig. 53).
	Taxonomic opinions	Von Huene (1932) referred the specimen to *Plateosaurus quenstedti* von Huene, 1905. Galton (2001b) placed it along with AMNH FARB 6810 as part of *Plateosaurus longiceps* Jaekel, 1913.	

Historical catalogue number	New catalogue numbers	Locality	Details
GPIT I (stored skull)	GPIT-PV-30784	Collected from the lower dinosaur bed, Obere Mühle	The skull is not mounted but stored in the basement collection. It is partially articulated, but the skull roof collapsed over the left side (von Huene 1932: pl. 25). The mounted skulls are casts of SMNS 13200 and is used in GPIT-PV-30784 and GPIT-PV-30785.
	Taxonomic opinions	Von Huene (1932) referred the specimen to *Plateosaurus quenstedti*. Galton (2001b) placed it along with AMNH FARB 6810 as part of *Plateosaurus longiceps*.	
GPIT II (composite of several individuals)	GPIT-PV-30785	Collected from the lower dinosaur bed, Obere Mühle	GPIT IIe.i refers to the dorsal 13–15, the sacrum, caudal vertebrae 1–42, pelvis with a closed obturator foramen), hindlimbs of mounted skeleton GPIT II (von Huene 1932: 166–174, fig. 14, pl. 25; fig. 15). GPIT IIq refers to some dorsal vertebrae mounted in the exhibit (von Huene 1932; fig. 14, pl. 5; Weishampel and Westphal 1986: fig. 3).
	Taxonomic opinions	GPIT II.e.i. was referred to *P. erlenbergiensis* von Huene, 1905 (von Huene 1932). GPIT IIq was referred to *P. quenstedti* (von Huene 1932). Galton (2001b) considered both species *nomina dubia* and does not give an opinion on the taxonomic placement for GPIT II. Nevertheless, in the literature, this composite is considered part of *P.* '*engelhardti*'.	
GPIT III	GPIT-PV-30786	Collected from upper dinosaur bed, Obere Mühle	Both ischia, a complete right hindlimb (von Huene 1932: pl. 41).
	Taxonomic opinions	The specimen was referred to as *G.* '*robustus*', the same species given to GPIT B. The species was considered a junior synonym of *P.* '*engelhardti*'.	
GPIT IV	GPIT-PV-30787	Collected from lower dinosaur bed, Obere Mühle	The specimen includes a pelvis with the sacrum, part of the tail, left hindlimb, right fibula, partial foot, all articulated, and a partial forelimb with a mandible.
	Taxonomic opinions	Von Huene (1932) referred it to as *P.* '*plieningeri*' von Huene, 1905, whose holotype (SMNS 80664) was collected from the Knollenmergel of Degerloch in Stuttgart. A recent morphological study placed the specimen from Degerloch within the range of variability for *P. trossingensis*, which includes some elements of GPIT II (Lefevbre et al. 2020), GPIT I and SMNS 13200. Galton (2001b) considered *P.* '*plieningeri*' as a *nomen dubium*. Here, we consider the elements found in articulation as the holotype of *Tuebingosaurus* n. gen.	
GPIT V	GPIT-PV-30788	Collected from upper dinosaur bed, Obere Mühle	Eight dorsals, incomplete third sacral vertebra, 13 caudal vertebrae, the distal two-thirds of the left humerus, the ventral half of the left ilium, both ischia and pubes, an almost complete left hindlimb (von Huene 1932: 105–111, pl. 12; Galton 2011: fig. 4e, 10e).
	Taxonomic opinions	The specimen was made the holotype of *Pachysaurus wetzelianus* von Huene, 1932, and considered as a junior synonym of *P.* '*engelhardti*' by Galton (1985c, 1990, 1992), but made a *nomen dubium* in Galton (2001b) due to the apparent poor preservation. The humerus is currently missing. GPIT V is also the largest specimen in the collection, with the hindlimb measuring about 3 meters long.	
GPIT VI	GPIT-PV-30789	Collected from the lower dinosaur bed, Obere Mühle	A left hindlimb with femur, tibia, fibula, distal tarsals, metatarsals and pedal phalanges.
	Taxonomic opinions	It was referred to as *P.* '*quenstedti*' in an unpublished drawing by von Huene.	
GPIT VII = GPIT C	See GPIT C	See GPIT C	See GPIT C

omy and the locomotory apparatus suggests that *Massospondylus carinatus* Owen, 1854, retained bipedality through its life (Neenan et al. 2018). Finally, the discovery of what seems to be juvenile specimens of *Plateosaurus* from Frick in Switzerland could hint at there being some ontogenetic stages preserved in the Trossingen area (Hofmann and Sander 2014).

However, as it is, the faunal composition of Germany is at odds with the faunal composition pattern identified in other well-studied tetrapod communities from the Late Triassic. For instance, in South Africa, Lesotho, and Zambia, there is an assortment of gracile bipedal animals, such as *Nyasasaurus* Nesbitt et al., 2012 (see Baron et al. 2017), and *Plateosauravus* von Huene, 1932 (see McPhee et al. 2017), and large, robust quadrupeds like *Meroktenos* Peyre de Fabrègues and Allain, 2016, *Melanorosaurus* Haughton, 1924 (see McPhee et al. 2017), and *Eucnemesaurus* van Hoepen, 1920 (see McPhee et al. 2015a) (Fig. 1). On the other hand, in western and southern Argentina, we have large-sized bipedal animals (*Mussaurus* Otero et al., 2019) and medium to large-sized quadrupeds (*Ingentia* Apaldetti et al., 2018); eastern Argentina shows

a more homogenous composition in terms of morphology but is equally diverse in identified groups. Moreover, in the Bristol archipelago, in what is today the United Kingdom, which was facing southwards relative to Germany, France and Switzerland (Galton et al. 2007; Lovegrove et al. 2021), a heterogeneous community existed both in morphological and phylogenetic terms, with very early diverging sauropodomorphs such as *Thecodontosaurus* Riley and Stutchbury, 1836, and *Pantydraco* Galton et al., 2007 (Lovegrove et al. 2021), coexisting with the melanorosaurid *Camelotia* Galton, 1985d, which has a more robust and massive constitution (Galton, 1985d) (Fig. 1).

Furthermore, the recent redescription of a sauropodiform dinosaur from the Klettgau Formation of Switzerland, *Schleitheimia* Rauhut et al., 2020, which was previously referred to as *Plateosaurus* (Galton 1986), strengthens the argument that much of the diversity of sauropodomorphs of Germany has been hidden under the '*Plateosaurus*' umbrella. The referral to *Plateosaurus* for all the material from Germany assumed that there are discrete taphonocoenoses and that all individuals represent a coherent population (Sander 1992; Galton 1999, 2001a,b). The sauropodomorph diversity likely originated during the Late Triassic through sympatric speciation, such as niche partitioning (McPhee et al. 2015b). Stratigraphy alone cannot be a criterion to define early diverging sauropodomorph species, as the same taphonocoenosis can contain several lineages (e.g., the Rhaetic bonebed, Galton 2005). However, a recent study on cranial morphology of skulls referred to as *Plateosaurus* has found that the characters in 18 specimens show a high degree of variation without the consistent combination that may indicate different species – a pattern consistent with intraspecific variation (Lallensack et al. 2021). The sample in Lallensack et al. (2021) includes mostly material from the lower and middle bonebeds of the Gruhalde Quarry, Klettgau Formation in Frick, Switzerland, and also GPIT-PV-30784 (formerly designated as "GPIT/RE/09392", housed in Tübingen), and SMNS 12949, SMNS 13200, SMNS 5297, SMNS 52968, and SMNS 1950 (housed in Stuttgart) from Trossingen, as well as MB.R.1936 and MB.R.4430.1 (housed in Naturkundemuseum Berlin) from Halberstadt in Germany.

The material of *Schleitheimia* was collected in the 1950s by Emil Schultz (Rauhut et al. 2020). Galton (1986) referred the material to the species *P.* '*engelhardti*'. The material was recently redescribed (Rauhut et al. 2020) based on the ilium and femur morphology. The ilium is one of the most variable elements amongst early diverging sauropodomorphs. There was constant "experimentation" and innovation in the locomotion, with many animals evolving toward an obligate bipedal stance and others with a clear trend toward quadrupedalism (Fig. 1). Regalado Fernandez (2019) suggested quadrupedality may have originated at least twice. In some cases, such as in sauropodomorphs of a mussaurid morphotype, the quadrupedality may have evolved through paedogenesis.

In the present contribution, we provide a revision of the taxonomic history of *Plateosaurus* and its usage in the literature, and we do a preliminary assessment of several characters that have been identified as varying from species to species in other sauropodomorphs from other Late Triassic communities in the material that has been previously referred to *Plateosaurus* housed in the University of Tübingen collection (see Table 1 for an inventory of specimens with old and new catalogue numbers).

1.1. Usage of *Plateosaurus* in phylogenetic analyses

The specimens that have been included as part of the operational taxonomic unit (OTU) of *Plateosaurus* through time have not been constant. Two matrices with different taxonomic and character compositions were produced in 2007, namely by Upchurch et al. (2007) and Yates (2007) (Fig. 2). These matrices were subsequently modified through eight iterations until 2019. Table 2 summarises the different specimen compositions of the OTU *Plateosaurus* and the number of species considered valid.

In 2019, the International Commission on Zoological Nomenclature (ICZN) resolved to replace the name of the type species, *P.* '*engelhardti*', whose holotype is UEN 552, by the type species *P. trossingensis* Fraas, 1913, and its type specimen SMNS 13200 (ICZN 2019). Therefore, the current consensus on *Plateosaurus* seems to treat GPIT-PV-30784, and AMNH FARB 6810 as syntypes of *P. trossingensis*, with *P. erlenbergiensis* von Huene, 1905 being a junior synonym of *P. trossingensis*. *P. longiceps* is the name given to the Halberstadt material. *P. gracilis* corresponds to the name given to the material from the Untere Mühle, the Stromberg region quarry 'Weißer Steinbruch' (Pfaffenhofen), and the quarry 'Goessel' (Ochsenbach) [sic] (Moser 2003; Galton 2012).

Finally, *P. ingens* is given to the material from Niederschönthal near Füllinsdorf, in Switzerland (syntypes NMB NB 1582, 1584, 1585, 1875). Material from Frick (MSF1-13) was described as part of *P.* '*engelhardti*', and thus *P. ingens* was considered as a junior synonym of *P.* '*engelhardti*' (Galton 2012). In Novas et al. (2011), all these specimens were included in *P. ingens*, and the composition of this OTU does not seem to have changed through the literature. Nevertheless, additional material from the same locality has also been referred to as *P. trossingensis* (= *P.* '*engelhardti*' in Galton 1986) rather than *P. ingens*, as it has been used in the iterations of phylogenetic analyses. Furthermore, *P. ingens* was initially the type species of *Gresslyosaurus* Rütimeyer, 1856, a genus that has been considered distinct from *Plateosaurus* (Moser 2003) and recently re-erected as valid (Rauhut 2020). Therefore, the taxonomy of the new material from Frick described in Lallensack et al. (2021) needs to be revisited.

1.2. Taxonomy of *Plateosaurus trossingensis* (= *Plateosaurus 'engelhardti'*)

The lectotype material of *Plateosaurus* '*engelhardti*' used to comprise seven bones that did not belong to the same individual as they form part of an allochthonous assem-

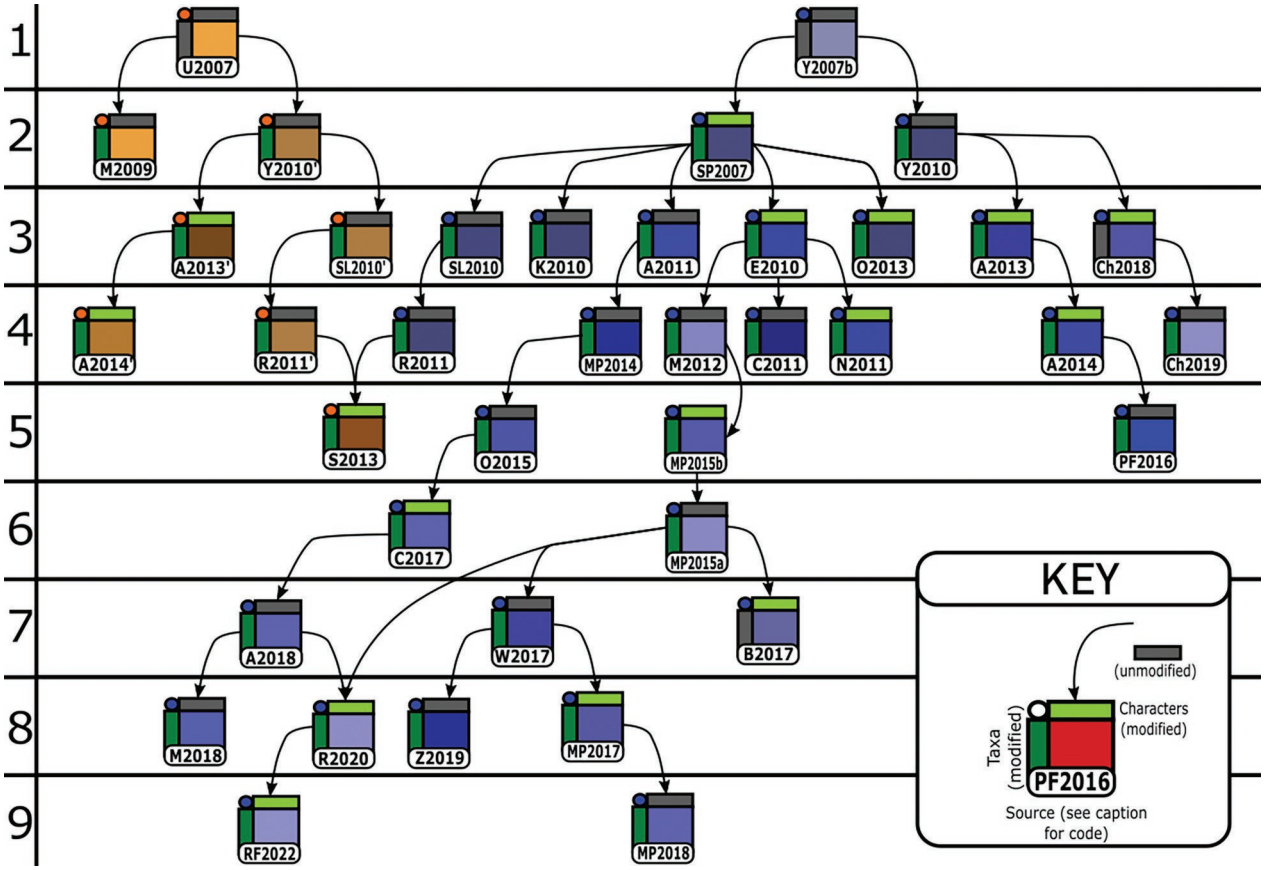

Figure 2. Iterations on the matrices originally built by Upchurch et al. (2007) and Yates (2007) and the addition of characters and operational taxonomic units (OTUs) as described in the text. Numbers on the left correspond to the iteration number. Abbreviations: The labels are abbreviations of the matrices compiled for this work (from stage 0 to stage 9): stage 1 [Y2007b – Yates (2007b); U2007 – Upchurch et al. (2007)], stage 2 [M2009 – Martínez and Alcober (2009), Y2010 – Yates et al. (2010), Y2010' – Yates et al. (2010) second analysis, SP2007 – Smith and Pol (2007)], stage 3 [A2013 – Apaldetti et al. (2013), A2013' – Apaldetti et al. (2013) second analysis; SL2010 – Sertich and Loewen (2010), SL2010' – Sertich and Loewen (2010) second analysis, K2010 – Knoll (2010), A2011 – Apaldetti et al. (2011), E2010 – Ezcurra (2010), O2013 – Otero and Pol (2013), Ch2018 – Chapelle and Choiniere (2018)], stage 4 [A2014 – Apaldetti et al. 2014, R2011 – Rowe et al. (2011), R2011' – Rowe et al. (2011), second analysis, MP2014 – McPhee et al. (2014), M2012 – Martinez et al. (2012), C2011 – Cabreira et al. (2011), N2011 – Novas et al. (2011), Ch2019 – Chapelle et al. (2019)], stage 5 [S2013 – Sekiya et al. (2013), O2015 – Otero et al. (2015), MP2015b – McPhee et al. (2015b), PF2016 – Peyre de Fabrègues and Allain (2016)], stage 6 [C2017 – Cerda et al. 2017, MP2015a – McPhee et al. (2015a)], stage 7 [A2018 – Apaldetti et al. (2018), W2017 – Wang et al. (2017), B2017 – Bronzati and Rauhut (2017)], stage 8 [M2018 – Müller et al. (2018b), Z2019 – Zhang et al. (2019), McPhee et al. (2017)], stage 9 [MP2018 – McPhee et al. (2018), RF2022 – Regalado-Fernandez and Werneburg 2022].

blage. The lectotype, UEN 552, corresponds to three incomplete sacral vertebrae, and the paralectotypes include three dorsal vertebrae (UEN 557, 561, 562), two caudals (UEN 550, 558), the distal half of a left femur (UEN 554, 555), a femoral head (UEN 559) and a left tibia (UEN 556). The rest of the material referred to as *P.* '*engelhardti*' was collected from three different mass deposits, Halberstadt in 1909, Trossingen in 1911 and Ellingen in 1962 (Moser 2003). The sacrum of the lectotype shows some recognisable characters that have been found to provide a phylogenetic signal. The second sacral shows evidence of a ventral keel (= *crista ventralis* in Moser 2003), damaged, and two deep fossae, each lateral to the keel (= *fovea paramediana* in Moser 2003). Furthermore, there is evidence of a centrodiapophyseal fossa delineated by a centrodiapophyseal lamina that connected the diapophysis with the centrum (= *crista diagonalis* in Moser 2003). This lamina divides the sacral rib into an anterior portion that connects to the lateral portion of the first sacral and a posterior portion that connects to the centrum of the second sacral. Although the sacral vertebrae seem to be co-ossified, the suture between sacral 1 and sacral 2 does have a distinct fissure, but this fissure is not discernible between sacral 2 and the caudosacral.

The morphology of the UEN 552 sacrum inspired coding new sacral characters to describe *Plateosaurus* taxonomy. However, many sacral characters have been found to vary from species to species. In *Plateosaurus* (= '*Sellosaurus*') *gracilis*, it has been recognised that there are two types of sacra: type I, which involves a dorsosacral, primordial sacral 1 and primordial sacral 2, and type II, interpreted as primordial sacral 1, primordial sacral 2 and caudosacral (Galton 1999, 2000). The differences were interpreted as either evidence of sexual dimorphism (Gal-

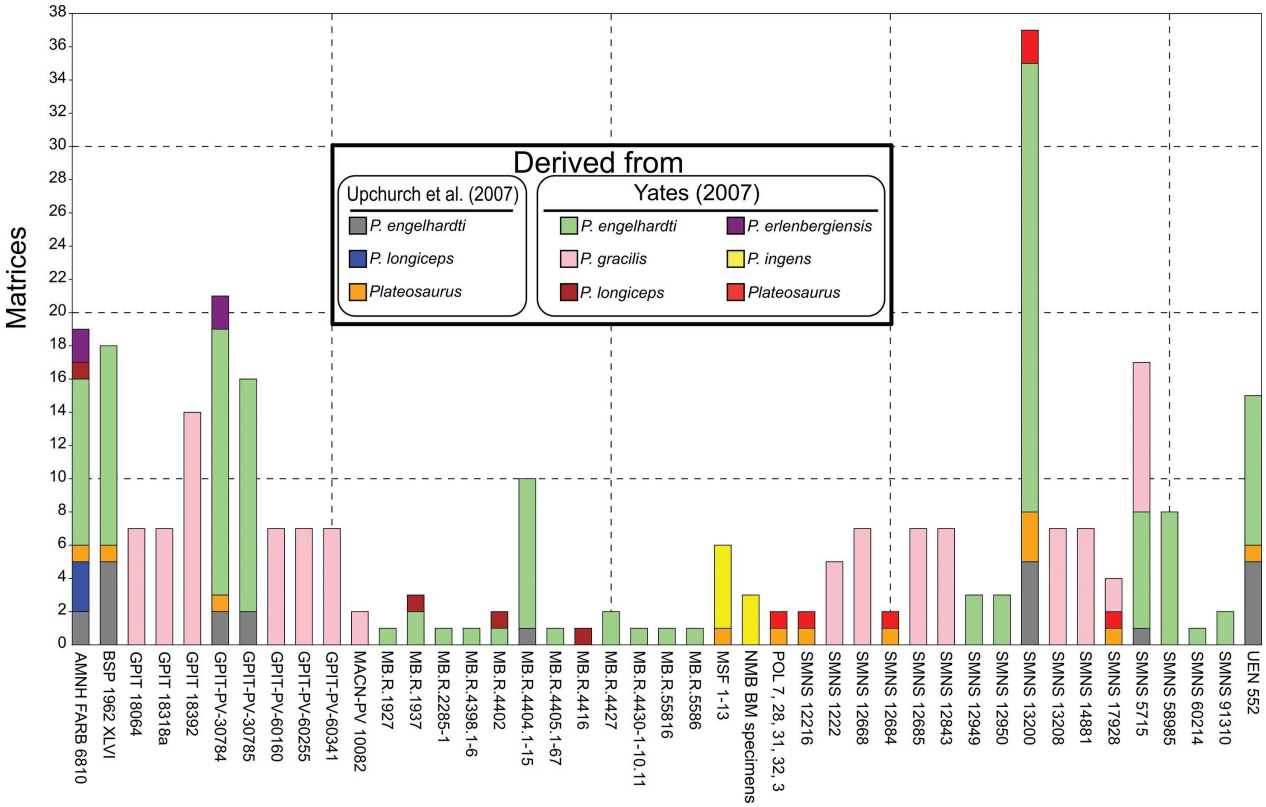

Figure 3. Bar chart summarising the frequency each specimen was used as either *P.* '*engelhardti*' alone, as *P. gracilis*, as *P. ingens*, as *P. longiceps* or as '*P. erlenbergiensis*'. Although *P. trossingensis* (*P.* '*engelhardti*' at the time) was considered the only valid species, several species were also used as part of *Plateosaurus*. Most phylogenetic analyses base their character scores on the same specimens: SMNS 13200, BSP 1962 XLVI and GPIT-PV-30784. *P. gracilis* is the second species more frequently used in phylogenetic analyses. The skull collected from the younger Stubensandstein, former specimen GPIT 18318a, illustrated in von Huene (1915) and Galton (1985c), left the GPIT collection at some point in 2004, and it is not clear if several works refer to the skull of GPIT I as *P. gracilis*. The collection recovered the skull in 2022. Specimens GPIT 18064, GPIT 18318a and GPIT 18392 have been used as part of *P. gracilis*, but they are not given new catalogue numbers because it is not clear if they each correspond to one individual. Specimen GPIT-PV-30787 has not been explicitly used in phylogenetic analyses as part of the OTU for *Plateosaurus* '*engelhardti*'.

ton 2000) or homeotic transformation (Galton and Upchurch 2000, Galton 2001b). Type I (dorsosacral, primordial sacral 1 and primordial sacral 2) is the most common condition among early-diverging sauropodomorphs, as in *Ruehleia* Galton, 2001b, and *Efraasia* Galton, 1973, taxa from Germany, and the persistent condition in Massospondylidae (Wang et al. 2017). Type II is only seen in *Plateosaurus*, and many of the specimens that Galton (2001b) regarded as type I have also been reinterpreted as type II (Moser 2003).

The specimen GPIT "Aixheim" corresponds to a type II sacrum, concordant with the UEN 552 holotype. However, there is no ventral keel in the sacrals, and the fossa lateral to the keel is not that pronounced, but the sutures between the sacrals 1 and 2 are present, and there is a centrodiapophyseal fossa present as well. The difference in size between UEN 552 and GPIT "Aixheim" could explain the changes in those characters as ontogenetic. In both specimens, the identity of the sacrum cannot be confidently asserted without seeing the morphology of the rib or the arrangement with the ilium. GPIT "Aixheim" seems different from the specimens with the current numbers GPIT-PV-60364, GPIT-PV-60446 and GPIT-PV-60448, specimens incorrectly associated with Aixheim in the literature (Fig. 3). See further discussion in the "Analysis 2" section.

1.3. The taxonomic history of other Central European genera of Late Triassic sauropodomorphs

The name *Gresslyosaurus ingens* was first given to material from Niederschönthal, canton Basel-Landschaft, Switzerland, which was discovered by the Swiss palaeontologist Amanz Gressly (Rütimeyer 1856). The holotype of *Gresslyosaurus ingens* (specimen numbers: NMB BM 1, 10, 24, 53, 530–1, 1521, 1572–74, 1576–78, 1582, 1584–85, 1591) includes a partial sacrum, four caudal vertebrae, a metacarpal, partial left and right tibiae, an almost complete fibula and pedal elements. During the late 19th century and early 20th century, *Gresslyosaurus* was applied to several remains in Switzerland and Germany. *Gresslyosaurus robustus* von Huene, 1905, includes only the specimen historically referred to as 'GPIT B', currently GPIT-PV-30786, from the Trossingen Formation

Table 2. History of the taxonomy of *Plateosaurus* and the specimens referred to as *Plateosaurus*. See Table 1 to refer to the old catalogue numbers from the GPIT.

Original taxon	**Specimen**	**Taxonomic history**
1830–1899		
Plateosaurus '*engelhardti*' Meyer, 1837	UEN-552, Heroldsberg, Feuerletten (Norian terrestrial conglomerate in the Trossingen Formation of Germany)	former **holotype** for the genus *Plateosaurus* (ICZN 2019)
Gresslyosaurus ingens Rütimeyer, 1856	NMB BM 1, 10, 24, 53, 530–1, 1521, 1572–74, 1576–78, 1582, 1584–85, 1591	referred to '*Plateosaurus engelhardti*' (Galton 1985a) referred to '*Plateosaurus longiceps*' (Galton 2001a,b)
Dimodosaurus poligniensis Pidancet and Chopard, 1862	POL 31–32, 57, 70, 76, Bois de Cassagne, Poligny (Norian terrestrial marl in the Marnes irisées supérieures Formation of France)	referred to *Plateosaurus poligniensis* (von Huene 1907) referred to '*Plateosaurus longiceps*' (Galton 2001a, 2001b)
Smilodon laevis Plieninger, 1846	SMNS 6045, Swäbisch Hall, Gaildorf (Ladinian terrestrial horizon in the Erfurt Formation of Germany)	referred to *Zanclodon lavis* (Plieninger 1847) referred to *Zanclodon plieningeri* (Fraas 1896) referred to *Zanclodon quenstedti partim* (Koken 1900) referred to *Plateosaurus quenstedti partim* (von Huene 1932) removed from Prosauropoda, assigned to phytosauria (Galton 2001a)
Zanclodon bavaricus Fraas, 1894	UW not listed briefly described by Sandberger (1894), described by Fraas 1894, from Altenstein, Würzburg, Lower Franconia	referred to '*Plateosaurus engelhardti*' (von Huene 1907) considered a *nomen dubium* (Galton 2001a).
Zanclodon plieningeri Fraas, 1896	SMNS 6045, Swäbisch Hall, Gaildorf (Ladinian terrestrial horizon in the Erfurt Formation of Germany)	
Avalonia sanfordi Seeley, 1898	Syntypes BMNH R2870–R2874, R2876–R2878	postcrania are referred to as *Gresslyosaurus ingens* (von Huene 1907) removed from *Plateosaurus* and referred to as *Camelotia borealis* (Galton 1985d)
1900–1930		
Zanclodon quenstedti Koken, 1900		initially referred to as *Zanclodon laevis* (Plieninger 1846) referred to *Plateosaurus quenstedti* (Weishampel and Chapman 1990) considered a *nomen nudum* (Galton 2001a)
Thecodontosaurus elizae Sauvage, 1907	Provenchères-sur-Meuse	referred to *Plateosaurus elizae* (von Huene 1907) referred to *Gresslyosaurus* (Lapparent 1967) removed from 'Prosauropoda', assigned to Saurischia (Galton 1985a)
Gresslyosaurus robustus von Huene, 1907	GPIT-PV-30786, Roter Graben, Bebenhausen	referred to as *Plateosaurus robustus* (von Huene 1932) referred to as '*Plateosaurus engelhardti*' (von Huene 1932) considered *nomen dubium* (Galton 2001a) includes GPIT III (Galton 2001a)
Pachysaurus ajax von Huene, 1907	GPIT C, Wüstenrot	referred to as *Pachysauriscus ajax* (Kuhn 1959) referred to as *Gresslyosaurus ajax* (Steel 1970) referred to as '*Plateosaurus engelhardti*' (Galton 1985a) considered *nomen dubium* (Galton 2001a)
Pachysaurus magnus von Huene, 1905b	GPIT D, Brandklinge, Pfrondorf	referred to as *Pachysauriscus magnus* (Kuhn 1959) referred to as *Gresslyosaurus magnus* (Steel 1970) referred to as '*Plateosaurus engelhardti*' (Galton 1985a) considered a *nomen dubium* (Galton 2001a)
Plateosaurus erlenbergiensis von Huene, 1905b	SMNS 6014, Erlenberg	referred to as *Zanclodon laevis* (Fraas 1879) referred to as '*Plateosaurus engelhardti*' (Galton 1985a) considered a *nomen dubium* (Galton 2001a) includes GPIT-PV-30785e.i (Galton 2001a) includes SMNS 13200b (Galton 2001a)
Plateosaurus quenstedti von Huene, 1905a	GPIT A, "Jachklinge" in Tübingen-Pfrondorf. GPIT-PV-30784 – Skelett I	referred to as '*Plateosaurus engelhardti*' (Galton 1985a) considered as *nomen dubium* (Galton 2001a) includes GPIT-PV-30785 (von Huene 1932; Weishampel and Westphal 1986) includes SMNS Fund I (Galton 2001a) includes SMNS 12951 (Galton 2001a)
Plateosaurus ornatus von Huene, 1905a	Schlösslesmühle bone bed	removed from Prosauropoda, assigned to Archosauriformes (Galton and Upchurch 2004)

Original taxon	Specimen	Taxonomic history
Plateosaurus reiningeri von Huene, 1905a	SMNS 53537, Degerloch	referred to as '*Plateosaurus engelhardti*' (Wellnhofer 1993) considered as a *nomen dubium* (Galton 2001a)
Gresslyosaurus plieningeri von Huene, 1907	SMNS 80664	referred to as *Plateosaurus plieningeri* (von Huene 1932) referred to as *Pachysaurus reiningeri* (Kuhn 1959) referred to as '*Plateosaurus engelhardti*' (Galton 1985a) considered *nomen dubium* (Galton 2001a) includes GPIT IV (Galton 2001a) included MB RvL 1, 2 and 3 (Rühle von Lilienstern 1952) then these were removed and referred to as *Ruehleia bedheimensis* (Galton 2001a)
Gresslyosaurus torgeri Jaekel, 1911	MB.R.4401.1-18	referred to as *Plateosaurus plieningeri* (von Huene 1932) referred to as '*Plateosaurus engelhardti*' (Galton 2001a) considered a *nomen dubium* (Galton 2001a)
Plateosaurus longiceps Jaekel, 1913	MB R.1937	renamed *Plateosaurus quenstedti* (von Huene 1932) referred to as '*Plateosaurus engelhardti*' (Galton 1985a) includes AMNH FARB 6810 (Galton 2001a) includes GPIT-PV-30784 (Galton 2001a) includes SMNS 12950 (Galton 2001a) includes SMNS 12949 (Galton 2001a)
Plateosaurus trossingensis Fraas, 1913	SMNS 13200	referred to as '*Plateosaurus engelhardti*' (Galton 1985c) referred to as '*Plateosaurus longiceps*' (Galton 2001) considered the neotype for *Plateosaurus* (ICZN 2019)
Plateosaurus integer Fraas, 1915	SMNS 13200	the name replaced by *Plateosaurus trossingensis*
Plateosaurus stormbergensis Broom, 1915	AMNH 6505	referred to as *Euskeosaurus* (Heerden 1979) considered a *nomen dubium* (Galton 2001a)
Plateosaurus cullingworthi Haughton, 1924	SAM 3341, 3345, 3347, 3350, 3351, 3603, 3607	referred to as *Euskelosaurus browni* (Heerden 1979) referred to as *Plateosauravus cullingworthi* (Galton et al. 2005)
1930–1940		
Pachysaurus giganteus von Huene, 1932	GPIT E	referred to as *Pachysauriscus giganteus* (Kuhn 1959) referred to as *Gresslyosaurus giganteus* (Steel 1970) referred to as '*Plateosaurus engelhardti*' (Galton 1985c) considered a *nomen dubium* (Galton 2001a)
Pachysaurus wetzelianus von Huene, 1932	GPIT V	referred to as *Pachysauriscus wetzelianus* (Kuhn 1959) referred to as *Gresslyosaurus wetzelianus* (Steel 1970) referred to as '*Plateosaurus engelhardti*' (Galton 1985c) considered a *nomen dubium* (Galton 2001a)
Plateosaurus fraasianus von Huene, 1932	SMNS 13200	the name replaced by *Plateosaurus trossingensis*

at Bebenhausen. *G.* '*robustus*' comprises a complete left hind limb, a left pes, a couple of ischia and pubes, and an almost complete tail. *Gresslyosaurus* '*torgeri*' Jaekel, 1911, was erected for a set of postcranial material from Baerecke-Limpricht clay, in Halberstadt, from a time equivalent to the Trossingen Formation (Sander 1992; Mudroch et al. 2006).

In 1932, von Huene synonymised the material of *Gresslyosaurus* with *Plateosaurus*, namely *P.* '*robustus*' and *P.* '*plieningeri*' von Huene, 1905, the latter including the material of *Gresslyosaurus* '*torgeri*'. This reserved the genus *Gresslyosaurus* only for material from Switzerland. However, in his plate 13, von Huene (1932) indicated that *G. ingens* had come from the Upper Keuper from Halberstadt, but the material listed corresponds to the Swiss specimen described in Rütimeyer (1856). Furthermore, material from Somerset, United Kingdom, was identified as *G. ingens* (von Huene 1907, 1932) and distinguished by the straight outline of the femur from the sigmoidal outline of *Plateosaurus*. Nevertheless, *G. ingens* from Somerset was later identified as the melanorosaurid *Camelotia borealis* Galton, 1985d.

Gresslyosaurus was considered a valid name by Steel (1970) and placed within Plateosauridae. Steel (1970) expanded the content of *Gresslyosaurus* to several specimens from the Upper Triassic of Switzerland and Germany, most of which were stored in Tübingen. The genus included: *G. ingens* (holotype); *G. cloacinus* von Huene, 1932, now a theropod from the Rhät bonebed in Bebenhausen (see Carrano et al. 2012); SMNS 52457, *G.* '*reiningeri*' from Trossingen Formation (first named *Plateosaurus reiningeri* von Huene, 1905a); SMNS 53537, *G.* (= *Pachysaurus*) *giganteus* (von Huene, 1932); *G.* (= *Pachysaurus*) *wetzelianus* (von Huene, 1932); *G.* (= *Pachysaurus*) *magnus* (von Huene, 1905); as well as *G.* (= *Pachysaurus*) *ajax* (von Huene, 1905). Galton (1985a) synonymised all the material previously referred to as *Gresslyosaurus* as *Plateosaurus* '*engelhardti*', and Galton (2001a,b) made all the *Gresslyosaurus*-bearing specimens *nomina dubia*.

The specimen SMNS 13200 has effectively been used as the reference specimen for *P.* '*engelhardti*' before being officially defined as the holotype for the species *P. trossingensis* (ICZN 2019). GPIT-PV-30784 ("GPIT I")

and GPIT-PV-30785 ("GPIT II") have also been used as reference material for *P.* '*engelhardti*', and although GPIT-PV-30785 is a composite of at least two similarly sized individuals, these two come from the same locality and could safely be considered the same species as SMNS 13200. Furthermore, AMNH FARB 6810 comes from the same site where GPIT-PV-30784 and GPIT-PV-30785 were excavated. Therefore, in cases where GPIT-PV-30784 and AMNH FARB 6810 are used instead of the neotype, these two specimens could be considered syntypes for *P.* '*engelhardti*' given the large amount of literature on them. Nevertheless, in the literature, AMNH FARB 6810 has been referred to as *P. longiceps* or *P. erlenbergiensis*. The holotype of *P. longiceps* is MB.R.1937, and the holotype of *P. erlenbergiensis* is SMNS 6014, coming from the localities of Halberstadt and Ellenberg, respectively. Moreover, the specimen SMNS 13200 is the holotype of *P. trossingensis*, which made *P. trossingensis* a junior synonym of *P.* '*engelhardti*' (Galton 1999, 2000, 2001a).

In the case of the Halberstadt material, it has been considered as part of *P. longiceps* based on the association within the bonebed and because of two cranial autapomorphies. These autapomorphies are 1) a medially directed peg on the palatine, a sub-vertical lamina between the basipterygoid processes, and 2) the combination of characters of a diapophysis from sacral 1 forming a broad sheet with a semicircular outline with a narrow distal half on the adjacent edge of the first sacral rib, a diapophysis from sacral 2 posterolaterally directed and tapering gradually, a sigmoid femur, articular end surfaces of the anterior caudal centra are sub-parallel rather than wedge-shaped (Galton 2001b). The two cranial autapomorphies have also been found in AMNH FARB 6810 (Prieto-Márquez and Norell 2011). Nevertheless, several cranial characters have been interpreted as displaying a wide range of variability in *Plateosaurus*. For instance, GPIT-PV-30784 and AMNH FARB 6810 (Prieto-Márquez and Norell 2011; Lallensack et al. 2021) have five premaxillary teeth, whereas SMNS 13200 has six (Galton 1976; Lallensack et al. 2021) as well as the holotype of *P. longiceps* (MB.R.1937; Galton 1985). Therefore, a revision of the material from Halberstadt is needed to understand the combination of cranial and postcranial characteristics compared to the rest of the plateosaurian material from Central Europe. The holotype of *P. erlenbergiensis*, specimen SMNS 6014, from the Knollenmergel of Ellenberg, contains a neurocranium with a sub-vertical lamina between the basipterygoid processes. Furthermore, Galton (2001b) noted that specimen GPIT-PV-30785 was referred to as *P. erlenbergiensis* due to the postcranial anatomy. Therefore, *P. erlenbergiensis* could be considered a junior synonym of *P.* '*engelhardti*' (Fig. 3).

The ilium of SMNS 80664 is incomplete and lacks most of the dorsal margin; however, its morphology is distinctively different from the one in GPIT-PV-30787. The preacetabular process in SMNS 80664 is short and with a triangular outline, whereas GPIT-PV-30787 is more quadrangular and more anteriorly expanded. On the postacetabular side, GPIT-PV-30787 bears a distinct brevis-fossa that gives the posterior margin an M-shaped outline, whereas the posterior margin in SMNS 80664 bears a reduced brevis fossa and a straighter-sided margin. SMNS 80664 has a more distinctive 'plateosaurian' morphology, i.e., like SMNS 13200, referred to as *P.* '*engelhardti*' and one of the most preserved skeletons. Here, we describe specimen GPIT-PV-30787 as a new sauropodomorph that shows affinities to more derived non-sauropod sauropodomorphs.

The GPIT collection houses five historical catalogue numbers that have been used as specimens in the literature, although they refer to several individuals collected in the same expedition and not necessarily to one individual. These historical catalogue numbers are "GPIT A", "GPIT B", "GPIT C", "GPIT D", and "GPIT E", and a detailed breakdown of their new catalogue numbers is provided in Table 2. Specimens of GPIT A–D were collected during the late 19th century. On the other hand, the specimens in the diorama are numbered GPIT I–IV. Except for GPIT VII, all the specimens in the diorama were collected from the Obere Mühle locality, as well as specimen GPIT E. GPIT C are fragments belonging to GPIT VII (see Table 2).

1.2. The specimens from Obere Mühle

Specimen SMNS 13200 was excavated from Obere Mühle in the summer of 1912 (Schoch 2011). The Obere Mühle outcrop has been the most productive site in the Trossingen locality, where 65 skeletons have been excavated (Schoch and Seegis 2014). The next round of excavations from 1921 to 1923 was organised by Friedrich von Huene (Tübingen University) and mainly financed by William Diller Matthew (American Museum of Natural History, New York) (Reinacher 2021). Half of the findings were sent to the AMNH, and the other half stayed at GPIT. This excavation yielded 12 skeletons (Schoch 2011; Schoch and Seegis 2014; Reinacher 2021), with seven staying in Tübingen. The specimen AMNH FARB 6810 was mounted and remained in the New York exhibition, and some other material was sent to the Museum of Comparative Zoology at Harvard University (Sander 1992). Of the material that remained in Tübingen, the complete skeleton was mounted, and two others were joined into a composite (Weishampel and Westphal 1986; Sander 1992). These two skeletons correspond to "GPIT I" (GPIT-PV-30784) and "GPIT II" (GPIT-PV-30785), respectively. Because the four specimens mentioned above, namely SMNS 13200, AMNH FARB 6810, GPIT-PV-30784, and tentatively GPIT-PV-30785, come from the same bonebed, known as the "*Plateosaurus*-bonebed", it is likely that these four specimens belong to the same species. These four specimens have been consistently referred to as *P.* '*engelhardti*' in the literature. A recent study on the morphological variation clusters "GPIT I" (GPIT-PV-30784) and "GPIT II" (GPIT-PV-30785) and SMNS 13200 as part of the same group, neatly separated from *Ruehleia* and *Efraasia* (Lefebvre et al. 2020).

A third excavation in the quarry was organised by Reinhold Seemann in 1932, in an expedition that lasted for six months and recovered 65 bones, most of which are stored at the SMNS (Schoch 2011). The *Plateosaurus* collection at Stuttgart is also likely monospecific.

Specimen GPIT-PV-30787, historically known as "GPIT IV", was initially referred to as *Plateosaurus* '*plieningeri*' (see Table 2). The holotype of *P. plieningeri* is specimen SMNS 80664 (von Huene 1907). It comprises 17 vertebrae, including the sacrum, ribs, ilium, pubis, distal ends of the femur, a fibula, metatarsal V, and the ends of other metatarsals found in 1847 by Theodor Plieninger in a bonebed at Degerloch, from the Knollenmergel, Trossingen Formation (now a district of Stuttgart) (Galton 2001a). The Degerloch specimen became the holotype of *Gresslyosaurus plieningeri* (von Huene 1907) and was referred to as *Plateosaurus* by von Huene (1932). Wellnhofer (1993), in a study on the stance of *Plateosaurus*, considered specimen SMNS 80664 as *P.* '*engelhardti*', since it was a younger, more robust specimen compared to the older and more gracile specimens from Trossingen. A recent morphometric analysis shows strong evidence that SMNS 80664, along with GPIT-PV-30784 ("GPIT I") and GPIT-PV-30785 ("GPIT II", a composite – see Table 2), cluster together with *P.* '*engelhardti*' and attribute the variability in the morphology to taphonomic effect (Lefebvre et al. 2020). However, the analysis did not include specimen GPIT-PV-30787.

According to Galton (2001a), *P.* '*plieningeri*' included two Trossingen specimens: SMNS 80664, housed in Stuttgart, and specimen GPIT-PV-30787 ("GPIT IV"), housed in Tübingen. Nevertheless, specimen GPIT-PV-30787 has more preserved elements than the holotype of *P.* '*plieningeri*', as it includes a complete pelvic girdle, the anterior and distal portion of the caudal vertebrae series, a fibula, a tibia, metatarsal I, and digits II and III and a femur. Galton (2001a) considered this specimen part of *P.* '*engelhardti*' and identified it as a large female (Table 2), based on comparisons with crocodiles and *Tyrannosaurus* Osborn, 1905, given the morphology of the femur and the small first chevron. Galton (2001a) included specimen SMNS 80664 as one of the historical referrals to *P.* '*plieningeri*', but he concluded that the palatine peg and the vertical lamina between the basipterygoid process corresponded to another species, *P. longiceps*. The status of *P.* '*plieningeri*' (von Huene 1907) is as a junior synonym of *P. longiceps* but restricted only to SMNS 80664.

The review of the literature presented here shows that there are two definitions of *Plateosaurus*: a phylogenetic definition with an inconsistent specimen composition, and a morphological definition that includes mostly the same specimens. Specimen GPIT-PV-30787 has been used as part of the morphological definition but has never been included in the phylogenetic or morphometric definition. In this work, we provide a framework to contextualise phylogenetic data with morphological data to help delimiting the specimen-composition of *Plateosaurus* as a taxonomic unit.

2. Materials and Methods

Institutional Abbreviations: **ACM**, Beneski Museum of Natural History, Amherst, Massachusetts, U.S.A.; **AMNH**, American Museum of Natural History, New York, New York, U.S.A.; **BP**, Bernard Price Institute, Johannesburg, South Africa; **FMNH**, Field Museum of Natural History, Chicago, Illinois, U.S.A.; **GPIT**, Paläontologische Sammlung, Universität Tübingen, Tübingen, Germany; **IVPP**, Institute of Vertebrate Paleontology and Paleoantropology, Beijing, People's Republic of China; **MACN**, Museo Argentino de Ciencias Naturales 'Bernardino Rivadavia,' Buenos Aires, Argentina; **MB**, Museum für Naturkunde, Humbolt-Universität, Berlin, Germany; **MCZ**, Museum of Comparative Zoology, Harvard University, Cambridge, Massachusetts, U.S.A.; **MLP**, Museo de La Plata, La Plata, Argentina; **MPEF**, Museo Paleontologico 'Egidio Feruglio,' Trelew, Chubut, Argentina; **MPM**, Museo Regional Provincial 'Padre M. J. Molina,' Rio Gallegos, Santa Cruz, Argentina; **NAA,** Naturama, Aargau, Kanton Aargau, Switzerland; **NHMUK**, The Natural History Museum, London, U.K.; **NMQR**, National Museum, Bloemfontein, South Africa; **PIMUZ**, Paläontologisches Institut und Museum der Universität Zürich, Zürich, Switzerland; **POL**, Musée de Poligny, now housed in the Musée Archéologique de Lons-le-Saunier, Jura, France; **PVL**, Instituto 'Miguel Lillo,' Tucuman, Argentina; **PVSJ-UNSJ**, Paleontología de Vertebrados–Museo de Ciencias Naturales, Universidad Nacional de San Juan, San Juan, Argentina; **SAM**, Iziko–South African Museum, Cape Town, South Africa; **SMA**, Sauriermuseum Aathal, Kanton Zürich, Switzerland; **SMNS**, Staatliches Museum für Naturkunde, Stuttgart, Germany; **TMM**; Texas Memorial Museum, Austin, Texas, U.S.A.; **UEN**, Universität Erlangen, Institüt für Geologie und Mineralogie**; UMNH**, Utah Museum of Natural History, Salt Lake City, Utah, U.S.A.; **USNM**, National Museum of Natural History, Smithsonian Institution, Washington, D.C., U.S.A.; **YPM**, Yale Peabody Museum, New Haven, Connecticut, U.S.A.

Specimen GPIT-PV-30787 was added to a character-by-taxon matrix that included two species of *Plateosaurus* and early diverging sauropodomorphs from Central Europe *Efraasia*, *Ruehleia*, *Schleitheimia* and *Ohmdenosaurus* Wild, 1978. Rauhut et al. (2020) used the character-by-taxon matrix of Apaldetti et al. (2018), but Rauhut et al. (2020) reported that they added some corrections performed by McPhee et al. (2015b). As shown in Fig. 2, these two matrices come from different iteration chains. McPhee et al. (2015b) defined the OTU *P.* '*engelhardti*' as containing AMNH FARB 6810, SMNS 13200 (neotype) and SMNS 91310, and the OTU *P. gracilis* as containing GPIT 18392 and SMNS 5715. McPhee et al. (2015b) had broader definitions of *P.* '*engelhardti*' and *P. gracilis*, but the changes reported in McPhee et al. (2015b) apply only to *Pulanesaura* McPhee et al., 2015 and *Spinophorosaurus* Remes et al., 2009. Apaldetti et al. (2018) employed the definition of

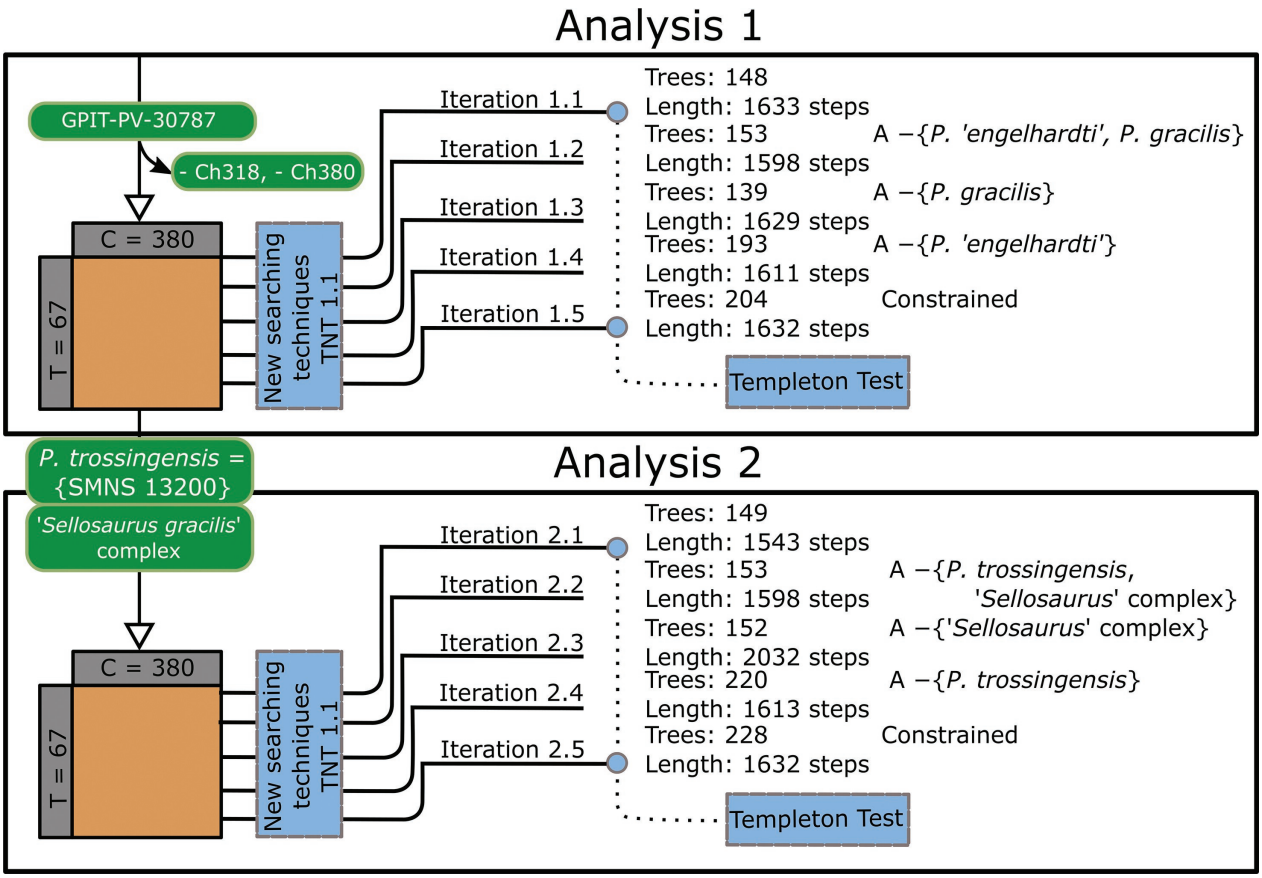

Figure 4. Diagram outlining the workflow of the phylogenetic analyses carried out in this work. The character-by-taxon matrix has 67 taxa and 380 characters. The number of trees obtained from each iteration is shown next to the name with their length. *A* stand for the character-by-taxon matrix and the elements inside the curly brackets represent the OTUs removed before the analysis was run. The constrain refers to forcing GPIT-PV-30787 inside a clade with *Plateosaurus*. The Templeton Test in the two iterations only compared the total evidence trees (iteration 1.1 against iteration 1.5 and iteration 2.1 against iteration 2.5). The original character-by-taxon matrix by Rauhut et al. (2020) includes *P. trossingensis* as *P.* '*engelhardti*', including several specimens (see text), and only two characters scored as polymorphisms: Ch. 17 (scored as 0 and 1), and Ch. 138 (scored as 0 and 1). In the second analysis, *P. trossingensis* is restricted to specimen SMNS 13200, where Ch. 17 is scored as 0, and Ch. 138 is scored as 1.

P. gracilis as it was in Otero et al. (2015) but amended the definition of *P. trossingensis* (there as *P.* '*engelhardti*') to specimens AMNH FARB 6810, SMNS 13200 and SMNS 91310 (=F65). Rauhut et al. (2020) used this character-by-taxon matrix, making it a good candidate to add specimen GPIT-PV-30787 without a noisy signal. Other than the changes outlined in the following paragraphs, the characters that were considered as ordered by Rauhut et al. (2020) are treated as such here, namely Chs. 8, 13, 19, 23, 40, 57, 69, 92, 102, 117, 121, 129, 132, 145, 148, 150, 151, 158, 168, 170, 171, 178, 210, 213, 232, 237, 245, 254, 263, 268, 282, 295, 316, 322, 330, 352, 365, 368, 370 and 375. Table 3 details the specimens and sources used for comparative purposes in this study.

Several characters were changed (Appendix 1). Ch. 318 refers to a paramarginal ridge on the lateral surface of the cnemial crest. Since the character was not illustrated, it is not easy to know what structure this refers to and has been removed. It was initially scored by Yates (2007) for *Lufengosaurus* Young, 1940 (specimens IVPP V15, and illustrations in Young 1941; Barrett et al. 2005a), *Yunnanosaurus huangi* Young, 1940 (specimens IVPP V94, V505, and illustrations in Young 1942, 1951) and *Jingshanosaurus* Zhang and Yang, 1995 (specimen LV 3, and illustrations in Zhang and Yang 1994), however, upon first-hand examination of the tibia in *Lufengosaurus* (IVPP V15) and *Yunnanosaurus huangi* (IVPP V20, the one illustrated in Young 1941), it was not possible to identify the paramarginal ridge, neither based on the illustrations or the descriptions for *Jingshanosaurus*.

Ch. 380, which refers to the femoral length alone, was removed. It was not possible to replicate the character states using gap-coding, and several specimens could refer to juveniles, complicating the scoring of this character. Furthermore, there is already a character on the tibia:femur ratio in the matrix.

Two more characters must be reinterpreted, namely Ch. 379, 'Growth marks (LAGs or annuli) in the cortex' and Ch. 381, 'Relative abundance of parallel-fibered bone (PFB) and woven fibered bone (WFB)'. These characters were proposed by Cerda et al. (2017) and assessed in *Riojasaurus* Bonaparte, 1969, *Coloradisaurus* Galton, 1990, *Massospondylus*, *Adeopapposaurus* Martinez, 2009, *Leyesaurus* Apaldetti et al., 2011, *Mussaurus*, *Leonerasaurus* Pol et al. 2011, *Lessemsaurus* Bonaparte 1999, *Volkheimeria* Bonaparte, 1979 and *Pa-*

Table 3. Source of comparative data used in this study. ‡ Indicates specimens that were observed in person by ORRF.

Taxon	Source	Specimens referred
Aardonyx celestae Yates et al., 2010	Yates et al. (2010)	BP/1/6510, BP/1/5379c, BP/1/5379d, BP/1/6602
Adeopapposaurus mognai Martinez, 2009	Martinez (2009)	PVSJ 610
Anchisaurus polyzelus (Hitchcock, 1865)	Yates (2004)	ACM 41109 (‡), YPM 208 (‡), YPM 209 (‡), YPM 1883 (‡)
Antetonitrus ingenipes Yates and Kitching, 2003	Yates and Kitching (2003)	BP/1/4952
Barapasaurus tagorei Bandyopadhyay et al., 2010	Bandyopadhyay et al. (2010)	ISIR 51, ISIR 52, ISIR 54, ISIR 741, ISIR 62, ISIR 743
Blikanasaurus cromptoni Galton and van Heerden, 1985	Galton and van Heerden (1998)	SAM-PK-K403
Buriolestes schultzi Cabreira et al., 2016	Müller et al. (2018b)	ULBRA-PVT280, CAPPA/UFSM 0035
Camarasaurus supremus Cope, 1877	Osborn and Mook (1921)	
Coloradisaurus brevis Galton, 1990	Apaldetti et al. (2011)	PVL 5904
Efraasia minor (von Huene, 1908)	Yates (2003)	SMNS 12354 (‡), SMNS 12684 (‡), SMNS 11838 (‡), SMNS 12667 (‡), SMNS 12668 (‡), SMNS 17928 (‡)
Eoraptor lunensis Sereno et al., 1993	Sereno et al. (2012)	PVSJ 559, PVSJ 745, PVSJ 860
Giraffatitan brancai (Janensch, 1914)	Janensch (1914)	HMN SII
Glacialisaurus hammeri Smith and Pol, 2007	Smith and Pol (2007)	FMNH PR 1823, 1822 (‡)
Herrerasaurus ischigualastensis Reig, 1963	Novas (1994)	PVSJ 373, PVL 2566
Jingshanosaurus xinwaensis Zhang and Yang, 1994	Zhang and Yang (1994)	LFGT-ZLJ0113
Lessemsaurus sauropoides Bonaparte, 1999	Bonaparte 1999; Pol and Powell (2007)	PVL 4822/8–4822/9, 4822/11–4822/79
Lufengosaurus huenei Young, 1942		IVPP V15 (‡)
Macrocollum itaquii Müller et al., 2018a	Müller et al. (2018a)	CAPPA/UFSM 0001a–c
Massospondylus carinatus	Young 1941; Barrett et al. (2019)	BP/1/4934, BP/1/5241, BP/1/4693, BP/1/4377
Melanorosaurus readi Haughton, 1924	Cooper (1981)	NM QR3314, NM QR 1551, SAM-PK-K3449
Meroktenos thabanensis Peyre de Fabreguès and Allain, 2016	Peyre de Fabreguès and Allain (2016)	MNHN.F.LES16, MNHN.F.LES351.
Mussaurus patagonicus Bonaparte and Vince, 1979	Otero and Pol (2013)	MLP 61-III-20–23, MLP 68-II-27-1, MLP 61-III-20–22
Pantydraco caducus Yates, 2003	Galton and Kermack (2010)	BMNH NHMUK P77/1 (‡)
Plateosauravus cullingworthi von Huene, 1932	van Heerden (1979)	SAM-PK-K3342, 3343, 3348, 3350, 3351, 3356, 3602, 3603
Riojasaurus incertus Bonaparte, 1969	Bonaparte (1972)	PVL 3808
Ruehleia bedheimensis Galton, 2001b		MB RvL1 (‡)
Sarahsaurus aurifrontalis Rowe et al., 2011	Rowe et al. (2011)	TMM 43646-2, 23646-3
Saturnalia tupiniquim Langer et al., 1999	Langer et al. (1999, 2007; Langer 2003)	MCP 3844-PV
Seitaad ruessi Sertich and Loewen, 2010	Sertich and Loewen (2010)	UMNH VP 18040 (‡)
Shunosaurus lii Dong et al., 1983	Zhang (1988)	T5401
Tazoudasaurus naimi Allain and Aquesbi, 2008	Allain and Aquesbi (2008)	CPSGM To1-38, CPSGM To1-103, CPSGM To1-129, CPSGM To1-31, CPSGM To1-114, CPSGM To1-265
Thecodontosaurus antiquus Morris, 1843	Benton et al. (2000)	See catalogue in Benton et al. (2000) (‡)
Unaysaurus tolentinoi Leal et al., 2004	Leal et al. (2004)	UFSM 11069
Vulcanodon karibaensis Raath, 1972	Cooper (1984)	
Yunnanosaurus huangi Young, 1940	Young (1942)	NGMJ 004546
Yunnanosaurus youngi, Lü et al., 2007	Lü et al. (2007)	CXMVZA 185 (‡)

tagosaurus Bonaparte, 1979. Apaldetti et al. (2018) incorporated these two characters from Cerda et al. (2007) and assessed them on *Ingentia*. The scores on *Plateosaurus* were based on the histological analyses performed by Klein (2004) and Sander and Klein (2005). Several specimens were sampled as part of *Plateosaurus*, based in collections in SMNS, AMNH, MSF, NAA, PIMUZ, SMA, and GPIT (there referred to as the IFG, "Institut für Geowissenschaften"). For this second analysis, where all the other *Plateosaurus* material was removed, and the OTU was restricted to the neotype SMNS 13200 and GPIT-PV-30784, this character was rescored based on the results reported in those two works. Two specimens from the GPIT collection were mentioned, one referred to as 'IFG, exhibition', and the other as 'IFG, compactus' (archive). The femur and tibia belong to GPIT-PV-30787, the scapula and the humerus used in that study have not been located yet, and the trunk vertebrae used (Rückenwirbel [RW]: RW12 and RW14) are part of GPIT-PV-30790 ('GPIT C').

In Klein (2004), the 'IFG compactus' left femur corresponds to the left femur from GPIT-PV-30787 described above. This femur was the only one in her sample with highly vascularised fibrolamellar bone, higher than the normal fibrolamellar bone in other material referred to as *Plateosaurus*. In the femur of GPIT-PV-30787, there are also single vascular canals and thicker laminae. This tissue appeared after the fifth growth cycle, confirming that this individual was already an adult. In Klein (2004) and Sander and Klein (2005), it was interpreted that this growth pattern corresponded to an exceptional growth cycle due to favourable environmental conditions during a restricted period. However, based on our "section Systematic Palaeontology", this tissue confirms our suggestion that this animal corresponded to a different species with a faster growth rate. Moreover, SMNS 13200 and GPIT-PV-30784 were not included in the histological sampling, and we have removed the two scores that refer to the histological characters from their string. Nevertheless, GPIT-PV-30787 can be confidently scored for these two characters.

To explore the relationship of GPIT-PV-30787, several iterations of phylogenetic analyses were performed (see Appendix 2 for the added OTUs). In the first round of analysis (Fig. 4), five iterations were run using TNT 1.1 (Goloboff et al. 2008), employing the new searching techniques, with the sectorial, ratchet, drift and tree fusing algorithms run through 1.000 random addition sequences. Iteration 1.1 included all taxa; in iteration 1.2, the two *Plateosaurus* OTUs were removed and were then alternatively removed in iterations 1.3 and 1.4 (see Fig. 4). Finally, specimen GPIT-PV-30787 was constrained to form a clade with *Plateosaurus*, and a Templeton Test was performed to contrast the trees obtained in iteration 1.5 against iteration 1.1.

For the second round of analysis, *P. trossingensis* was restricted to the neotype. Characters were checked against the descriptions of the neotype (Moser 2003) and with notes on first-hand observations of SMNS 13200. The species *P. gracilis* was restricted to the material available in the GPIT collection (Fig. 3). The historical catalogue numbers GPIT 18064, GPIT 18318a and GPIT 18392 have not been given new catalogue numbers because documental evidence suggests the material in each catalogue number belongs to several individuals. Furthermore, the skull of specimen GPIT 18318a has been reported missing in the collection. To avoid confusion, in this iteration, we are referring to this OTU as the '*Sellosaurus*' von Huene, 1907, complex, removing the scores for cranial characters. The same conditions as in Analysis 1 were repeated for Analysis 2 (Fig. 4).

A third phylogenetic analysis was performed, using the implied weighting on TNT 1.1, setting a 'gentle' concavity of k=12 as suggested in Goloboff et al. (2018).

Finally, a bivariate analysis of the morphology of the tibia following Ezcurra and Apaldetti (2011) was performed in this work. To the character-by-taxon matrix by Rauhut et al. (2020), the following specimens were added: GPIT-PV-30787, and *Plateosaurus* was represented by the specimens BSP 1962, MB.R.4405.1-67, SMNS 17928, SMNS 13200 (holotype of *P. trossingensis*) and GPIT-PV-30784 (referred to *P. trossingensis*), *Mussaurus*, *Xingxiulong* Wang et al., 2017, *Yunnanosaurus huangi* and *Lufengosaurus*. According to Ezcurra and Apaldetti (2011), the ratio between the total length and the anteroposterior depth at the mid-length of the tibia show a phylogenetic signal. Nevertheless, the character they proposed is not added to the version of the character-by-taxon matrix used in our recursive analysis.

The character-by-taxon matrices of Analysis 1 and Analysis 2 are stored in MorphoBank Project 4301 (http://morphobank.org/permalink/?P4301), along with high-definition pictures of the different elements that comprise GPIT-PV-30787.

3. Results

3.1. Systematic palaeontology

Tuebingosaurus gen. nov.

http://zoobank.org/F3A918A4-DC5B-4263-9169-8AA-647BA1989

Dinosauria Owen, 1842
Sauropodomorpha von Huene, 1932
Massopoda Yates, 2007a

Etymology. The genus name refers to the city of Tübingen, Germany. The holotype described here has been housed in the university's palaeontological collection since 1922, when it was discovered during an excavation of the nearby Trossingen Formation.

Tuebingosaurus maierfritzorum sp. nov.

http://zoobank.org/B60C4F76-5CFA-4E9A-8745-E98E1CD6D8FC

Diagnosis. As for the type and only species.

Etymology. The species name refers to Uwe Fritz and Wolfgang Maier. The former is the editor-in-chief of the journal Vertebrate Zoology, and, in his journal, he facilitated the *Festschrift* edited by Ingmar Werneburg and Irina Ruf in honour of Wolfgang Maier. The latter was a professor of evolutionary zoology in Tübingen from 1987 to 2007, and the *Festschrift* was published on the occasion of his 80th birthday in 2022.

Holotype. GPIT-PV-30787, specimen historically referred to as 'GPIT IV', comprising a complete pelvis (three sacral vertebrae, two ilia, two pubes, two ischia), five anterior caudal vertebrae, four chevrons, left femur,

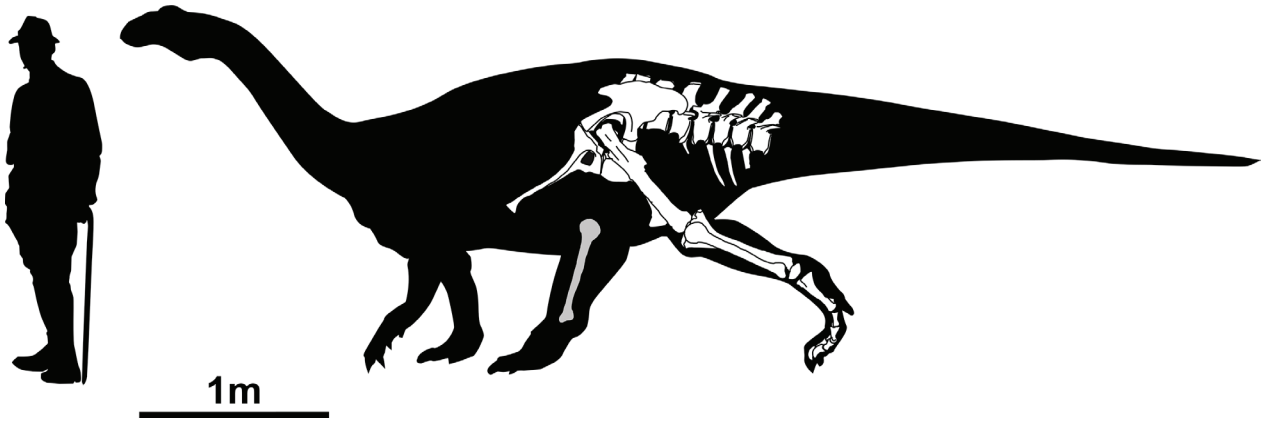

Figure 5. Reconstruction of *Tuebingosaurus maierfritzorum* **gen. et sp. nov.** as a quadruped dinosaur, using the outline of *Riojasaurus* as a base – next to the silhouette of Friedrich von Huene. The drawing of the bones is based on and modified from the original illustrations of specimen "GPIT IV" in von Huene (1932, pl. 38) that have been replicated in the literature. The right fibula is marked in grey as it was found nearby with similar measurements to the left fibula and has been assumed to be part of the same individual.

left tibia, left and right fibulae, left astragalus, left calcaneum, metatarsal I, pedal fingers 3 and 4 (Fig. 5).

Diagnosis. Sauropodomorph with a unique combination of features: a fused pair of primordial sacrals; a robust and rugose expansion in the postacetabular process of the ilium; a pentagonal outline in the distal surface of the tibia, characterised by an additional posterior projection; a deep lateroventral fossa on the anterior margin of the astragalus; a ventrally directed heel with a lateral projection on the lateral articulation of the astragalus supporting the reduced calcaneum.

Description and comparison. The anatomic terminology adopted in this work follows Galton and Upchurch (2004) for general anatomy, Wilson (1999) for vertebral laminae, Wilson et al. (2011) for vertebral fossae, and Wilson (2011) for the sacrum. Stacked photographs of the bones produced the plates Figs 6–18, and the scale is an approximate reference. Every object has a scale in a different plane, roughly scaled up to the same size. However, for accurate measurements, please refer to the tables or the raw photographs stored in Morphobank.

Specimen GPIT-PV-30787 was referred to as *P.* '*longiceps*' by Galton (2001b). The specimen was first illustrated by von Huene (1932) in his plate 38 and includes elements of the left forelimb (radius, metacarpal IV, phalanges from the fingers I, II and III), a sacrum with a pelvic girdle (including left and right ilia, left and right pubes, and left and right ischia), the first five anterior caudal vertebrae, and the left hindlimb (femur, tibia, fibula, and pes) (von Huene 1932; Galton 2001a).

3.1.1. **Sacrum** (Figs 6–7, Table 4)

The sacrum of *Tuebingosaurus maierfritzorum* is composed of two sacrals and one caudosacral. Sacral 1 and sacral 2 have co-ossified neural spines, whereas the caudosacral is broken at the anterior corner of the neural spine, and it is not possible to know if the co-ossification extends all the neural height of the caudosacral (Fig. 6). Most early-diverging sauropodomorphs possess three sacral vertebrae, unlike early sauropods with four. Due to the distortion, it is possible to see more fine details through the left-hand side (Fig. 6). The neural spines of sacral 1 and sacral 2 have an expanded spinal table. The intercostal fenestrae are small and face ventrally (Fig. 6); the alar process of the sacral rib is extensive, articulating with most of the medial iliac surface, and the acetabular process is thinner and posteriorly displaced compared to the alar process (Fig. 7). The sacral ribs between sacrals 1 and 2 form a large dorsal intercostal foramen (icf1) (Fig. 7). Sacral 1 has an intercostal foramen that is anteriorly facing. The anterior articular surface of sacral 1 is slightly concave, with parallel lateral margins and a rounded ventral margin. The centrum of sacral 1 is fused to sacral 2, but the suture between them is still visible. The prezygapophyseal centrodiapophyseal fossa (prcdf) is discernible, with very thick centroprezygapophyseal lamina (cprl) and a thicker prezygodiapophyseal laminae (prdl). Sacral 1 has a spinoprezygapophyseal laminae (sprl) with a rounded margin that meets at the base of the neural spine, where they merge into a prespinal lamina (prsl). Sacral 1 also has a thick strut in the spinopostzygapophyseal lamina (spol) position. It is unclear if there is an intracostal foramen in the second sacral rib. The centrum of sacral 2 is not completely fused into the caudosacral, with a pronounced suture. Through icf1, it is possible to see that sacral 2 also has a prezygodiapophyseal lamina (prdl) and a prezygodiapophyseal fossa. The second ala of the sacrum is thicker than the first one, with a developed dorsal shelf in the alar process.

The anterior corner of the neural spine of the caudosacral is broken. The neural spine of the caudosacral also has an expanded dorsal table. The morphology of the caudosacral rib is similar to that of sacral rib 2, with the alar process expanding towards the iliac surface after a median depression that expands into the intracostal foramen 2. The caudosacral rib is not separated into alar and acetabular projections. The caudosacral rib articulates with the medial side of the brevis fossa, and a suture between these two elements is quite clear (Fig. 6). A cavity sug-

Table 4. Measurements (in mm) of the sacral vertebrae of *Tuebingosaurus maierfritzorum*.

Measurements	S1	S2	CS
Anterior centrum height (ACH)	117.5	101.2	134.3
Anterior centrum width (ACW)	126.4	103.47	136.6
Centrum length (CL)	104.8	117.2	95.3
Neural spine length (NSL)	153.3	147.8	100
Posterior centrum height (PCH)	94.3	109.7	128.2
Posterior centrum width (PCW)	131	130	127
Sacral rib length (mediolateral) (SRL)	122.7	128.7	86
Total height of vertebra (VH)	255	262.7	211.1*

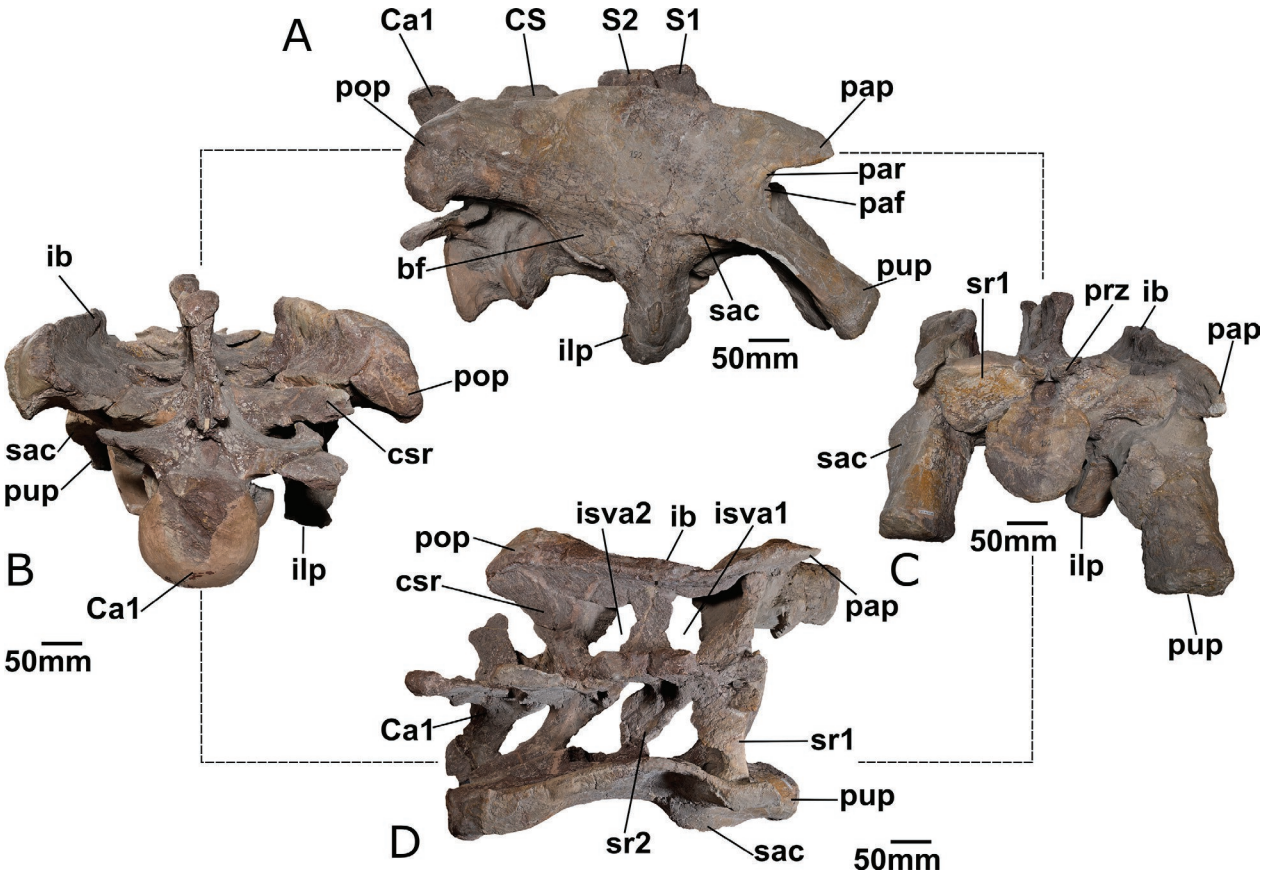

Figure 6. Ilia, sacrum and anterior caudal vertebra of *Tuebingosaurus maierfritzorum* (GPIT-PV-30787). **A** right lateral view; **B** posterior view; **C** anterior view; **D** dorsal view. Abbreviations: bf, brevis fossa; Ca1, anterior caudal 1; CS, caudosacral; csr, caudal sacral rib; ib, iliac blade; ilp, ischiadic peduncle; isva1,2, intercostal space ventral aperture; paf, preacetabular fossa; pap, preacetabular process; par, iliac preacetabular ridge; pop, postacetabular process; prz, prezygapophyses; pup, pubic peduncle; S1, sacral 1; S2, sacral 2; sac, supracetabular crest; sr1, sacral rib 1; sr2, sacral rib 2.

gests a spinodiapophyseal lamina (spdl) in sacral 2 and a prespinal lamina (prsl) in the caudosacral (Fig. 6). The caudosacral has two developed rounded struts in the position of the spinopostzygapophyseal lamina (spol); they remain separated along with the height of the neural spine (Fig. 6).

3.1.2. Anterior caudal vertebrae (Fig. 8–9, Table 5)

The first five anterior caudal vertebrae are preserved (Fig. 8). The morphology of the vertebrae is typical of non-eusauropodan sauropodomorphs, amphicoelous, and constricted mediolaterally with a deeply concave ventral surface in lateral view. The ventral margin of the articular surfaces has a thickened lip that serves as the articulation point for the chevrons (= haemal arches). In *Lufengosaurus* and *Antetonitrus* Yates and Kitching, 2003, the centrum is higher than long, a trait also observed in *Tuebingosaurus*, and as in many early sauropodomorphs, the lamination is reduced. The neural arches extend along the centrum length, starting at the anterior articular surface and ending short of the posterior centrum margin.

The first caudal vertebra is attached to the sacrum (Figs 6–7). The posteroventral corner of the centrum has been remodelled with plaster. Unlike the sacrals, the

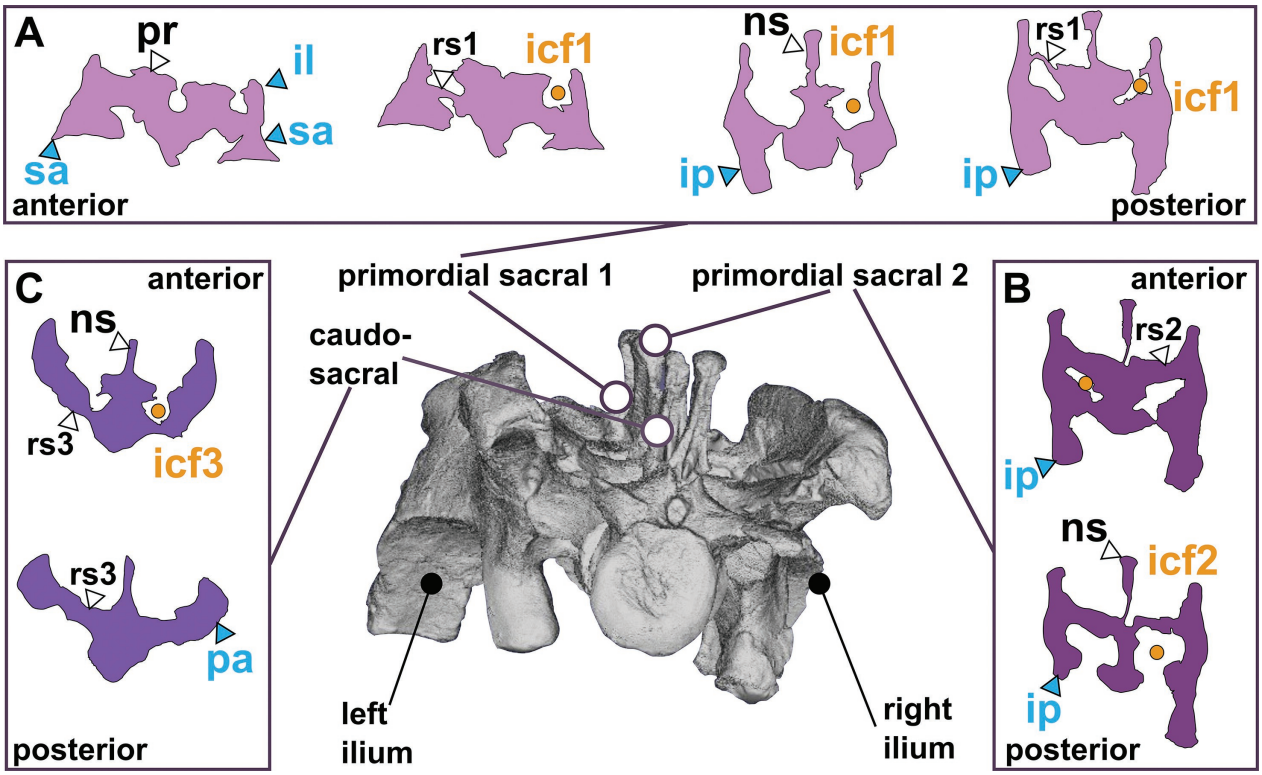

Figure 7. Surface scan of the pelvis of *Tuebingosaurus maierfritzorum* (GPIT-PV-30787) in posterodorsal view and some cross sections organised from the anterior to the posterior views. **A** Cross sections in sagittal planes along the first primordial sacral 1 ordered along the anteroposterior axis. **B** Cross sections in sagittal planes along the primordial sacral 2 ordered along the anteroposterior axis. **C** Cross sections in sagittal planes along the caudosacral vertebra are ordered along the anteroposterior axis. Abbreviations: icf1, intracostal fenestra 1; icf2, intracostal fenestra 2; icf3, intracostal fenestra 3; il, ilium; ip, ischidiac peduncle; ns, neural spine; rs1, sacral rib 1; rs2, sacral rib 2; rs3, sacral rib 3; sa, supraacetabular crest.

first caudal is apneumatic. The posterior articular surface is markedly convex on the ventral end, but a concavity extends below the neural arch. The neural spine ends in a knob-like structure, not a dorsal table like the preceding sacral vertebrae. The spinoprezygapophyseal lamina (sprl) meets at the midline at the base of the neural spine and forms an expanded pre-spinal lamina. The spinopostzygapophyseal laminae (spol) run from this knob-like structure to the postzygapophyses without forming a postspinal lamina. The diapophyses and the parapophyses are fused, but the former is longer than the latter allowing to distinguish both processes.

The second anterior caudal vertebra is obliquely twisted, with a deeply concave anterior articular surface and a shallow concave posterior articular surface (Fig. 8). The prezygapophyses, the postzygapophyses and the distal tip of the neural spine are broken. The ventral margin of the anterior articular surface has a large ventral lip for the chevron articulation, but the morphology of this process is difficult to assess due to distortion and breakage (Fig. 8). On both sides of the central body, there is a shallow concavity corresponding to a shallow centrodiapophyseal fossa (Fig. 7). The anterior articular surface is also more prominent than the posterior articular surface. The anterior margin of the neural spine is set more posteriorly than the position of the prezygapophyses, lending it a saddle-shaped outline, possibly due to a prominent spinoprezygapophyseal lamina (sprl) (Fig. 8). A distinct and broad anterior centrodiapophyseal lamina (acdl) is discernible. The spinopostzygapophyseal laminae run along the posterior margin of the neural spine, but the cortical bone is lost towards the tip, and it is impossible to know if they meet (Fig. 8).

Two anterior caudal vertebrae are preserved fused, and according to the illustration made by von Huene (1932) documenting the specimen, they correspond to the third and fourth caudal vertebrae. The vertebrae are dorsoventrally compressed on the right side (Fig. 8). The posterior part of the third anterior caudal neural arch is damaged, but a hypanthrum was present (Fig. 8). The neural canal is circular, and the diapophyses are oriented laterally (Fig. 8). It is not possible to discern the shape of the articular surface's outline due to the distortion (Fig. 8). The ventral lips on the posterior surfaces are wider than the ventral lips on the anterior surfaces. The neural arch is twice as high as the central height in both vertebrae. The spinoprezygapophyseal laminae meet at the base of the neural spine, whereas the spinopostzygapophyseal laminae remain separated throughout the neural spine, and in the third anterior caudal, there is a somewhat deep sulcus separating the two laminae (Fig. 8). The neural spines retain a constant width and end in a rounded dorsal surface with no mediolateral expansion. The prezygapophyses of the third anterior caudal are broken at the tips, and they seem to be dorsolaterally oriented, whereas the prezygapophyses of the fourth anterior caudal end in a

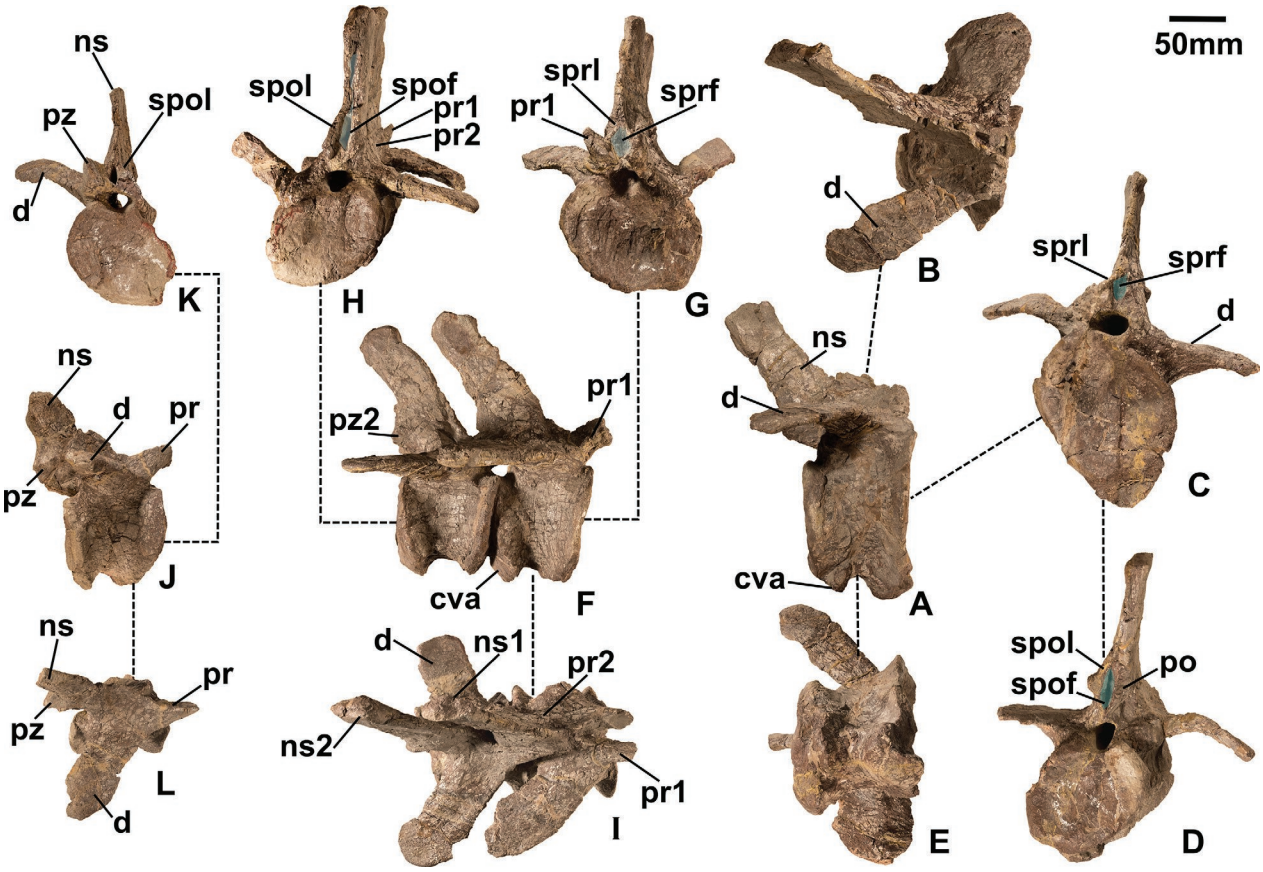

Figure 8. Anterior caudal vertebrae of *Tuebingosaurus maierfritzorum* (GPIT-PV-30787): **A**–**E** second anterior caudal vertebrae; **F**–**I** third and fourth anterior caudal vertebrae; **J**–**L** fifth anterior caudal vertebrae; in right lateral (A, F, J), in dorsal (B, I, L), in anterior (C, G, K), in posterior (D, H), and ventral (E) views. Abbreviations: cva, chevron articular surface, d, diapophysis, ns, neural spine, pr, prezygapophyses, pr1, prezygapophysis in third anterior caudal, pr2, prezygapophysis in fourth anterior caudal, pz, postzygapophysis, spof, spinopostzygapophseal fossa, spol, spinopostzygapophyseal lamina, sprf, spinoprezygapophseal fossa, sprl, spinoprezygapophyseal lamina.

point and are dorsally oriented. The anterior centrodiapophyseal lamina (acdl) is broad and short, only present in the second anterior vertebra (Fig. 8). The postzygapophyses are placed higher than the prezygapophyses in both neural arches.

The fifth anterior caudal vertebra is broken with part of the posterior half missing and has the same oblique twisting, even more markedly than in the preceding vertebrae (Fig. 8). As in the previous caudal vertebrae, the anterior articular surface is deeply concave, but the ventral margins are damaged, and the outline is unclear. The neural arch is slightly shorter than the centrum length, set posterior to the anterior articular surface and anterior to the posterior articular surface. The anterior margin of the neural spine is well set posterior to the anterior articular surface, aligned with the diapophysis. The prezygapophyses do not have the same tip morphology as the preceding vertebrae; instead, they are dorsoventrally widened in the proximal part.

Four chevrons are preserved and based on the description by von Huene (1932), corresponding to the three anterior-most chevrons. The chevrons have a closed Y-shaped chevron, with two proximal rami placed on each side of the haemal canal and distally composed of a laterally compressed blade. Proximally, the haemal canal is closed by a bony bridge connecting both rami and closing the canal dorsally. The chevrons have a straight outline in lateral view (Fig. 9). All chevrons show signs of compressive deformation, and two are complete. In the two complete chevrons, it is possible to see a posterior grove extending until the blade's mid-shaft (Fig. 9).

3.1.3. **Ilium** (Fig. 6, Table 6)

The pre-acetabular process resembles other early-diverging sauropodomorphs in being a triangular projection rather than a vertically tall subtriangular plate seen in more advanced sauropodomorphs. The pre-acetabular process is facing anteriorly in both lateral and dorsal views, and on both ilia, there is a bulge on the lateral surface of the processes. In addition, a preacetabular ridge is present in both ilia (Fig. 6).

The dorsal margin of the ilium is different on the left and right sides, suggesting a diagenetic distortion of the specimen that has slightly compressed the right-hand side and expanded the left-hand side (Fig. 6). The dorsal margin in the lateral view is convex in the middle portion, with two slight inflexions at the pre- and post-acetabular processes. The ilium of *P. trossingensis* (GPIT-PV-30784) has a sigmoid dorsal margin in lateral view,

Table 5. Measurements (in mm) of the anterior caudal vertebrae of *Tuebingosaurus maierfritzorum*. The "—" indicates that the element does not have the landmarks to measure it. The * indicates minimum length due to breakage.

Measurements	ACa1	ACa2	ACa3	ACa4	ACa5
Anterior centrum height (ACH)	131.3	148.7	101.2	101.6	94.2
Anterior centrum width (ACW)	205.9	114.3	118.6	102.0	—
Centrum length (CL)	103.3	88.2	82.0	80.3	80.1
Length of diapophysis	105.1	84.0	103.7	96.8	106.6
Length of prezygapophysis	73.4	—	31.9	55.9	39.6
Neural spine height (NSH)	126.9	165.0	185.0*	153.5	—
Posterior centrum height (PCH)	122.2	105.4	91.4	88.4	—
Posterior centrum width (PCW)	215.1	105.6	91.4	103.6	—
Total height of vertebra (VH)	260	285.0	270.0	245.9	205*

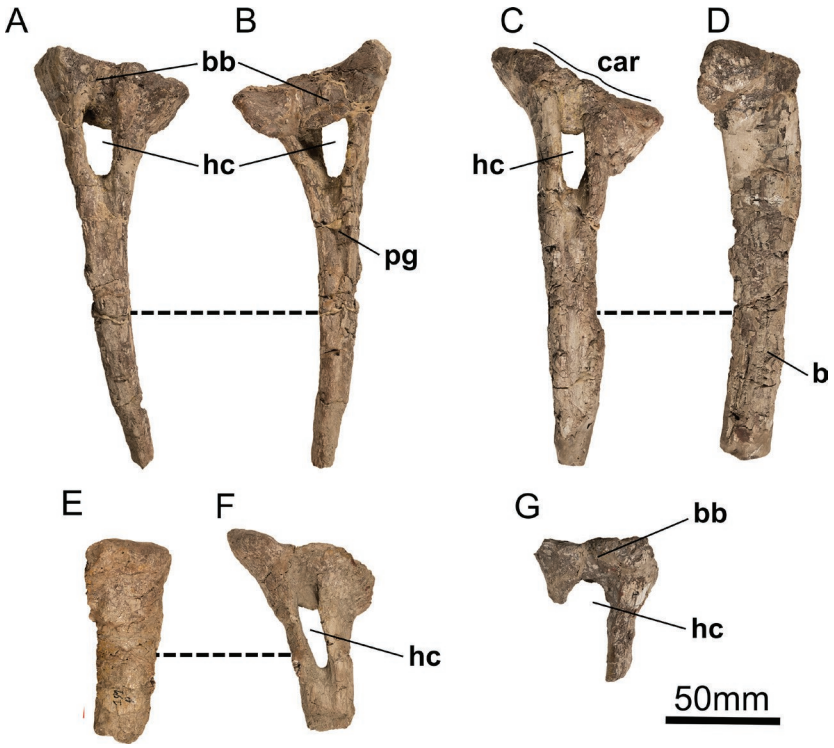

Figure 9. Chevrons of *Tuebingosaurus maierfritzorum* (GPIT-PV-30787) in anterior (**A**, **C**, **F**, **G**), posterior (**B**) and right lateral (**D**, **E**) views. Abbreviations: b, chevron blade, bb, bony bridge, car, chevron articular surface, hc, haemal canal, pg, posterior groove.

and in *Melanorosaurus* and *Riojasaurus*, the ilium is stepped. A stepped ilium is also present in the Ellingen material (Moser 2003). The iliac blade is thinner dorsal to the acetabulum than the postacetabular process. The lateral surface of both ilia is concave along the anteroposterior and dorsoventral axes, but the degree of the concavity is different on both sides due to the distortion. This concave surface extends ventrally to a point close to the acetabular margin, as *Meroktenos*. In non-sauropod sauropodomorphs, this surface is restricted to the dorsal half of the iliac blade, as illustrated in *Lufengosaurus* (Young 1941), the Ellingen material (Moser 2003) and *Riojasaurus* (Bonaparte 1971). The iliac blade of *Tuebingosaurus* is very high, approximately two-thirds of the iliac height, a condition shared with *Meroktenos*.

The acetabulum is fully open like in most sauropodomorphs, except for *Pantydraco* (Galton and Kermack, 2010), *Eoraptor* Sereno et al., 1993 and *Buriolestes* Cabreira et al., 2016. The acetabular region is dorsoventrally high with a pronounced medial wall, similar to the morphology described for *Anchisaurus* Marsh, 1885 (Galton and Cluver 1976), and *Yunnanosaurus youngi* Lü et al., 2007.

The pubic peduncle is prominent and projects anteriorly to the anterior tip of the pre-acetabular process (Fig. 6). The transverse cross-section through the pubic peduncle is laterally expanded and medially narrow, giving it a D-shape in distal view. The lateral margin is expanded into a supraacetabular ridge extending well above the acetabulum, similar to *P. trossingensis* (GPIT-PV-30784). The pubic peduncle is distally expanded lateral view when compared to its base.

The ischial peduncle is prominent and anteroposteriorly wide, and the articular surface extends posteriorly, forming a 'heel' (Fig. 6), and this character is present in the Ellingen material (Moser 2003), *Riojasaurus* (Heerden 1979) and *Melanorosaurus* (Galton et al. 2005). However, the ischial heel in *P. trossingensis* (GPIT-PV-30785) and BSP 1962 (Moser 2003) is more acute than in *Tuebingosaurus*. In addition, the ischial peduncle

Table 6. Measurements (in mm) of both ilia of *Tuebingosaurus maierfritzorum*. Left ilium was tectonically deformed (δ).

Measurements	Left (mm)	Right (mm)
Total length (between tips of the preacetabular and postacetabular processes)	438	428.5
Total length (between distal tips of the ischiadic and pubic peduncles)	314.8	269.5
Main body height dorsal to supraacetabular flange	164.4	176
Preacetabular process length	76.1	83.5
Postacetabular process length	171.3	142.6
Pubic peduncle length	177.4	154.4
Pubic peduncle, transverse width	84.3	83.8
Pubic peduncle distal end, anteroposterior length	59.4	67.6
Ischiadic peduncle length	71.6	86.9
Ischiadic peduncle, transverse width	65.4	65
Maximum acetabulum length (between peduncles)	214.5 δ	170.3 δ

is positioned at the mid-length of the ilium, producing an elongated postacetabular process.

The postacetabular process comprises about 48% of the ilium length and is widened transversely towards the posterior-most corner of the postacetabular process, in contrast to the narrow dorsal margin like in *Ruehleia* (pers. obs.) and *Lufengosaurus* (pers. obs.). The ventral margin of the postacetabular process is ventrally deflected at the most posterodorsal corner and does not meet the posterodorsal margin of the postacetabular process (Fig. 6). The lateral profile of the postacetabular process is square-ended with rounded margins, as also occurs in more derived sauropodomorphs and contrasts with the acute lateral outline seen in other early-diverging sauropodomorphs such as *Ruehleia* (pers. obs.) and *Jingshanosaurus*. The base of the postacetabular process and the base of the ischial peduncle are connected by a strongly developed brevis fossa with an M-shaped posterior margin (Fig. 6). The brevis shelf is lost in sauropods but present in most dinosaurs as a plesiomorphic state (Gaton and Kermack, 2010). The postacetabular process of the ilium is 1.08 times longer than the distance between the ischiadic and the pubic peduncle (Table 6).

3.1.4. **Pubis** (Fig. 10, Table 7)

Both pubes are preserved, although the left pubis has the obturator plate medially broken and is deformed in the proximal end (Fig. 10). As in most early-diverging sauropodomorphs, the pubis is long and slender, whereas sauropods have broad pubes (Galton and Upchurch 2004). The proximal end is slightly twisted and laterally expanded in the anterior view, followed by a plate-like shaft that continues towards the distal end (Fig. 10). The overall morphology is similar to that of *Plateosaurus* (SMNS 13200) and *Antetonitrus* (BP/1/4952), but in the medial view, the proximal end is anterodorsally expanded, as the condition in the Ellingen material (BSP 1962, in Pl. 30, Moser 2003). The iliac peduncle is not laterally expanded, giving the pubis straight medial and lateral margins in the anterior view, unlike the more derived condition in *Antetonitrus* and *Vulcanodon* Raath, 1972, that have a waisted outline, and the 'intermediate' slightly concave condition in *Lufengosaurus* and *Massospondylus carinatus*.

In *P. trossingensis* (SMNS 13200), the ischiadic articular surface is separated by an ample nonarticular surface from the iliac articular surface (Moser 2003). In contrast, in *Tuebingosaurus*, the ischiadic articular surface is separated from the iliac articular surface by a deep borrow, giving the distinctive sauropodomorph morphology of inflexion in the proximal anterior pubic profile. This borrow is present on both pubes, although the iliac articular surface in the left pubes is broken off (Fig. 10). The obturator foramen is relatively large and fully visible in lateral view, unlike in *Antetonitrus*, where the iliac peduncle obscures the obturator foramen. The iliac pedicel of the pubis partially occludes the obturator foramen in anterior view, a character shared with *Saturnalia* Langer et al., 1999, and *Guaibasaurus* Bonaparte et al., 1999. The pubic plate is approximately one-quarter of the total pubic length, measured from the proximal articular surface of the iliac peduncle to the distal surface of the pubic apron, a condition also observed in the Ellingen material (BSP 1962, Pl. 30, Moser 2003), *Adeopapposaurus*, *Lufengosaurus* (pers. obs.), *Antetonitrus* and *Meroktenos*. In *Lessemsaurus* and *Vulcanodon*, the pubic plate is closer to a third of the pubic length and is almost half the length in eusauropods, e.g., *Giraffatitan brancai* (Janensch, 1914) (MB.R.2180). As in *Coloradisaurus* and *Plateosaurus*, the distal end of the pubic apron is markedly anteroposteriorly expanded, and unlike *Antetonitrus*, *Riojasaurus* and *Meroktenos*. There is a pubic tubercle present on the left pubis, very prominently and directly ventral to the obturator foramen, but the same area on the right pubis is damaged. This pubic tubercle is present in *Efraasia*, *Plateosaurus* and *Plateosauravus* (Yates 2003b, 2007).

The conjoined width of the pubes represents 38% of the total length of the pubis (Table 7), unlike in more derived sauropodomorphs where the conjoined width of the pubes is larger than 75% of the pubic length. In addition, the minimum transverse width of the apron is 28% larger than the distance between the pubic and ischiadic peduncle of the ilium; a condition shared with most early-diverging sauropodomorphs and like more derived sauropodomorphs, where the width of the pubic apron is smaller than 40% of the distance between the iliac peduncles (Table 7).

Table 7. Measurements (in mm) of both pubes of *Tuebingosaurus maierfritzorum*. Left pubis is tectonically deformed. The * indicates minimum length due to breakage. The δ indicates deformation.

Measurements	Left (mm)	Right (mm)
Total length (iliac articulation to distal end)	560.0	560.0
Proximal end, maximum width	230.0	160.0
Obturator foramen, maximum diameter (anterposterior)	85.1	69.9 δ
Obturator foramen, minimum diameter (mediolateral)	50.3	61.9 δ
Shaft, minimum width	14.9	8.7
Shaft, distal width	46.6	52.4
Shaft, anteroposterior length distal end	43.6*	54.8

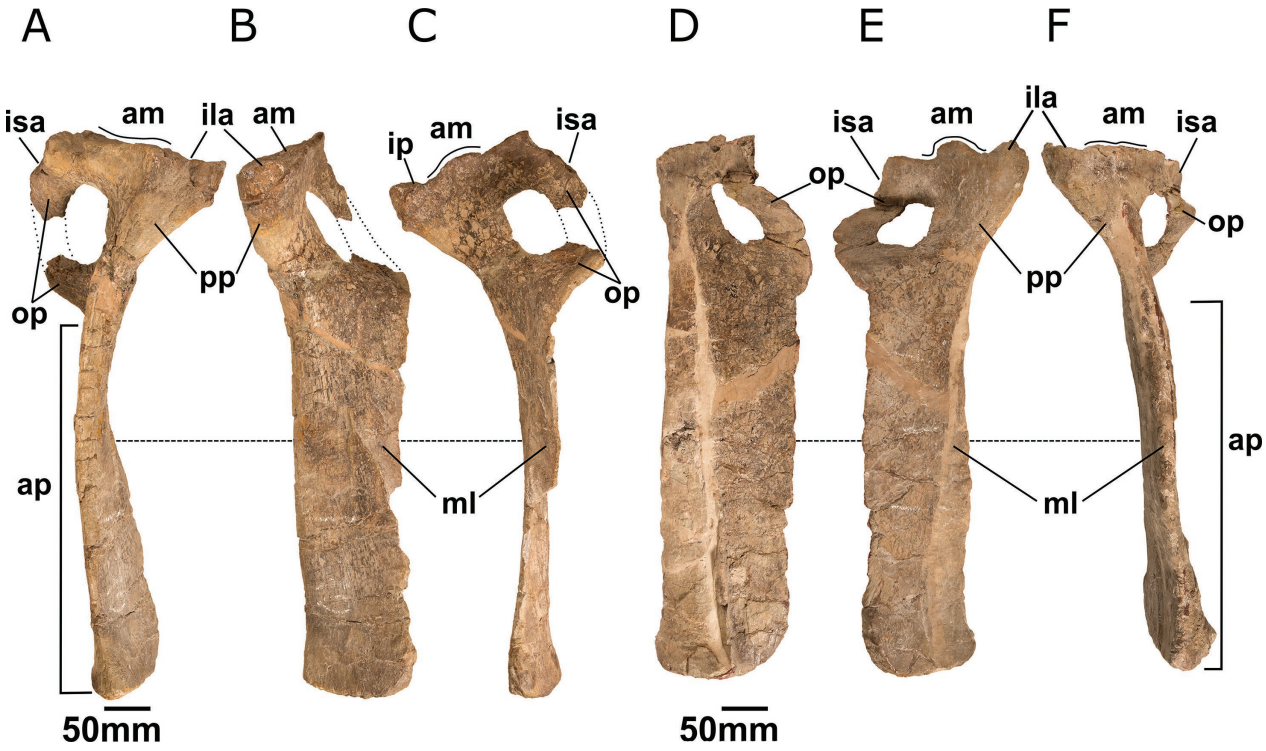

Figure 10. Pubes of *Tuebingosaurus maierfritzorum* (GPIT-PV-30787). **A**–**C** Right pubis in (A) lateral, (B) anterior, (C) medial views. **D**–**F** Left pubis in (D) posterior, (E) anterior, (F) lateral views. Abbreviations: am, acetabular margin; ap, pubic apron; ila, iliac articular surface; ip, ischiadic peduncle; isa, ischiadic articular surface; ml, median lamina; op, obturator plate; pp, proximal plate. Scale bar: 50 mm.

3.1.5. **Ischium** (Fig. 11, Table 8)

Both ischia in *Tuebingosaurus* are preserved and fused along the midline (Fig. 11). As in many early-diverging sauropodomorphs, the ischia are almost rod-like and subtriangular structures where the ischiadic plate is the thinnest region and occupies the proximal third of the bone. As in *Colorodisaurus*, *Plateosaurus* and *Lufengosaurus*, the proximal plate is medially concave and laterally convex, but unlike *Coloradisaurus* and *Plateosaurus*, the distal end is not as dorsoventrally expanded and lacks their sub-ovoid morphology. The cortical end on the distal end is not preserved, and only the general morphology can be discerned, and it is not possible to know if there was a posteriorly directed heel as seen in SMNS 13200. *Tuebingosaurus* has a more strongly dorsoventrally expanded axis than the mediolateral axis, a condition shared with *Lufengosaurus*.

The pubic process is widest transversely at the acetabular margin and tapers ventrally, giving it a V-shaped outline (Fig. 11). The mediolateral expansion corresponds to a medial projection that makes the internal border of the acetabular foramen. The ventral margin is expanded in the proximal part of the ischium forming an obturator plate but drastically decreases where the ischiadic shaft starts, with a notch separating the posteroventral end of the ischial obturator plate and the ischial shaft, which then retains a constant dorsoventral width up to the distalmost third where the distal expansion starts (Yates and Kitching, 2003) (Fig. 11). The iliac peduncle has a distinctive morphology, as posterior to the iliac articular surface, there is a concavity followed by a posteriorly oriented projection, which is not seen in the original illustration (von Huene 1932) nor other sauropodomorphs. Along the proximal part of the ischium is a well-developed and deep longitudinal dorsolateral sulcus, a common condition in

Table 8. Measurements (in mm) of both ischia of *Tuebingosaurus maierfritzorum*. Left pubis is tectonically deformed. The "—" indicates that the element does not have the landmarks to measure it.

Measurements	Left (mm)	Right (mm)
Total length (from the distal end to the point where the acetabular margin meets the pubic articulation)	490	485
Length of the pubic articulation	94.1	108.7
Transverse width of the pubic articulation at its dorsal end	61.6	73.3
Width of the proximal end (from iliac articulation to the ventral end of the pubic articulation)	24.0	23.5
Minimum dorsoventral width of the distal shaft (at approximately mid-length of the shaft).	22.8	23.1
Dorsoventral width of the distal end	—	87.8
Maximum transverse width of the distal end	—	94.6
Transverse width of iliac articulation	96.7	104.0

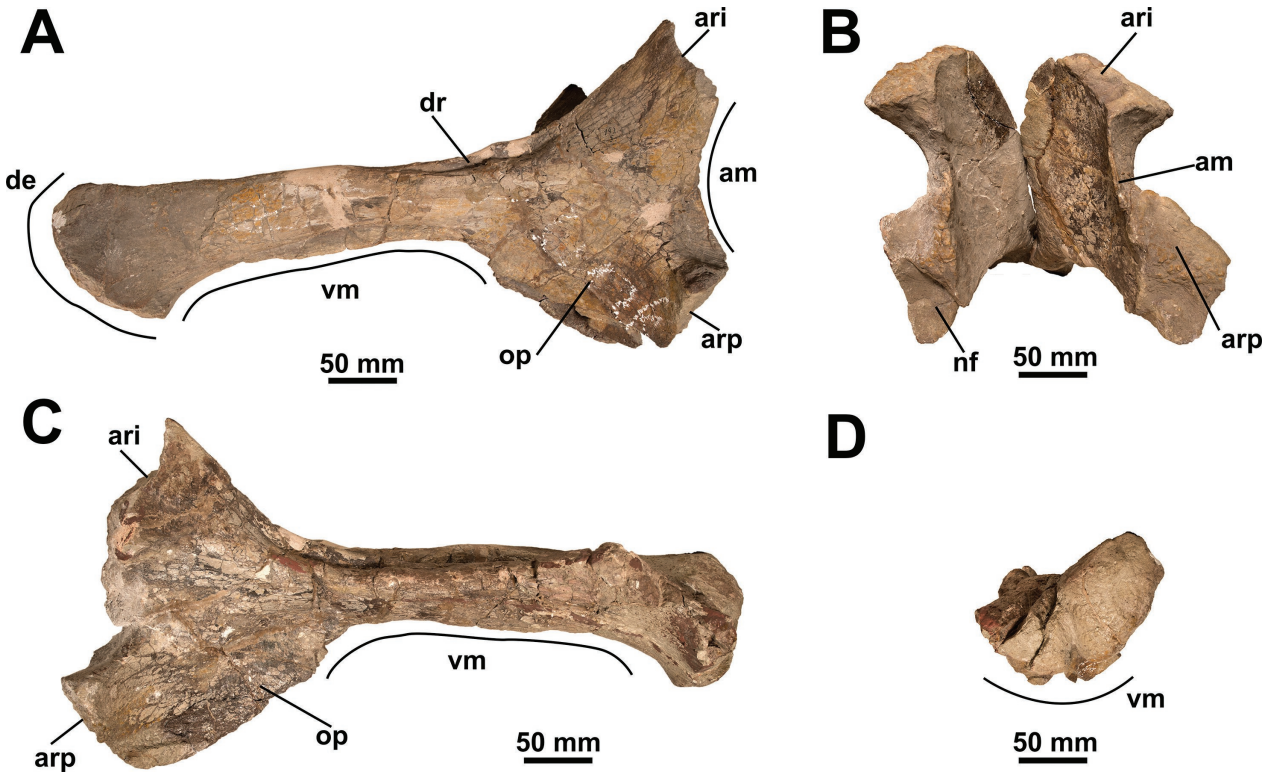

Figure 11. Conjoined ischia of *Tuebingosaurus maierfritzorum* (GPIT-PV-30787). **A** right lateral view; **B** proximal view; **C** left lateral view; **D** distal view. Abbreviations: am, acetabular margin; ari, articular surface for the ilium; arp, articular surface for the pubis; de, distal expansion; dr, dorsal ridge; nf, non-articular fossa; op, obturator plate; vm, ventral margin.

sauropodomorphs (Fig. 11). In *Tuebingosaurus*, the ventral margins of the pubic process meet up to a third of the length of the ischiadic shaft, unlike in *P. trossingensis* (GPIT-PV-30784 and GPIT-PV-30785, as illustrated in Yates 2003a), and *Lufengosaurus*, where the margins met by the beginning of the ischium.

In *Tuebingosaurus*, the distal end of the ischiadic shaft ends in a distal expansion (Fig. 11). In the distal view, the medial margin that meets the antimere is higher than the lateral margin. Only the left ischium has the distal surface of the distal expansion preserved, showing a subquadrangular outline (Fig. 11). In *Plateosaurus* (SMNS 13200), the distal expansion has a more subtriangular outline, where the medial expansion is four times larger than the lateral margin, and the lateral margin ends more in a point. In *Tuebingosaurus*, the anteroposterior length of the medial margin is slightly shorter than the lateromedial length of the distal surface.

In contrast, in *Plateosaurus* (SMNS 13200), the anteroposterior length of the medial margin is almost three times as big as the lateromedial length, giving the distal expansion in *Plateosaurus* a more gracile shape. The morphology of the distal expansion is similar, then, to *Lufengosaurus* (pers. obs.) and *Mussaurus* (Otero and Pol 2013). However, in the lateral view, the distal expansion has a small anterior projection, that in *Plateosaurus* (SMNS 13200) has more of a heel-like morphology, in *Tuebingosaurus* is more triangular; this triangular expan-

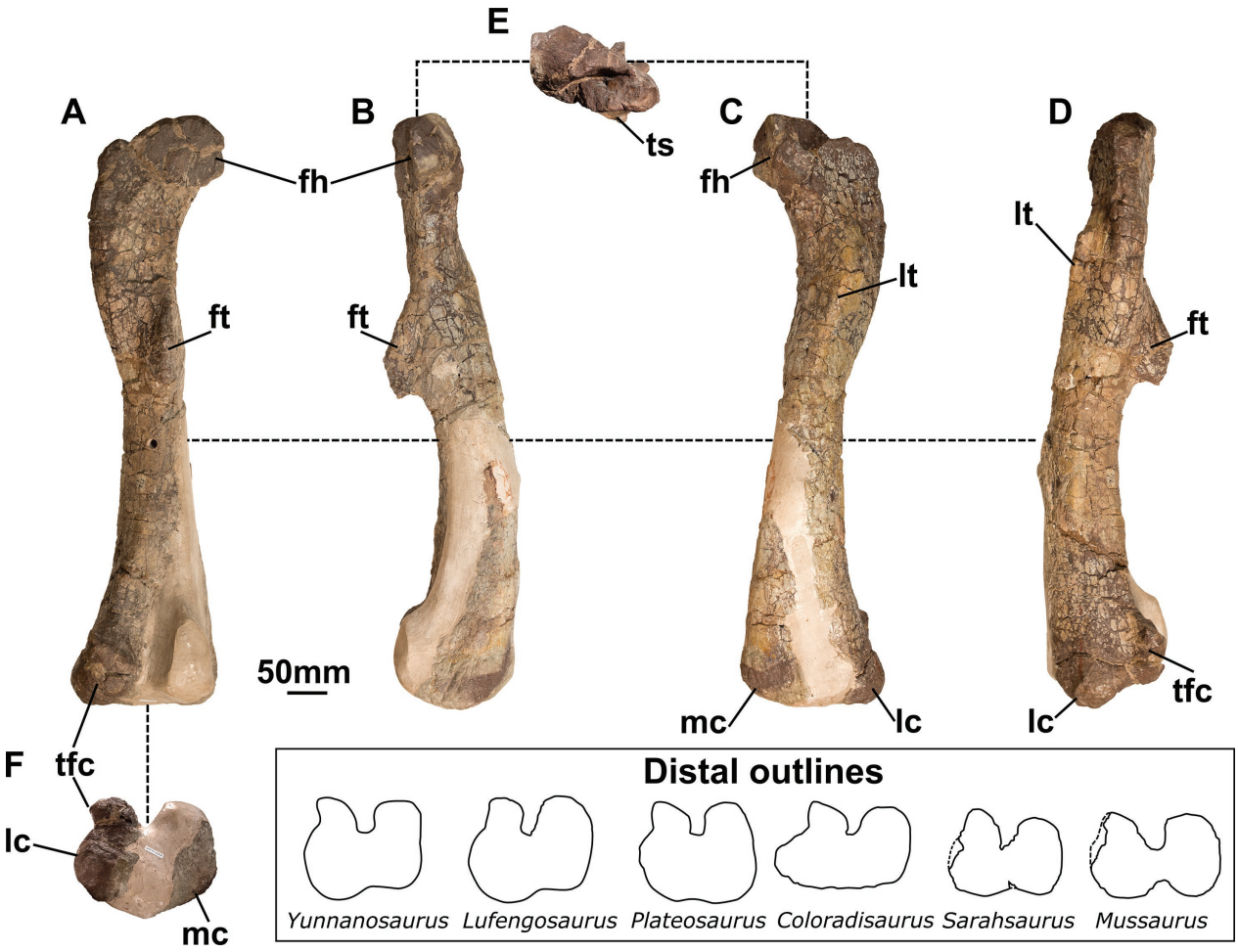

Figure 12. Left femur of *Tuebingosaurus maierfritzorum* (GPIT-PV-30787) in (**A**) posterior, (**B**) medial, (**C**) anterior, (**D**) lateral, (**E**) proximal, (**F**) distal views. The medial condyle is separated from the rest of the bone by plaster, and the shape of the medial condyle is reconstructed as a square, following a typical morphology in early diverging sauropodomorphs. The panel below shows the distal outlines in other non-sauropod sauropodomorphs: *Yunnanosaurus huangi* (IVPP V20), *Lufengosaurus* (IVPP V15), *Plateosaurus* (SMNS 13200), *Coloradisaurus* (PVL 5904), *Sarahsaurus* (TMM 43646–2), *Mussaurus* (MLP 68-II-27-1 specimen A). Abbreviations: fh, femoral head; ft, fourth trochanter; lc, lateral condyle; lt, lesser (= anterior) trochanter; mc, medial condyle; tfc, tibiofibular crest; ts, trochanteric shelf.

sion is unlike *Mussaurus* (Otero and Pol 2013) and *Lufengosaurus* (pers. obs.), where is a continuous expansion that starts from the midshaft.

3.1.6. **Femur** (Fig. 12, Table 9, 10)

In *Tuebingosaurus*, only the left femur is partially preserved, missing most of the medial condyle, and the medial condyle is reconstructed in the distal end with plaster (Fig. 12). The femur has the general morphology seen in early sauropodomorphs, straight in an anterior view and curved in a lateral view (Galton and Upchurch 2004, Fig. 12). In the earliest forms, like *Buriolestes* (Müller et al. 2018), the femur is curved in the anterior and lateral view, whereas in more derived forms, like in *Barapasaurus* Jain et al., 1975 (Bandyopadhyay et al. 2010), it is straight in both views. In specimen SMNS 13200, the femoral head is slightly visible in lateral view, not fully medially inturned, whereas, in *Tuebingosaurus*, the femoral head is completely inturned and hidden in lateral view.

The femoral head is broken on its anterior half, missing the anteromedial and anterolateral features. The sulcus for the ligamentum capitis femoralis is flat, compared to the marked concavity in *Buriolestes* (Müller et al. 2018), followed by a markedly concave but narrow facies articularis antitrochanterica. No proximal groove is on the proximal surface, like the one seen in *Buriolestes* (Müller et al. 2018).

The lesser trochanter is prominent, a feature shared with specimen SMNS 13200 (Moser 2003), but unlike in SMNS 13200, the dorsolateral trochanter (= trochanter major) is only a small bump, whereas in SMNS 13200 is a more developed protuberance. In the fourth trochanter in SMNS 13200, the dorsal margin and the ventral are parallel and similarly slope dorsoventrally (Moser 2003). The femur in *Tuebingosaurus* has the fourth trochanter with a dorsal margin running dorsoventrally and a ventral margin running more horizontally, giving the fourth trochanter a somewhat trapezoid shape (Fig. 12), quite similar to the morphology seen in *Riojasaurus* (Bonaparte 1972). In *Coloradisaurus*, the dorsal margin

Table 9. Measurements (in mm) of the left femur of *Tuebingosaurus maierfritzorum*. Eccentricity index is expressed as a ratio of mediolateral width at midshaft/anteroposterior width at midshaft. The robustness index is expressed as a total length/circumference ratio under the fourth trochanter.

Measurements in *Tuebingosaurus maierfritzorum*	**Length (mm)**
Total femoral length	755.0
Mediolateral width of the femoral head	75.5
Anteroposterior width of the femoral head	—
Midshaft mediolateral width	91.7
Midshaft anteroposterior width	82.2
Distal mediolateral width	90.5
Distal anteroposterior width	153.3 with condyle
	111.2 without condyle
Circumference under the fourth trochanter	306.0
Distal expansion of the fourth trochanter	127
Eccentricity index	1.15
Robustness index	2.46

Table 10. Comparative femoral measurements of massopodans. The specimens are ordered according to the femoral length (a). a. Total femoral length, b. Mediolateral width of the femoral head, c. Anteroposterior width of the femoral head, d. Midshaft mediolateral width, e. Midshaft anteroposterior width, f. Distal mediolateral width, g. Distal anteroposterior width, h. Circumference under the fourth trochanter, i. Distal expansion of fourth trochanter, j. Eccentricity index, k. Robustness index. Eccentricity index is expressed as a ratio of mediolateral width at midshaft/anteroposterior width at midshaft. The robustness index is expressed as a ratio of total length/circumference under the fourth trochanter. Data was taken from Peyre de Fabreguès and Allain (2016) and first-hand assessments.

Specimens	**a.**	**b.**	**c.**	**d.**	**e.**	**f.**	**g.**	**h.**	**i.**	**j.**	**k.**
Massospondylus (SAM-PK-402)	247	72	30	32	27	—	—	96	125	1.18	2.57
Massospondylus (SAM-PK-393)	390	87	51	43	51	98	70	141	183	0.84	2.77
Meroktenos (MNHN.F.LES16c)	480	153	57	82	52	136	78	230	280	1.58	2.09
Coloradisaurus (PVL 5904)	508	118	74	65	62	147	112	—	—	—	—
Gryponyx (SAM-PK-7919)	535	—	44	67	68	107	121	205	290	0.99	2.61
Melanorosaurus (NM QR1551)	623	139	80	93	66	183	88	266	305	1.41	2.34
Melanorosaurus (SAM-PK-3450)	624	173	69	103	77	172	110	273	350	1.34	2.29
Aardonyx (BP/1/6510)	682	188	—	91	90	169	110	284	380	0.96	2.4
Mussaurus (MLP 68-II-27-1)	700	169*	73	96	77	169	110	—	—	1.2	—
Tuebingosaurus (GPIT-PV-30787)	755	75.5	—	92	82	91	111	306	127	1.15	2.46
Lessemsaurus (PVL 4822/65)	772	211	107	—	106	243	—	—	—	1.5	—
Antetonitrus (BP/1/4952)	775	208	114	142	94	270*	150	410	450	1.51	1.89
Plateosaurus (GPIT-PV-30784)	580	125	72	66	60	121	107	198	60	1.1	2.92
Plateosaurus (GPIT-PV-30785)	580	149	74	74	69	146	98	224	90	1.07	2.59

runs dorsoventrally but not so steeply, whereas the ventral margin runs ventrodorsally with a more pronounced slope, giving the fourth trochanter a distinctive trapezoidal shape in an inverted orientation compared to *Riojasaurus* (Apaldetti et al. 2013). In *Buriolestes* (Müller et al. 2018) and *Anchisaurus* (Galton 1976), the fourth trochanter has a trapezoidal shape, with the dorsal margin running dorsoventrally and the ventral margin running ventrodorsally, both with similar slopes, giving the fourth trochanter a regular trapezoid shape. In *Mussaurus* (Otero and Pol 2013), the dorsal and ventral margins run somewhat parallel, close to the horizontal, but have markedly curved edges. In *Buriolestes* (Müller et al. 2018), the fourth trochanter is closer to the medial margin along the mediolateral axis. In the medial view, the medial surface expands continuously onto the fourth trochanter; in the lateral view, there is an inflexion separating the lateral surface from the fourth trochanter. This same condition is observed in SMNS 13200, where the medial surface is continuously expanded onto the fourth trochanter plate in anteromedial view but separated from the lateral surface by an inflexion. The fourth trochanter in *Tuebingosaurus* has the same morphology, and this condition can be found in other early sauropodomorphs, e.g., *Riojasaurus* (Bonaparte 1972), *Anchisaurus* (Galton 1976), and *Coloradisaurus* (Apaldetti et al., 2014). In *Mussaurus* (Otero and Pol 2013), the fourth trochanter is closer to the lateral side, and the lateral surface continuously expands onto the fourth trochanter, whereas a marked inflexion separates the posterior surface from the fourth trochanter.

In the distal view, the median portion of the femur is reconstructed by plaster, but the outline seems more

ovoid (Fig. 12). For instance, in SMNS 13200 and *Coloradisaurus*, the mediolateral axis is considerably longer than the anteroposterior one, giving the distal surface a more flattened elliptical shape. In *Mussaurus*, the distal end is hourglass-shaped, with a marked popliteal fossa posterior and a deep extensor depression anteriorly. Due to the plaster, it is impossible to know which of these two morphotypes is present in the femur. An extensor depression is present in most sauropodomorphs, except for the earliest forms, such as *Buriolestes*, *Saturnalia*, *Pantydraco* and *Efraasia* (SMNS 12216, pers. obs.). The plaster in the specimen does not outline an extensor depression, imitating the plesiomorphic condition. In *Buriolestes* (Müller et al. 2018), the medial condyle and the anterolateral tuber are similar, with a very lateromedially reduced lateral condyle. In *Coloradisaurus*, the medial condyle is the most prominent of the three condyles, and the tibiofibular condyle has a triangular outline, unlike the quadrangular one seen in earlier forms. The lateral condyle is laterally projected and separated from the tibiofibular condyle by a significant inflexion. The condylar morphology of *Coloradisaurus* is also seen in SMNS 13200 and *Anchisaurus* (Galton 1976). Despite the plaster, the medial condyle is larger in the lateromedial axis than the tibiofibular condyle. The lateral condyle is laterally projected and separated from the tibiofibular condyle by an inflexion, although not as marked as in *Coloradisaurus*. The morphology in *Mussaurus* is unclear, as this portion is broken off (Otero and Pol 2013). Furthermore, a Ward clustering of the measurements in sauropodomorph femora in Table 10, showing *Tuebingosaurus* is placed in a cluster with *Mussaurus* and *Lessemsaurus* (Appendix 3, Figure A1).

3.1.7. **Tibia** (Fig. 13, Table 11)

The tibia is approximately 0.85 times the length of the femur (Tables 9 and 11), a proportion similar to all non-eusauropod sauropodomorphs (Apaldetti et al. 2013). The anteroposterior axis of the proximal end is horizontal in lateral view as in *Mussaurus* and *Anchisaurus*, whereas the anteroposterior axis in specimen SMNS 13200 and *Coloradisaurus* is dorsoventrally skewed. In the proximal view, the proximal end of the tibia has a scalene shape, with the medial condyle posteriorly expanded relative to the medial condyle and the cnemial crest facing laterally (Fig. 13). In specimen SMNS 13200, the medial and lateral condyles are roughly aligned, and the cnemial crest is more anteriorly oriented. In *Coloradisaurus*, the medial and lateral condyles are roughly aligned, but the cnemial crest is laterally oriented, whereas, in *Mussaurus*, the proximal outline is similar to that of specimen *Tuebingosaurus*. In earlier forms, such as in *Buriolestes*, the cnemial crest is laterally oriented, forming a 90 degrees angle with the anteroposterior axis of the proximal end of the tibia. In *Tuebingosaurus*, the fibular articular surface has a large protuberance, similar to the outline in SMNS 13200, although this protuberance is less pronounced. In *Mussaurus* and *Coloradisaurus*, this protuberance is more like a small tuber (Fig. 13).

The shaft of the tibia is straight with a sub-elliptical cross-section. The distal end has a quadrangular outline, with two lateral processes, the anterolateral and posterolateral processes, and a posteromedial and an anterolateral condyle (Fig. 13). The anterolateral process is twice as wide as the posterolateral process. In *Tuebingosaurus*, the medial surface has an additional projection not seen in other sauropodomorphs. In *Coloradisaurus*, the anteromedial process is medially expanded relative to the posteromedial condyle, a feature seen in *Adeopapposaurus*, *Mussaurus* and SMNS 13200. The distal end is lateromedially elongated, and in the posterior view, the posterolateral process (= posteroventral process, = caudoventral process) is distally expanded relative to the anterolateral process and reaches the lateral margin of the distal tibia, a condition shared with SMNS 13200, *Riojasaurus, Adeopapposaurus* and *Coloradisaurus*, but unlike *Mussaurus*, *Anchisaurus* and *Aardonyx* Yates et al., 2010, and other advanced sauropodomorphs, where the posterolateral process does not reach the lateral margin. As in most early sauropodomorphs, the posterolateral process distally exceeds the limits of the anterolateral process. The distal surface of the posterolateral process is horizontally oriented, whereas the distal surface of the anterolateral process is distolaterally oblique for the articulation of the ascending process of the astragalus.

Tuebingosaurus sits between the morphospaces outlined for Massospondylidae and "Melanorosauridae" in a bivariate plot of the ratios between the total length and anteroposterior depth of the proximal end of the tibia (L/Pw) concerning the ratio between the total length and anteroposterior depth at mid-length of the tibia (L/Mw) (Fig. 14). Noteworthy, *Plateosaurus* has a large morphospace, compared to the other sauropodomorphs in the sample. First, this could represent that the morphospace of *Plateosaurus* captures better the intraspecific variability in the tibiae given the larger sample compared to other sauropodomorphs; however, the gradual increase in the robustness through time is quite clear. Furthermore, a restricted definition of *Plateosaurus* (SMNS 13200 and GPIT-PV-30785) occupies a similar space in the bivariate plot. Specimen BSP 1962 is, on the other hand, nested within "Melanorosauridae", close to *Tuebingosaurus* and *Mussaurus*, and supports the idea that the similarity between *Tuebingosaurus* and BSP 1962 outlined above in the pubis, ischia and the tibiae are better explained by considering BSP 1962 as a massopodan as well (Appendix 3 – Figure A2).

3.1.8. **Fibula** (Fig. 15, Table 12)

The two fibulae are preserved and have similar sizes. The fibula is a slender and long bone with an anteroposteriorly expanded proximal end and, to a lesser degree, the distal end (Fig. 15), similar to the condition in *Riojasaurus*, unlike in *Anchisaurus* and *Mussaurus*, where the distal end is not expanded. The proximal articular surface has a concave medial margin and a convex lateral margin, forming a crescent-shaped outline as in SMNS 13200, *Adeopapposaurus* and *Mussaurus*. However, in *Tuebingosaurus*, the

Table 11. Measurements (in mm) of the left tibia of *Tuebingosaurus maierfritzorum.*

Measurements	Length (mm)
Total length	640
Transverse width of the proximal end	130
Anteroposterior length of the proximal end	240
Transverse width of the shaft at midlength	82.2
Anteroposterior length of the shaft at midlength	59.3
Anteroposterior length of the distal end	87.9
Transverse width of the distal end	130.1

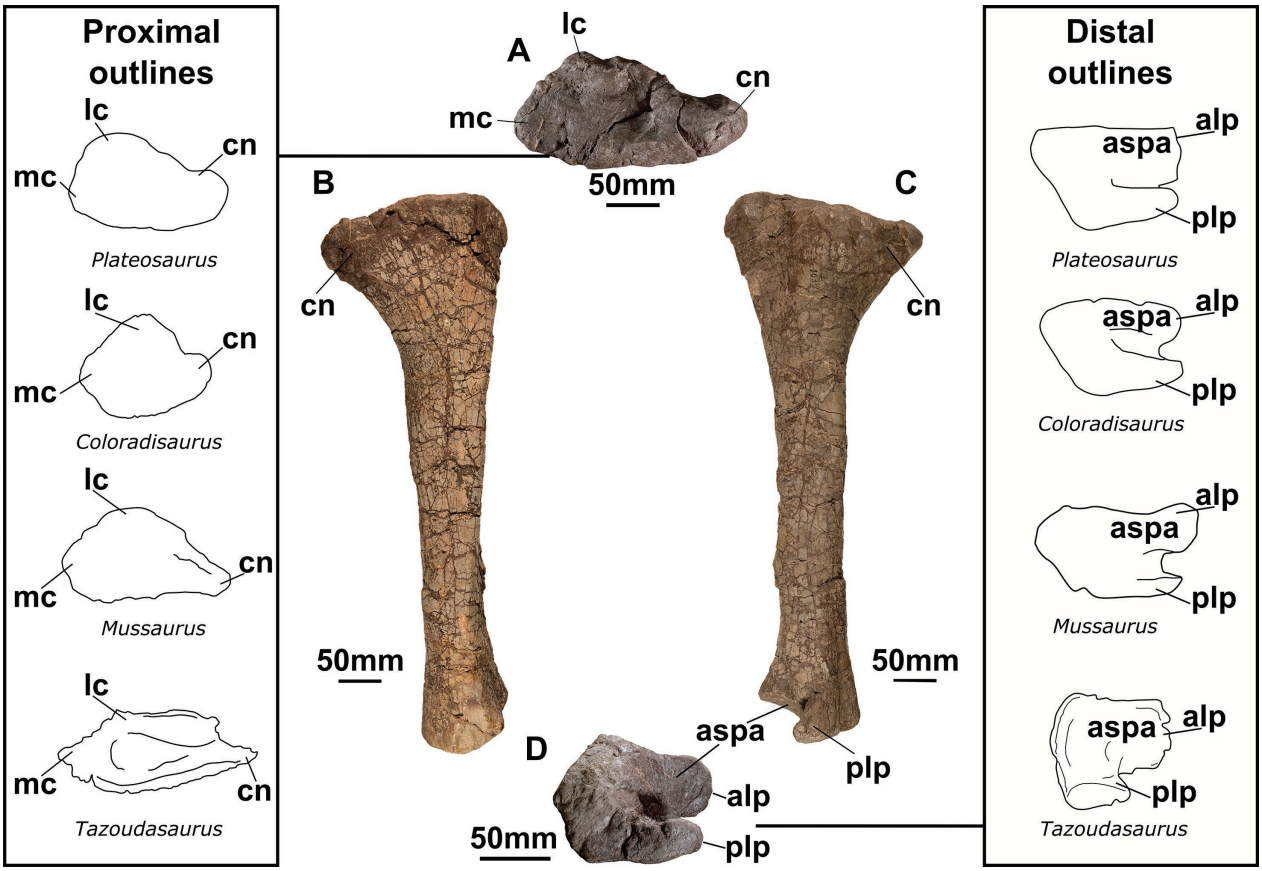

Figure 13. Left tibia of *Tuebingosaurus maierfritzorum* (GPIT-PV-30787) in the centre, and outlines in other sauropodomorphs for comparisons. The left tibia is shown in (**A**) proximal, (**B**) lateral, (**C**) medial and (**D**) distal views. The panels to the left and right show the proximal and distal outlines, respectively, of four sauropodomorphs: *Plateosaurus* (SMNS 13200), *Coloradisaurus* (PVL 5904), *Mussaurus* (MLP 68-II-27-1) and *Tazoudasaurus* (To1-380). The outlines are not set to scale. Abbreviations: alp, anterolateral process, aspa, articular surface for the ascending process, cn, cnemial crest, lc, lateral condyle, mc, medial condyle, plp, posterolateral process.

medial margin is concave only in the anterior portion and straight in the posterior one. The shaft is straight in lateral and anterior views, unlike in *Adeopapposaurus* and *Mussaurus*, where the fibula is curved in anterior view. The distal end in lateral view is anteriorly slanted but horizontal in posterior view, as in *Mussaurus* and *Adeopapposaurus*. There is a small protuberance on the anteromedial surface, a feature that has not been reported for sauropodomorphs and is present on both fibulae, discarding a noticeable pathological feature (mfp in Fig. 15). The medial condyle is larger than the lateral condyle, and a shallow triangular fossa is visible on the medial face of the distal end of the fibula. The lateral face of the fibula is, in turn, flat.

3.1.9. **Astragalus** (Fig. 16, Table 13)

The astragalus has the classic non-eusauropod sauropodomorph morphology, with a somewhat kidney-shaped outline (Fig. 16). In dorsal view, the medial margin is about 50% larger than the lateral margin; the lateral margin has a sigmoidal articulation, and the medial margin is posteriorly curved. The posterior margin is convex, as in *Mussaurus* (Otero and Pol 2013), *Blikanasaurus* Galton and van Heerden, 1985 (Galton and van Heerden 1998), *Vulcanodon* (Cooper 1984), and *Tazoudasaurus* Allain et al., 2004 (Allain and Aquesbi 2008); nevertheless, a con-

Table 12. Measurements (in mm) of both fibulae of *Tuebingosaurus maierfritzorum*

Measurements	Left (mm)	Right (mm)
Total length	584.0	590.0
Transverse width of the proximal end	145.3	129.5
Anteroposterior length of the proximal end	52.0	53.9
Transverse width of the shaft at midlength	51.0	49.9
Anteroposterior length of the shaft at midlength	29.6	30.6
Transverse length of the distal end	89.2	88.3
Transverse width of the distal end	47.6	47.5

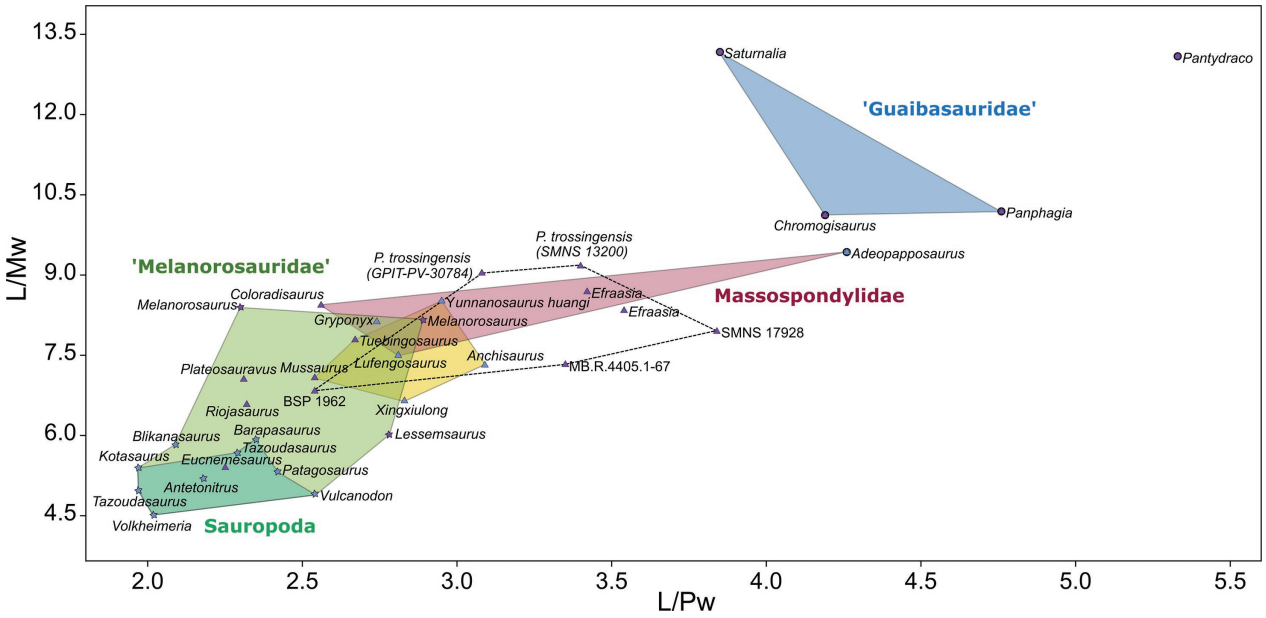

Figure 14. Bivariate plot showing the ratio between the total length and anteroposterior depth of the proximal end of the tibia (L/Pw) concerning the ratio between the total length and anteroposterior depth at mid-length of the tibia (L/Mw). Data was taken from Ezcurra and Apaldetti (2011) and first-hand assessments obtained by ORRF. The convex hulls with solid lines show the morphospace generated by the groups 'Guaibasauridae', Massospondylidae, 'Melanorosauridae' and Sauropoda. The name 'Melanorosauridae' is here used to refer to sauropodomorphs that are not traditionally considered as sauropods. The triangles represent taxa traditionally considered sauropods, and the stars represent non-sauropod sauropodomorphs. The colours of the points represent the age of the taxa, with purple for the Late Triassic and blue for the Early Jurassic. The dashed convex hull represents the morphospace corresponding to *Plateosaurus* as currently defined. The yellow convex hull represents the taxa placed in a polytomy before the diversification of Massospondylidae and Sauropodiformes.

vex posterior margin is also present in *P. trossingensis* (as illustrated in von Huene 1926).

The posterior margin is straight in *Unaysaurus* Leal et al., 2004 (McPhee et al. 2019) and *Macrocollum* Müller et al., 2018. The medial margin in *Unaysaurus*, *Macrocollum* and *Blikanasaurus* has a prominent triangular process anteromedially projected, similar to the outline in *Tuebingosaurus*. At the midlength of the posterior margin, there is a prominent bulge like that present in *Mussaurus*, and a bulge is present in *Blikanasaurus* and *P. trossingensis* but not as pronounced (Fig. 16). The anterior margin has its highest point on the medial side, whereas the posterior margin has its highest point on the lateral side. The proximal surface is divided into two distinct articular facets: a lateral facet, with a deep socket-like concavity for the articulation with the distal end of the fibula, and a flat medial facet occupying most of the proximal surface, where the distal end of the tibia articulates with the astragalus. These two facets are divided by a rounded ridge that continues to form the posterior margin of the ascending process. As in many other early sauropodomorphs, the ascending process is not as prominent, and in anterior view, the ascending process rises slightly above the posterior bulge. Towards the lateral end of the anterior margin, there is a deep depression similar to those in early saurischians, e.g., *Herrerasaurus* Reig, 1963, *Eoraptor* (Sereno et al., 2012), and *Saturnalia* Langer (2003), but faces anterolaterally rather than lateroventrally, and it is placed right beneath the anterior margin of the ascending process. This fossa occupies a prominent space of the anterior margin, and it is not a feature seen in other early sauropodomorphs. Ventral to this fossa, a ventrally directed projection with a heel-like morphology supports the calcaneum by a laterally oriented projection. The distal surface has the characteristic rugose roller-shaped articulation in other sauropodomorphs.

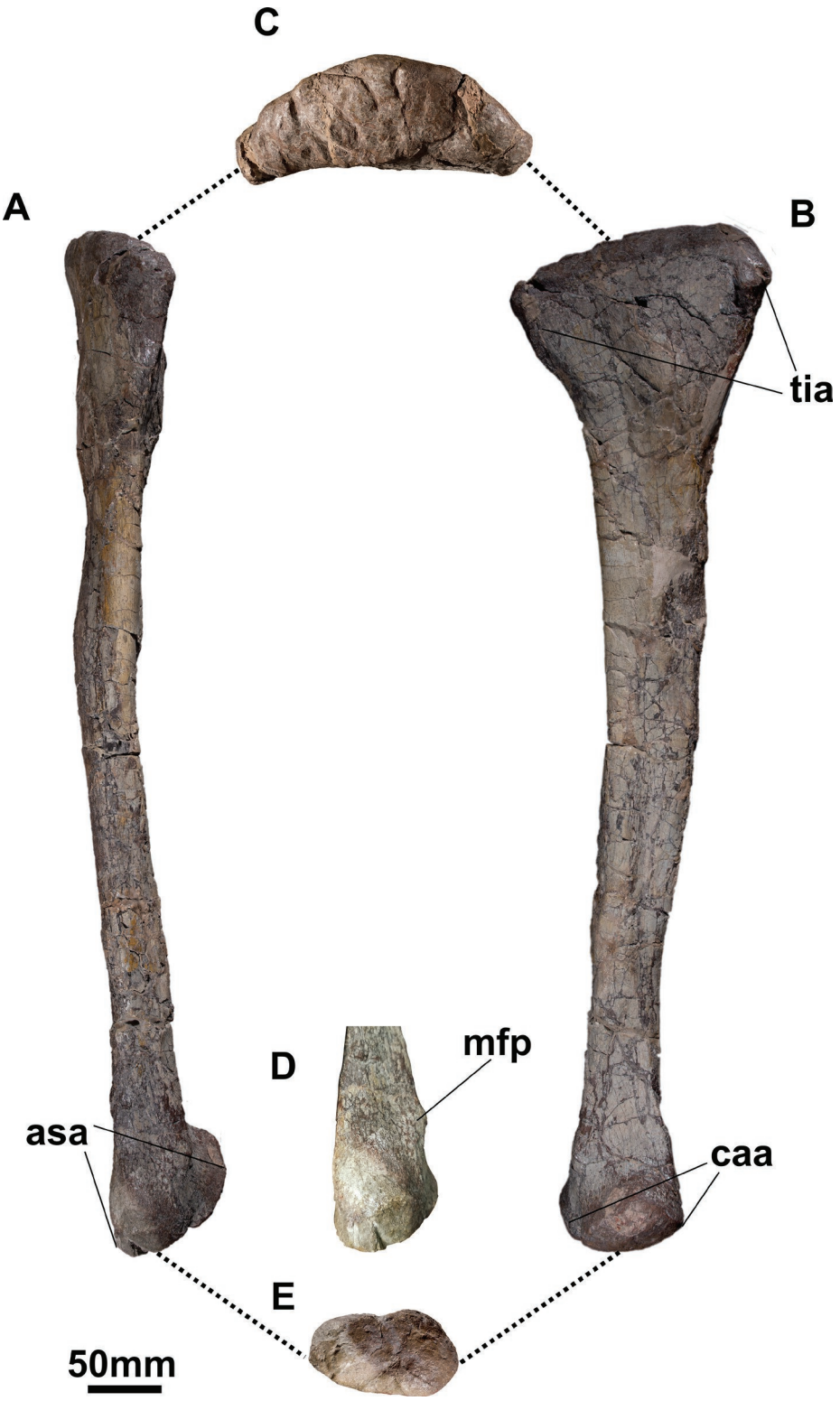

Figure 15. Left fibula of *Tuebingosaurus maierfritzorum* (GPIT-PV-30787) in (**A**) anterior, (**B**) medial, (**C**) proximal, (**D**) distal anteromedial view of the fibular, (**E**) distal views. Abbreviations: asa, astragalar articular surface, caa, calcaneum articular surface, mfp, anteromedial fibular process, tia, tibial articular surface.

3.1.10. Calcaneum (Fig. 16–A, D, Table 13)

The calcaneum in *Tuebingosaurus* is significantly reduced, albeit conserving the early-diverging sauropodomorph triradiate morphology. The calcaneum is lateromedially flattened, but the anterior end is thicker than the posterior end and lacriform in dorsal view. The anterior end is not straight but bears a distinct anterior projection in the anterolateral margin. The ventral process rests on the anterolateral projection of the lateral margin of the astragalus. The medial margin of the calcaneum is concave and articulates along the sigmoidal lateral margin of the astragalus. This articulation generates a pocket between the two elements that were probably filled with cartilage. The mediolateral length of the calcaneum represents 21% of the astragalar mediolateral length. In early sauropodomorphs, such as *Saturnalia*, the calcaneal length is roughly 50% of the astragalar length, and in *Coloradisaurus*, it is 40%, and towards the more derived sauropodomorphs, we have values lower than 30%, such

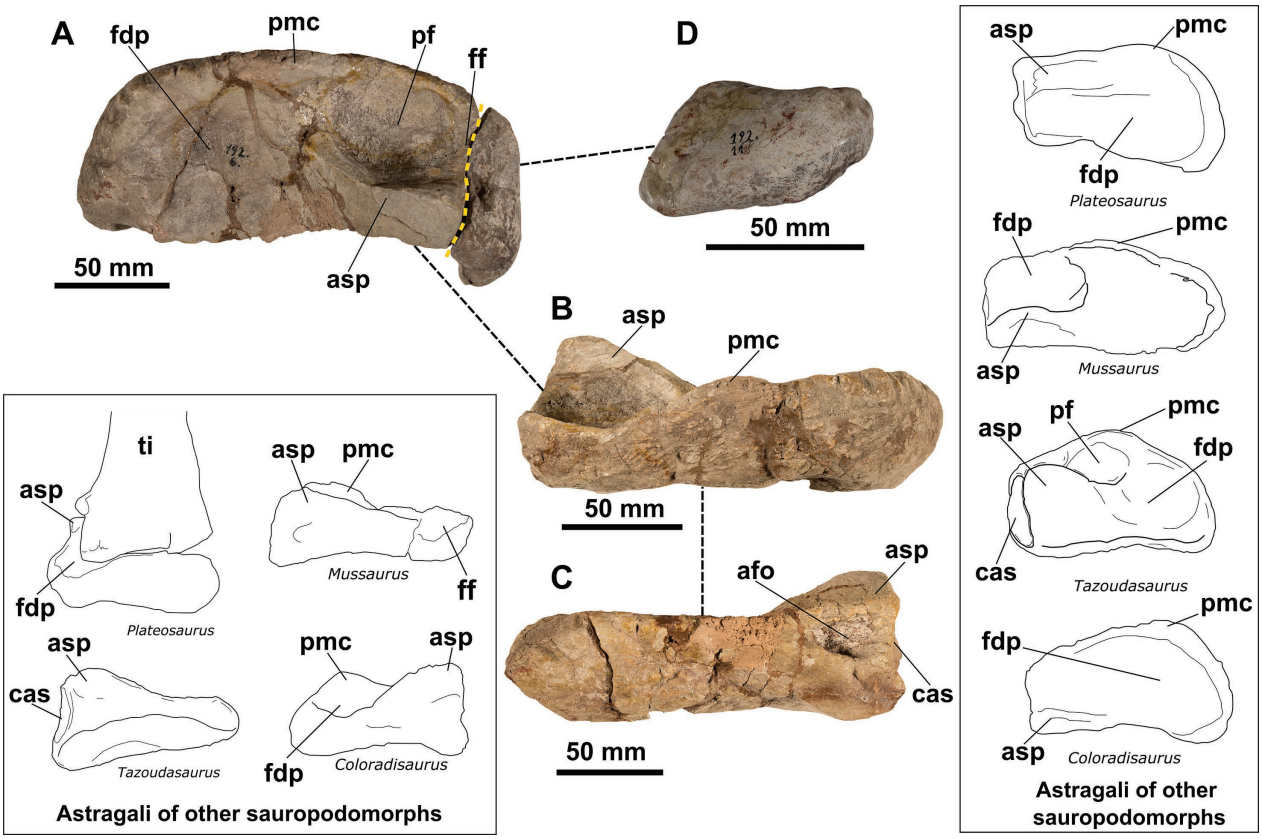

Figure 16. Astragalus of *Tuebingosaurus* in (**A**) dorsal, (**B**) posterior and (**C**) anterior views. Calcaneus in A) dorsal and D) lateral views. The panel to the bottom left shows the astragali in other sauropodomorphs: *Plateosaurus* (SMNS 13200, in posterior view and articulated with the tibia), *Mussaurus* (MLP 68-II-27-1 specimen A), *Tazoudasaurus* (To1-31, mirrored), *Coloradisaurus* (PVL 3967). The panel to the right shows the astragali in other sauropodomorphs in dorsal view: *Plateosaurus* (SMNS 13200), *Mussaurus* (MLP 68-II-27-1 specimen A, mirrored), *Tazoudasaurus* (To1-31, mirrored), *Coloradisaurus* (PVL 3967, mirrored). Abbreviations: asp, ascending process; afo, anterior foramen; cas, concavity of the posterior surface of the ascending process; fdp, facet for descending process of the tibia; ff, fibular facet; pf, posterior fossa; pmc, posteromedial corner. The yellow dotted line represents the astragalar-calcaneum articulation.

as in *Anchisaurus*, *Vulcanodon*, *Shunosaurus* Dong et al., 1983 and *Camarasaurus* Cope, 1877. This reduced calcaneum is consistent with what we expect in more obligated quadrupedal animals, such as sauropods.

3.1.11. Metatarsal IV (Fig. 17, Table 13)

According to the early drawings by von Huene (unpublished), an almost complete pes was recovered from the block as part of specimen "GPIT IV". The drawings show metatarsals I, II, III, and IV articulated to their respective phalanges. Currently, only metatarsal IV, the complete digits II and III, and one phalange of digit I are preserved in the collection (Fig. 17).

The only metatarsal element preserved is metatarsal IV. The metatarsal IV is a robust element with a constriction along the mid-section. Its proximal end is expanded lateromedially and flattened dorsoplantarly, whereas the distal end is expanded not as lateromedially but expanded dorsoplantarly, with a morphology similar to *Massispondylus carinatus* (BPI/I/4377) and *Mussaurus* (MLP 61-III-20-22) (Fig. 17). A well-developed crest on the proximal end extends proximodistally along the dorsal surface of the proximal end. This crest delimits a concave medial surface where metatarsal III articulates. The dorsoventral length at the crest level represents 30% of the lateromedial length of the proximal end of metatarsal IV, as in *Mussaurus* and *Massospondylus*, whereas this ratio reaches 50% in *Saturnalia*, *Coloradisaurus*, *Plateosaurus*, and *Blikanasaurus*.

The dorsal and plantar edges of the lateral half are parallel through the metatarsal length (Fig. 17), as in *Mussaurus*. The cross-section is ovoid, where the lateral margin is narrower than the medial one. The medial margin of metatarsal IV has a bulge close to the proximal end, a feature in *Massospondylus*, *Mussaurus* and *Plateosaurus*. In other early-branching sauropodomorphs, this bulge fits in a slight depression on the lateral margin of the shaft of metatarsal III. Distally, there is another bulge along the distal end of the shaft of metatarsal IV, a condition shared with *Mussaurus*.

The distal articular surface is quadrangular in distal view with an undivided and marked convexity, similar to *Riojasaurus* (PVL 3526). The lateral margin on the distal end has two processes that project laterally in distal view, whereas the medial margin has a marked expansion in the medio-plantar corner. On the lateral margin, the two projections are separated by a well-developed concavity; the medial margin is roughly straight.

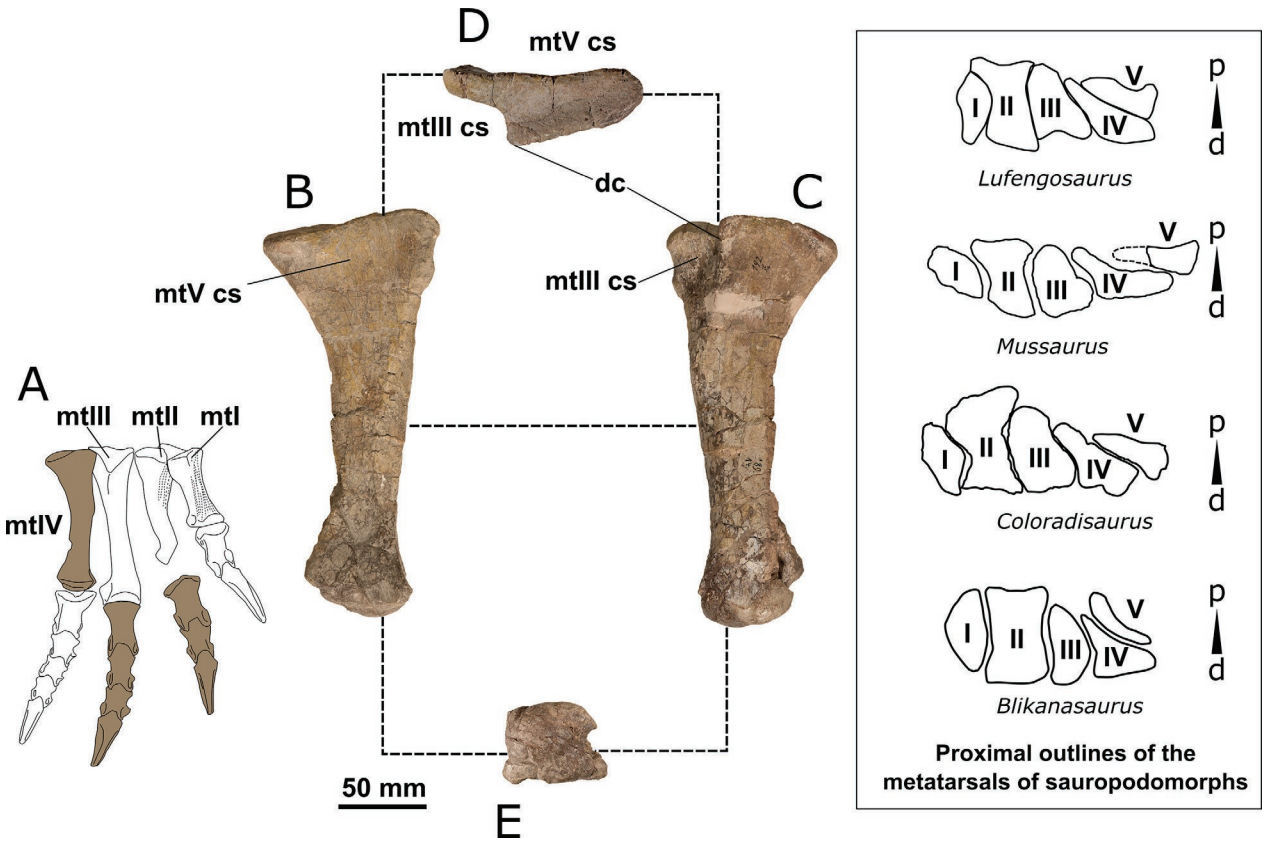

Figure 17. Pes of *Tuebingosaurus maierfritzorum* (GPIT-PV-30787). **A** Reconstruction of the pes of *Tuebingosaurus maierfritzorum* as illustrated by von Huene (Pl. 38, fig. 10). The elements coloured in brown correspond to the only material that has been located in the collection. Metatarsal IV in (**B**) plantar, (**C**) dorsal, (**D**) proximal, and (**E**) distal views. The panel to the right shows the proximal outlines of the metatarsals of four sauropodomorphs: *Lufengosaurus* (IVPP V15), *Mussaurus* (MLP 61-III-20-22, Otero and Pol 2013, mirrored), *Coloradisaurus* (PVL 5904, Apaldetti et al. 2013, mirrored), and *Blikanasaurus* (Galton and Van Heerden 1998). Abbreviations: d, dorsal; p, plantar; dc, dorsal crest; mtI (I), metatarsal I; mtII (II), metatarsal II; mtIII (III), metatarsal III; mt III cs, contact surface of metatarsal III; mtIV (and IV), metatarsal IV; mtV cs, metatarsal V contact surface; V, metatarsal V.

3.1.12. Pedal digits (Fig. 18, Table 13)

Only two digits are preserved, pedal digit II and pedal digit III, with two and three phalanges, respectively, and the first phalanx of digit I. Phalanx I.1 is identified due to the morphology, with a proximomedial projection (Fig. 18) like the morphology reported in *Plateosaurus* (von Huene 1926) but more developed. The proximal lateromedial width corresponds to 84% of the total proximodistal length of the phalange (Table 14). The proximal articular surface is concave, reniform and undivided with a concave dorsal edge and a convex ventral edge. The major axis of the proximal articular surface is twisted 5° to the lateromedial axis of the distal surface. The shaft has subparallel lateral and medial margins, with a flat dorsal surface and a deeply concave plantar surface. The distal margin has two well-developed condyles separated by an intercondylar groove. The dorsoplantar length of the lateral and medial condyles is roughly the same, but the medial collateral ligament pit is more deeply concave.

Pedal digit II has two non-terminal phalanges and a well-developed ungual. Phalanx II.1 is robust, where the proximal lateromedial length is 78% of the proximodistal length. In phalanx II.1, the distal lateromedial length is similar to the lateromedial length, with a distinctive shaft with concave lateral and medial margins. The dorsal margin of the proximal articular surface of phalanx II.1 is shorter than the ventral margin. On the distal end, there is a distinctive dorsal depression (Fig. 18). The collateral ligament pits are not deeply excavated. A markedly concave intercondylar groove separates the lateral and medial condyles. Phalanx II.2 is shorter than II.1, with similar robustness to phalanx II.1 (proximal lateromedial length is 79% of the proximodistal length). The lateral and medial margins of phalanx II.2 are more concave, and the shaft is comparatively shorter than the one in phalanx II.1 (Fig. 18). The collateral ligament pits of phalanx II.2 are more deeply marked and seem to face dorsally, although this could be the product of deformation. Phalanx II.2 has a distinctive dorsal flange. The ungual pedal digit II is lateromedially flattened and distinctively curved. The articular surface is undivided.

Pedal digit III has three non-terminal phalanges. Phalanx III.1 is robust, with the proximal lateromedial length being 72% of the proximodistal length. The shaft of phalanx III.1 is defined by markedly concave lateral and medial margins (Fig. 18). The dorsal surface is slightly concave, but the plantar one is strongly concave. Phalanx III.1 has a more hour-glass shape than phalanx II.1. The

Table 13. Measurements (in mm) of the pedal elements of *Tuebingosaurus maierfritzorum*

Astragalus	
Mediolateral width, anteriorly	143.1 and 175.0
Anteroposterior length	73.7
Lateral height	67.7
Medial height	49.3
Calcaneum	
Mediolateral width at widest point	31.6
Anteroposterior length at longest point	75.1
Metatarsal IV	
Length across anteromedial face	225.0
Anteroposterior width at midshaft	24.2
Mediolateral width at midshaft	47.9
Proximal width	71.4
Proximal height	99.6
Distal dorsal width	61.6
Distal ventral width	52.7
Distal height	46.6
Phalange I.1	
Total length	79.5
Distal width	48.4
Proximal width	67.0
Pedal digit II	
Total length	220
Length of phalange III.1	76.9
Proximal width of phalange III.1	60.4*
Distal width of phalange III.1	51.1
Length of phalange III.2	62
Proximal width of phalange III.2	49.5
Distal width of phalange III.2	33
Length of ungual for phalange III	88.9
Pedal digit III	
Total length	282.3
Length of phalange II.1	83.9
Proximal width of phalange II.1	60.7
Distal width of phalange II.1	52
Length of phalange II.2	66.6
Proximal width of phalange II.2	49
Distal width of phalange II.2	43.5
Length of phalange II.3	55.8
Proximal width of phalange II.3	46.5
Distal width of phalange II.3	46.7
Length of ungual for phalange II	76

dorsal margin of the proximal articular surface of phalanx III.1 is shorter than the ventral margin, and this morphology is also seen in the other non-terminal phalanges of pedal digit III. Phalanx III.1 has a very developed dorsal flange and a very developed ventral flange. Phalanx III.2 is also robust (proximal lateromedial length is 73% of the proximodistal length), with a more open concave lateral margin. The dorsal flange of phalanx III.2 is more reduced than in phalanx III.1, but the ventral flange is still prominent. The collateral ligament pits are deeply excavated (Fig. 18). Phalanx III.3 is more robust than the preceding phalanges, with the proximal lateromedial length representing 83% of the proximodistal length of the phalanx. The medial and lateral condyles are more defined than the preceding phalanges, and the collateral ligament pits are more deeply excavated. The pedal ungual III is more curved than pedal ungual II (Fig. 18).

3.1.13. Other material previously associated with specimen "GPIT IV"

According to von Huene (1932), during the expedition of 1922 in the Trossingen Formation near Tübingen. It is impossible to know how nearby these elements were to the pelvis and hind limb of *Tuebingosaurus*, as von Huene (1932) did not provide details on this. In two separate blocks located near the semi-articulated specimen described above, there was a mandible (in block 169), a partially articulated forearm (block 185) and a cervical vertebra (block 159). The mandible has a similar outline to *P. trossingensis*, with 24 alveoli and 23 preserved (3rd tooth is missing); the mandible is damaged due to post-excavation preparation. The forearm elements correspond to a radius, a metacarpal (possibly metacarpal III, and manual digits I to III (digit I is complete, digit II is probably missing one phalange, and digit III only has two phalanges). The radius is more straightened and less mediolaterally twisted than that of GPIT-PV-30785 and has a proximal outline that is more similar to *Plateosauravus* (based on the drawings in Remes 2007). The preservation of the bone is also slightly better than the preservation of the elements outlined above. There is no evident distortion; the cortical bone is not flaked like the other long elements in *Tuebingosaurus*, suggesting a faster burial and less environmental exposure. It could be possible that the forearm got buried earlier than the rest of the carcass. The cervical vertebrae could not be located in the collection.

Furthermore, there are no relevant details or documentation regarding the excavation from 1922 available to us. The pelvis, the hind limb, and the caudal vertebrae articulate with each other, and it is possible to associate them with a single individual, whereas the other bones are associated with this based on their distance to the larger block. These specimens were embedded into a plastic matrix as part of the diorama display to simulate the mud-burial. When trying to remove the mandible, it was clear that the material was glued to the plastic, and its removal may endanger the specimens. Thus, the mandible and the forearm are removed from specimen GPIT-PV-30787 and, as such, from the holotype of *Tuebingosaurus*. However, further work should test whether these specimens can be referred to the holotype.

3.2. Phylogenetic analyses

3.2.1. Analysis 1

For the first analysis, *Tuebingosaurus* was added to the character-by-taxon matrix by Rauhut et al. (2020). Five iterations were run on this character-by-taxon matrix: 1) including all 67 taxa, b) removing *P.* '*engelhardti*' and *P. gracilis*, c) removing *P. gracilis* only, d) removing *P.*

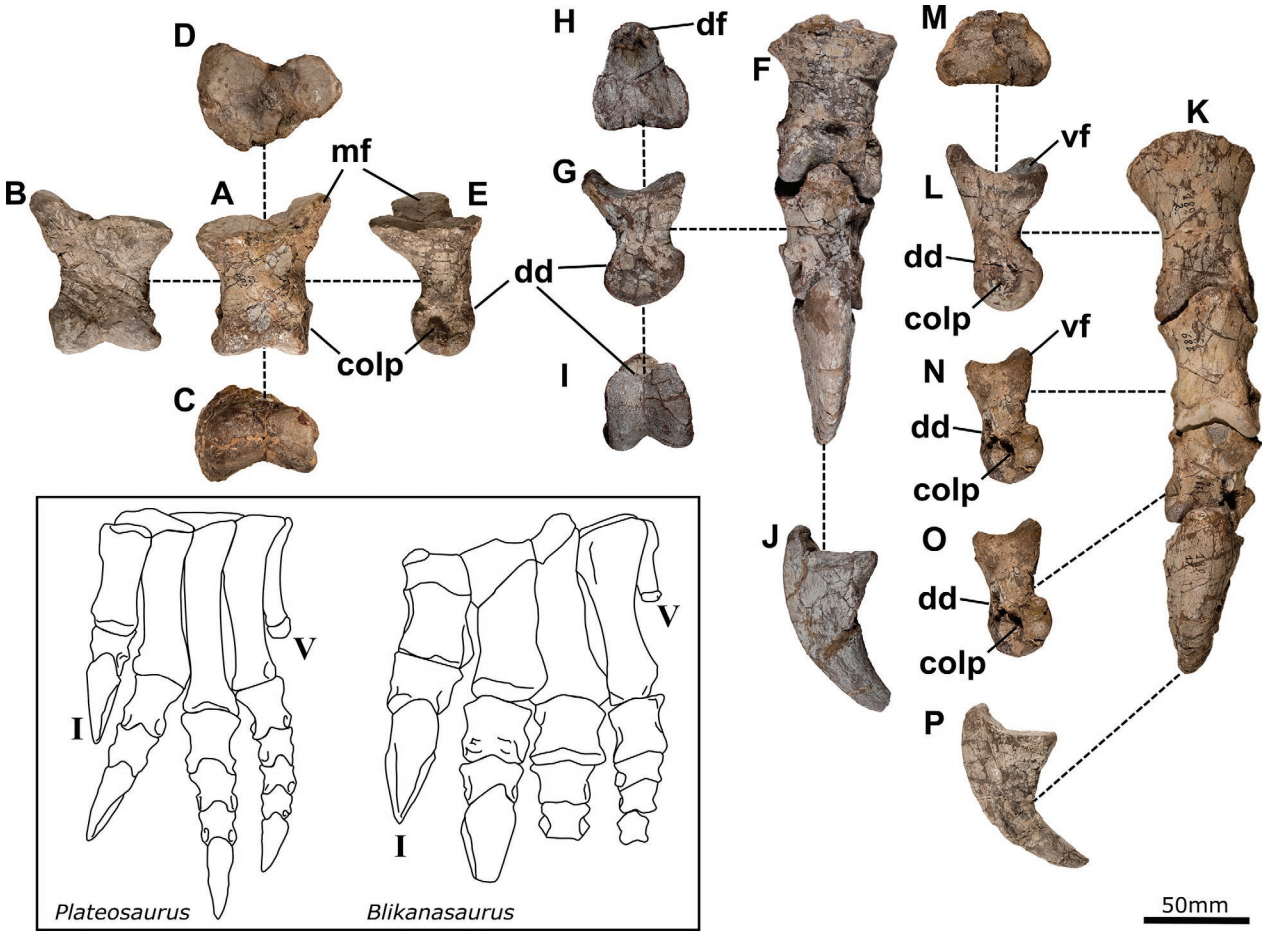

Figure 18. Pedal phalanges I to III of *Tuebingosaurus maierfritzorum* (GPIT-PV-30787). **A**–**E** Phalanx I.1, in dorsal (**A**), ventral (**B**), distal (**C**), proximal (**D**), right lateral I views (**F**). Pedal digit II in dorsal view: **G**–**I** Phalanx II.2 in left lateral (**G**), proximal (**H**) and distal (**I**) views, (**J**) ungual II in left lateral view, (**K**) Pedal digit III in dorsal view. **L**–**M** Phalanx III.1 in left lateral (**L**) and distal (**M**) views, (**N**) Phalanx III.2 in left lateral view, (**O**) Phalanx III.3 in left lateral view and, (**P**) ungual III in left lateral view. The outlines on the left corner, reconstructions of the feet of *Plateosaurus* (SMNS 13200), and *Blikanasaurus* (Galton and van Heerden 1998). Abbreviations: colp, collateral ligament pit, dd, dorsal depression, mf, medial flange, I, pedal digit I, V pedal digit V.

'*engelhardti*' only, e) constraining GPIT-PV-30787 to the genus *Plateosaurus*. The tree space was explored using the 'Clade Frequency in Trees' function in Mesquite. The key result from Analysis 1 is that *Tuebingosaurus* is consistently placed nested within Massopoda, alternatively paired with *Meroktenos*, *Mussaurus*, *Isanosaurus* Buffetaut et al. 2000 and *Pulanesaura*. The trees from iteration 1.5 are very similar to the topologies with a broad definition of *Plateosaurus*, which supports the idea that several specimens included in *Plateosaurus* have a combination of plesiomorphic and derived traits that are not seen when the definition is reduced. The phylogenetic definitions used in the following descriptions are given in Table 14.

Iteration 1.1
Addition of *Tuebingosaurus* (Fig. 19)

Massopoda is found in 100% of the MPTs. Plateosauridae and Massospondylidae are recovered in 100% of the MPTs. Lessemsauridae is found in 71% of the MPTs. In the 149 MPTs, *Tuebingosaurus* is deeply nested within Sauropodiformes: 1) paired with *Meroktenos* in 64.7% of the MPTs, 2) at the base of a pectinate arrangement towards Eusauropoda in 25%, 3) in a clade with *Meroktenos* and *Pulanesaura* in 11.3%, 4) paired with *Schleitheimia* in 10%, and 5) paired with *Isanosaurus* in 6.7%.

Iteration 1.2
Exclusion of *P.* '*engelhardti*' and *P. gracilis*

Massopoda is found in 87% of the MPTs. Massospondylidae is found in 100% of the MPTs. Lessemsauridae is found in 89% of the MPTs. In the 153 MPTs, *Tuebingosaurus* is nested closer to Eusauropoda than in iteration 1.1: 1) at the base of a pectinate arrangement towards Sauropoda in 72% of the MPTs, 2) paired with *Mussaurus* in 17%, 3) paired with *Pulanesaura* in 4%, 4) at the base of Sauropoda (the most inclusive clade that includes *Saltasaurus* but not *Melanorosaurus* sensu Yates 2007a) in 4%, 5) paired with *Meroktenos* in 5 MPTs, and 6) in a clade with *Meroktenos* and *Pulanesaura* only in 1 MPT.

Iteration 1.3
Exclusion of *P. gracilis*

Massopoda is found in 100% of the MPTs. Plateosauridae and Massospondylidae are recovered in 100% of

Table 14. Phylogenetic names used to compare the different cladograms. The content refers to the taxa included in that name from the character-by-taxon matrix employed here and used to identify groups in the different trees.

Name	Definition	Content
Plateosauridae	The most inclusive clade containing *Plateosaurus trossingensis* but not *Saltasaurus* (Yates 2007a)	*Unaysaurus*, *Plateosaurus trossingensis*, *Plateosaurus gracilis*
Massopoda	The most inclusive clade containing *Saltasaurus* but not *Plateosaurus trossingensis* (Yates 2007a,b)	Massospondylidae and Sauropodiformes
Massospondylidae	The most inclusive clade containing *Massospondylus* but not *Plateosaurus trossingensis* or *Saltasaurus* (Sereno 2007)	*Massospondylus*, *Leyesaurus*, *Adeopapposaurus*, *Glacialisaurus* Smith and Pol, 2007, *Coloradisaurus*, *Lufengosaurus*.
Sauropodiformes	The most inclusive clade containing *Saltasaurus* but not *Massospondylus* (McPhee et al. 2015)	*Jingshanosaurus*, *Yunnanosaurus* Young, 1942, *Seitaad*, *Anchisaurus*, *Mussaurus*, *Sefapanosaurus* Otero et al., 2015, *Aardonyx*, *Leonerasaurus*, *Meroktenos*, *Camelotia*, *Melanorosaurus*, Lessemsauridae, *Pulanesaura*, *Gongxianosaurus* He et al., 1998, *Schleitheimia*, *Isanosaurus*, *Tazoudasaurus*, Eusauropoda
Anchisauria	The most recent common ancestor of *Anchisaurus* and *Melanorosaurus*, and all its descendants (Yates 2007b)	*Anchisaurus*, *Leonerasaurus*, *Mussaurus*, *Aardonyx*, *Sefapanosaurus*, *Meroktenos*, *Camelotia*, *Melanorosaurus*, Lessemsauridae, *Blikanasaurus*, *Pulanesaura*, *Gongxianosaurus*, *Schleitheimia*, *Isanosaurus*, *Tazoudasaurus*, Eusauropoda
Lessemsauridae	All the descendants of the most recent common ancestor of *Lessemsaurus* and *Antetonitrus* (Apaldetti et al. 2018)	*Lessemsaurus*, *Antetonitrus*, *Ingentia*
Eusauropoda	The least inclusive clade containing *Shunosaurus* and *Saltasaurus* (Upchurch et al. 2004)	*Shunosaurus*, *Amygdalodon* Cabreira, 1947, *Volkheimeria*, *Spinophorosaurus*, *Cetiosaurus*, *Omeisaurus*, *Mamenchisaurus*, Neosauropoda

the MPTs. Lessemsauridae is found only in 55% of the MPTs. In the 139 MPTs, the position of *Tuebingosaurus* is similar to the positions obtained in iteration 1.3: 1) paired with *Meroktenos* in 53.6% of the MPTs, 2) at the base of Sauropoda in 39%, 3) paired with *Schleitheimia* in 11%, 4) paired with *Isanosaurus* in 8%, 5) at the base of a pectinate arrangement towards Sauropoda only in 5%, 6) in a clade with *Meroktenos* and *Pulanesaura* in 6 MPTs.

Iteration 1.4
Exclusion of *P.* '*engelhardti*'

Massopoda is found in 81% of the MPTs. Plateosauridae and Massospondylidae are recovered in 100% of the MPTs. Lessemsauridae (sensu Apaldetti et al. 2018) is found in 77% of the MPTs. The position of *Tuebingosaurus* is similar to the previous iterations: 1) at the base of Eusauropoda in 57%, 2) paired with *Meroktenos* in 19%, 3) nested within Gravisauria (sensu Allain and Aquesbi 2008) in 17%, 4) at the base of a pectinate arrangement towards Sauropoda only in 11 MPTs, 5) paired with *Isanosaurus* in 10 MPTs, 6) paired with *Pulanesaura* in 6 MPTs.

Iteration 1.5
Forcing *Tuebingosaurus* within *Plateosauridae*

Unlike the previous iterations, the tree becomes more unstable. Massospondylidae is recovered in 100% of the MPTs but is nested within a clade with *Seitaad* Sertich and Loewen, 2010, *Yunnanosaurus* and *Jingshanosaurus* in 60% of the MPTs. The clade Sauropodiformes is found in all the trees, but *Xingxiulong* is placed as the sister taxon to Sauropodiformes in 60% of them. In iteration 1.1, *Xingxiulong* is placed at the base of Massopoda. A Templeton Test was performed to compare the trees between iteration 1.1 against 1.5, and although the trees are longer in iteration 1.1, there is no statistical significance.

3.2.2. Analysis 2

For this second analysis, *P. trossingensis* is restricted to the neotype (SMNS 13200), and *P. gracilis* was replaced by an OTU defined as '*Sellosaurus*' complex, restricted to the material in the GPIT collection. The skull characters were removed from the '*Sellosaurus*' complex. The material GPIT 18392 does not correspond to one individual, but there is not enough documentation to know which elements belong together. Further work is needed to determine the anatomic identity of GPIT 18392. The tree space was explored using the 'Clade Frequency in Trees' function in Mesquite.

Iteration 2.1
Addition of *Tuebingosaurus* (Fig. 19, Table 15)

In most of the trees (63%), *Tuebingosaurus* is paired with *Meroktenos*, supported by the morphology of the lesser trochanter, where the lesser trochanter is closer to the near centre of the anterior face of the femoral shaft and not visible in posterior view, characters shared with *Plateosaurus*. However, they are bracketed by Lessemsauridae and Eusauropoda, where the lesser trochanter is close to the lateral margin of the anterior face of the femoral shaft and visible in posterior view. In 30%, *Tuebingosaurus* is placed within a gradient towards Eusaropoda due to a combination of derived traits. In 7% of the MPTs, *Tuebingosaurus* is paired with *Schleitheimia*, with a projecting heel at the distal end of the ischial peduncle, a

Table 15. Positions of *Tuebingosaurus* in the tree space obtained from Analysis 2.

Iteration	Position of *Tuebingosaurus*	Found in % of MPTs	Synapomorphies
2.1 CI: 0.326 RI: 0.652	Paired with *Meroktenos*	66	Ch. 305, the lesser trochanter is closer to the centre of the anterior face of the femoral shaft.
			Ch. 306, the lesser trochanter is not visible in posterior view
	Within a gradient towards Eusauropoda	30	Ch. 190, deep bases of the anterior caudal diapophyses, extending from the centrum to the neural arch (shared with *Anchisaurus*)
			Ch. 268, a much shorter ischial peduncle of the ilium than the pubic peduncle (shared with *Sarahsaurus*)
			Ch. 331, a wedge-shaped astragalar body (shared with *Melanorosaurus*)
	Paired with *Isanosaurus* (Eusauropoda)	9	Ch. 308, fourth trochanter in the proximal half of the femur.
	Paired with *Schleitheimia*	7	Ch. 267, posteriorly projecting heel at the distal end of the ischial peduncle.
2.2 CI: 0.332 RI: 0.647	At the base of a gradient towards Eusauropoda	72	Ch. 189, prezygodiapophyseal laminae on anterior caudals.
			Ch. 266, strongly anteroposteriorly convex articular surface of the ischial peduncle of the ilium.
			Ch. 330, fibular trochanter laterally facing.
			Ch. 341, convex posterior margin of the astragalus.
	Paired with *Mussaurus*	17	Ch. 193, longitudinal ventral sulcus on proximal and middle caudal is absent.
			Ch. 270, well-developed brevis fossa with sharp margins on the ventral surface of the postacetabular process of the ilium ventrally facing.
			Ch. 330, fibular trochanter laterally facing.
			Ch. 341, convex posterior margin of the astragalus.
	Paired with *Meroktenos*	4	Ch. 305, lesser trochanter near the centre of the anterior face of the femoral shaft in anterior view.
			Ch. 306, lesser trochanter not visible in posterior view.
	Paired with *Pulanesaura*	4	Ch. 187, postzygapophyses placed on either side of the caudal end of the base of the neural spine in anterior caudal vertebrae.
			Ch. 315, the distal surface of the tibiofibular crest is wider mediolaterally than deep anteroposteriorly.
2.3 CI: 0.326 RI: 0.647	Paired with *Meroktenos*	59	Ch. 305, lesser trochanter near the centre of the anterior face of the femoral shaft in anterior view.
			Ch. 306, lesser trochanter not visible in posterior view.
	At the base of Eusauropoda	30	Ch. 190, deep bases of the proximal caudal transverse processes extend from the centrum to the neural arch.
			Ch. 268, ischial peduncle of the ilium much shorter than pubic peduncle.
			Ch. 331, wedge-shaped astragalar body.
	Paired with *Isanosaurus*	11	Ch. 308, fourth trochanter straddling midpoint along the femoral length.
	Paired with *Schleitheimia*	9	Ch. 267, posteriorly projecting 'heel' at the distal end of the ischial peduncle.
	In a clade with *Meroktenos* and *Pulanesaura*	7	Ch. 187, postzygapophyses placed on either side of the caudal end of the base of the neural spine in anterior caudal vertebrae (scored as '?' in *Meroktenos*).
			Ch. 277, obturator foramen of the pubis partially occluded by the iliac pedicel (scored as '?' in *Pulanesaura*).
			Ch. 305, lesser trochanter near the centre of the anterior face of the femoral shaft in anterior view (scored as '?' in *Pulanesaura*).
			Ch. 306, lesser trochanter not visible in posterior view (scored as '?' in *Pulanesaura*).
			Ch. 315, the distal surface of the tibiofibular crest is wider mediolaterally than deep anteroposteriorly (scored as '?' in *Meroktenos*).

Iteration	Position of *Tuebingosaurus*	Found in % of MPTs	Synapomorphies
2.4 CI: 0.329 RI: 0.648	At the base of a gradient towards Eusauropoda	64	Ch. 187, postzygapophyses placed on either side of the caudal end of the base of the neural spine in anterior caudal vertebrae.
			Ch. 189, prezygadiapophyseal laminae on anterior caudal vertebrae.
			Ch. 266, articular surface of the ischial peduncle of the ilium.
			Ch. 330, fibular trochanter laterally facing.
			Ch. 341, convex posterior margin of the astragalus.
	Base of Eusauropoda	20	Ch. 190, deep bases of the proximal caudal transverse processes extend from the centrum to the neural arch.
			Ch. 268, a much shorter ischial peduncle of the ilium than the pubic peduncle.
			Ch. 331, medial end of the astragalar body in anterior view much shallower creating a wedge-shaped astragalar body.
	Paired with *Meroktenos*	14	Ch. 305, lesser trochanter near the centre of the anterior face of the femoral shaft in anterior view.
			Ch. 306, lesser trochanter not visible in posterior view.
	Paired with *Schleitheimia*	4	Ch. 267, posteriorly projecting 'heel' at the distal end of the ischial peduncle.
	Paired with *Pulanesaura*	3	Ch. 187, postzygapophyses placed on either side of the caudal end of the base of the neural spine in anterior caudal vertebrae.
			Ch. 315, the distal surface of the tibiofibular crest is wider mediolaterally than anteroposteriorly deep.

derived character present in Plateosauridae and Massospondylidae but absent in Sauropodiformes, except for *Schleitheimia*, *Tuebingosaurus*, and *Melanorosaurus*. In 9% of the MPTs, *Tuebingosaurus* is paired with *Isanosaurus*, with a fourth trochanter in the proximal half of the femur as in most early sauropodomorphs such as Plateosauridae and Massospondylidae; in most Sauropodiformes, the fourth trochanter is straddling at the midpoint of the femoral shaft.

Iteration 2.2
Exclusion of *P.* '*engelhardti*' and *P. gracilis* (Table 15)

In most of the trees (72%), *Tuebingosaurus* is at the base of a gradient towards Eusauropoda due to several derived characters: prezygodiapophyseal laminae in the anterior caudal vertebrae, strongly anterior posteriorly convex articular surface of the ischial peduncle of the ilium, a laterally facing fibular trochanter, and a convex posterior margin of the astragalus. The latter is present also in *Mussaurus*, *Blikanasaurus* and early sauropods, later reversing to a straight posterior margin in Eusauropoda. In 17% of the *Tuebingosaurus* is paired with *Mussaurus*, the brevis fossa is well developed but absent in Sauropodiformes.

Iteration 2.3
Exclusion of *P. gracilis* (Table 15)

This iteration produces trees similar to iteration 2.1, with *Tuebingosaurus* paired with *Meroktenos* in 59% of the MPTs, and at the base of Eusaropoda in 30% of the MPTs. *Tuebingosaurus* is also paired with *Schleitheimia* (in 9%) and *Isanosaurus* (in 11%). Something new is the appearance of a clade containing *Meroktenos* and *Pulanesaura* in 7% of the MPTs; this clade is supported by synapomorphies that are scored as "?" in either *Pulanesaura* or *Meroktenos*.

Iteration 2.4
Exclusion of *P.* '*engelhardti*' (Table 15)

In 64% of the trees, *Tuebingosaurus* is placed at the base of a gradient towards Eusauropoda, supported by the same synapomorphies in the previous iterations. In 20% of the MPTs, *Tuebingosurus* has an even more derived position at the base of Eusaropoda, supported by derived characters such as deep bases of the diapophyses in the anterior caudal vertebrae, a much shorter ischial peduncle of the ilium than the pubic peduncle, and a wedge-shaped astragalar body. In 14% of the MPTs, *Tuebingosaurus* is paired with *Meroktenos*.

Iteration 2.5
Forcing *Tuebingosaurus* within *Plateosauridae*

In the trees of this iteration (228), Plateosauridae is supported by the following synapomorphies: medial margin of the supratemporal fossa (Ch60-1), basipterygoid processes and parasphenoid rostrum are roughly aligned (Ch81-1), symphyseal end of the dentary strongly curved ventrally (Ch99-1), ventrolateral twisting of the transverse axis of the distal end of the first phalanx of manual digit I is much less than 60 degrees (Ch245-1), concave

lateral margin of the proximal surface of metatarsal II (Ch356-1). Interestingly, all these characters are scored as "?" for *Tuebingosaurus*. In all the trees, an Anchisauria clade is supported by one unequivocal synapomorphy, a lateral margin of the descending posteroventral process of the distal end of the tibia set well back from the anterolateral corner of the distal tibia (Ch327-1), which is also scored as 1 in *Tuebingosaurus*. Another clade found in 100% of the trees is Gravisauria sensu Allain and Aquesbi (2008), supported by several synapomorphies: shallow lateral depression in the cervical vertebral centra (Ch129-1), spinodiapophyseal lamina on dorsal vertebrae joining to create a composite lamina (Ch171-2), deep bases of the anterior caudal diapophyses, extending from the centrum to the neural arch (Ch190-1), absence of the longitudinal ventral sulcus on the anterior and middle caudal vertebra (Ch193-1), strongly anteroposteriorly convex articular surface of the ischial peduncle of the ilium (Ch. 266-1), ischial peduncle of the ilium much shorter than pubic peduncle (Ch. 268-1), a straight longitudinal axis of the femur in lateral view (Ch. 295-2), intensely rugosely pitted articular surface of the long bones of the limbs (Ch. 378-1), and growth marks in the cortex absent or restricted to the outer cortex (Ch. 379). *Tuebingosaurus* shares Ch190-1, Ch193-1, Ch266-1, and Ch268-1. Although these trees are longer (1632 steps) and have similar consistency and retention indexes (CI=0.325, RI=0.651), a Templeton Test shows that there is no statistical significance between the constrained trees and the trees from iteration 2.1, thus the position of *Tuebingosaurus* nested within Plateosauridae seems to rely on the impact of missing information.

3.2.3. Analysis 3

The final analysis took the character-by-taxon matrix from Analysis 2, and a standard implied weighting was performed using the same searching settings described in Analysis 1 and 2. The implied weighting used a 'gentle' concavity of 12 as recommended in Goloboff. Down-weighting the homoplasies, *Tuebingosaurus* moves closer to the base of Sauropoda than the previous topologies. Fig. 20 shows the strict consensus of 3 MPTs, and *Tuebingosaurus* is placed as the sister taxon to a lineage that leads to Sauropoda, and *Schleitheimia* is the earliest member of the rest of the clade. The groups recovered in the iterations from Analysis 1 and 2 are also found in Analysis 3: Plateosauridae, Massopoda, Massospondylidae, Sauropodiformes, Lessemsauridae and Eusauropoda. The bootstrap values of the 3 MPTs in absolute frequencies are 62 for Sauropodomorpha, 85 for Riojasauridae (*Riojasaurus* and *Eucnemesaurus* sensu Yates 2007b), 78 for Plateosauridae, 52 for a reduced Massospondylidae (*Massospondylus*, *Adeopapposaurus*, and *Leyesaurus*). These values are consistent with the values in the other two analyses, which can be explained as an oversampling of characters applied to *Plateosaurus*, *Massospondylus*, *Riojasaurus* and sauropods, which make up the OTUs with the most complete specimens.

4. Discussion

4.1. Phylogenetic position of *Tuebingosaurus maierfritzorum*

Based on our three phylogenetic analyses, there is support for *Tuebingosaurus* being one of the earliest massopodan sauropodomorphs (Figs 19–20). *Tuebingosaurus* shares several characters with early massopodans but simultaneously retains several plesiomorphic characters that show some derived features seen in sauropodiformes. This combination of characters explains the various placements of *Tuebingosaurus* from the base of Massopoda to Sauropodiformes. This specimen may form part of the rapid radiation of massopodan sauropodomorphs that originated in Gondwana.

Unlike most sauropodomorphs at that level, *Tuebingosaurus* does not show a dorsosacral vertebra, but it does have a caudosacral like *Xingxiulong*, *Leonerasaurus* and *Mussaurus*. The sacral rib is narrower than the diapophysis of the first primordial sacral vertebra, as *Lufengosaurus*, *Massospondylus* and *Adeopapposaurus*, and unlike *Anchisaurus*, *Xingxiulong* and *Yunnanosaurus*. The iliac articular facets are divided into dorsal and ventral facets, like in *Mussaurus*, *Leonerasaurus*, *Yunnanosaurus*, *Lufengosaurus*, *Massospondylus* and *Adeopapposaurus*. The length of the first caudal centrum is greater than its height, like in *Xingxiulong* and *Mussaurus*, but unlike *Yunnanosaurus*. The postzygapophyses in the anterior caudals are placed on either side of the caudal end of the base of the neural spine, like in *Xingxiulong*, *Mussaurus* and *Coloradisaurus*, but unlike in *Jingshanosaurus*, *Yunnanosaurus* and *Lufengosaurus*, where a notch is visible in dorsal view. *Tuebingosaurus* lacks a longitudinal ventral sulcus on the anterior and middle caudals, a feature that it shares with *Lufengosaurus* and *Mussaurus*. There is a supracetabular crest on the anterodorsal margin of the acetabulum like in *Xingxiulong*, *Yunnanosaurus*, *Coloradisaurus* and *Lufengosaurus*. The distal articular surface of the pubic peduncle of the ilium is not divided into a more anteriorly facing a more ventrally facing facet, like in most sauropodomorphs, and unlike *Xingxiulong*, *Leonerasaurus*, *Mussaurus*, *Coloradisaurus* and *Lufengosaurus*. There is a posteriorly projected 'heel' at the distal end of the ischial peduncle of the ilium, a plesiomorphic character shared with other massopodans like *Xingxiulong*, *Coloradisaurus*, *Lufengosaurus*, and *Adeopapposaurus*, but gets lost towards Sauropodiformes. There is a well-developed and ventrally facing brevis fossa with sharp margins on the ventral surface of the postacetabular process of the ilium; a feature shared with *Mussaurus*, *Massospondylus* and *Adeopapposaurus*. There is no interischial fenestra, a trait shared with *Mussaurus*, *Anchisaurus*, *Coloradisaurus*, *Lufengosaurus* and *Massospondylus*. The proximal tip of the lesser trochanter is at the level of the femoral head like in other massopodans such as *Anchisaurus*, *Jingshanosaurus*, *Yunnanosaurus*, *Mussaurus*, *Coloradisaurus*, *Lufengosaurus*, *Massospondylus*, and *Adeopapposaurus*,

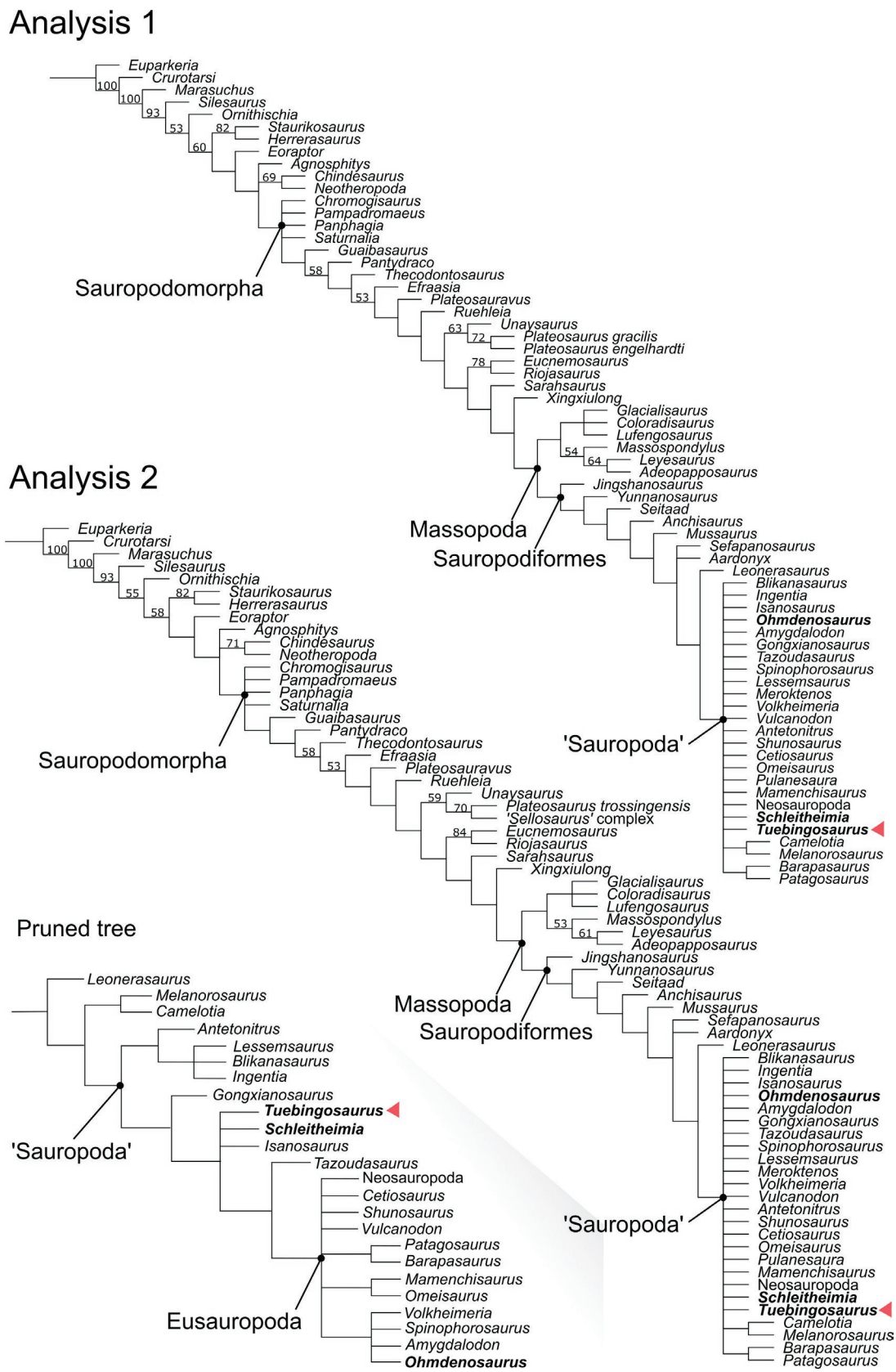

Figure 19. Analysis 1 Strict consensus from 148 MPTs obtained from iteration 1.1. **Analysis 2** Strict consensus from 149 MPTs. The values on the branch are bootstrap values from 100 replicates, reported in absolute values. The clade 'Sauropoda' is here used sensu lato to include all the taxa that collapsed in a polytomy with eusaropods since there is not a phylogenetic definition of Sauropoda. The **pruned tree** was calculated by performing an iterative positional congruence (reduced) analysis (iterPCR, Pol and Escapa 2009) in TNT; the analysis identified *Chromogisaurus*, *Pulanesaura* and *Meroktenos* as unstable taxa, and the new tree comes from a new technology search excluding these three taxa. Sauropoda and Eusauropoda, both sensu Sander et al. (2011), are better displayed in the pruned tree, and *Tuebingosaurus* and *Schleitheimia* are better displayed grouped with *Isanosaurus* as very derived early-diverging sauropods, and *Ohmdenosaurus* as a eusauropod.

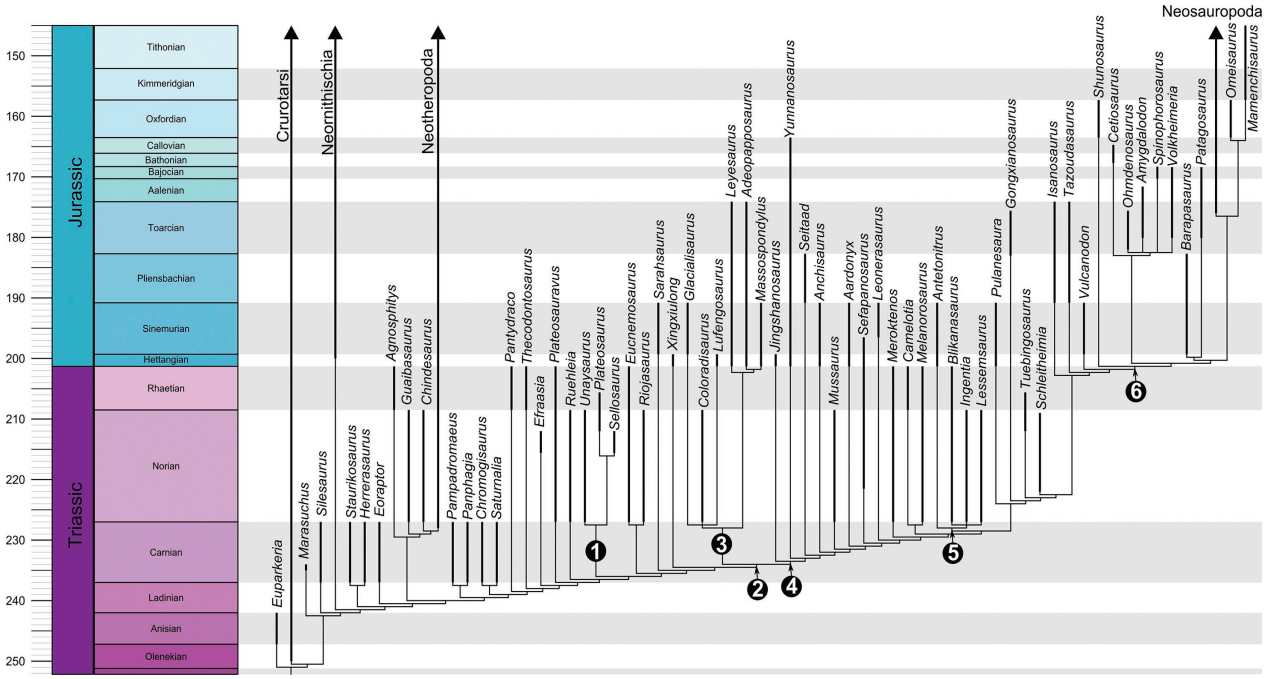

Figure 20. Strict consensus of three MPTs obtained from implied weighting (k=12). Down-weighting the homoplasies places *Tuebingosaurus* as having a common ancestor with the lineage that leads to Sauropoda and earlier than *Schleitheimia*. Numbers correspond to 1) Plateosauridae, 2) Massopoda, 3) Massospondylidae, 4) Sauropodiformes, 5) Lessemsauridae, 6) Eusauropoda. The ages of *Plateosaurus* and *Tuebingosaurus* are restricted to the Obere Mühle outcrop, which has been assigned to the Sevatian, an informal unit used in the stratigraphy of the Late Triassic in Central Europe, from 211 to 203.6 Mya (Olsen et al. 2011). The base of Massopoda is not clear in the topologies (see discussion in the text), but *Tuebingosaurus* is placed at this level with several other Early Jurassic sauropodomorphs and *Mussaurus* from the Late Triassic. This suggests that a very rapid diversification event occurred in the Carnian, and the groups that originated during this time experienced further diversifications during the Norian.

whereas in most sauropodomorphs, this tip is distal to the femoral head. The fourth trochanter is located on the medial margin of the femur, like in *Mussaurus*, *Jingshanosaurus*, *Anchisaurus*, *Coloradisaurus*, and *Lufengosaurus*, but unlike *Massospondylus*, *Adeopapposaurus*, and *Plateosaurus*, where it is centrally located along the mediolateral axis.

Several characters in *Tuebingosaurus* show a large degree of plesiomorphy, with reversals being very common in the phylogenetic analyses in this work. The position of the obturator foramen of the pubis is partially occluded by the iliac pedicel in anterior view, a plesiomorphic character present in *Seitaad* and *Jingshanosaurus*, unlike most of the sauropodomorphs where it is completely visible. The lateral margins of the pubic apron in the anterior view also retain the plesiomorphic straight morphology, like *Seitaad*, *Anchisaurus*, *Leonerasaurus* and *Yunnanosaurus*. It also retains an ilium shorter than the pubis and an ischial component larger than the pubic component of the acetabular rim, both plesiomorphic conditions found in non-sauropodiform sauropodomorphs. The femur has the plesiomorphic condition of being strongly bent with an offset between the proximal and distal axes; a plateosaurian-type femoral morphology shared with *Anchisaurus*, *Jingshanosaurus*, *Xingxiulong*, *Yunnanosaurus*, *Coloradisaurus*, *Lufengosaurus*, *Massospondylus* and *Adeopapposaurus*. In *Tuebingosaurus*, the fourth trochanter is on the proximal half of the femur, a plesiomorphic condition that changes in Sauropodiformes but is retained in some (i.e., *Melanorosaurus*, *Isanosaurus*, *Patagosaurus* and *Shunosaurus*), where the fourth trochanter is straddling around the midpoint. Furthermore, the fourth trochanter is asymmetrical, with a steeper distal slope and a plateosaurian-type femoral morphology, a feature also present in *Anchisaurus*, *Jingshanosaurus*, *Yunnanosaurus* and *Mussaurus*, and unlike *Coloradisaurus*, *Lufengosaurus*, *Massospondylus* and *Adeopapposaurus*, where the fourth trochanter is more symmetrical.

Unlike any other massopodan, *Tuebingosaurus* displays a prezygodiapophyseal lamina on the anterior caudal vertebrae and the anterior caudal diapophyses extending from the centrum to the neural arch, both of which are derived characters that are seen in sauropods, the former appearing in *Pulanesaura* and the latter in *Schleitheimia*. The length of the ischial peduncle of the ilium is much shorter than the pubic peduncle, a derived trait in sauropods and *Sarahsaurus*. The angle between the long axis of the femoral head and the transverse axis of the distal femur is close to 0°, a derived trait that originated early in massopodan evolution but about 30° in early sauropodomorphs, like *Thecodontosaurus*, *Efraasia* and *Plateosaurus*. The articular surface of the tibia has an anteroposterior length twice or larger than the transverse width, a derived trait shared with Sauropodiformes but absent in earlier massopodans. The lateral margin of the descending posteroventral process of the distal end of

the tibia is set well back from the anterolateral corner of the distal tibia – a derived trait shared with *Anchisaurus*, *Mussaurus* and most Sauropodiformes. The position of the fibular trochanter is laterally facing, as in sauropods – a trait shared with *Mussaurus*.

Tuebingosaurus and *Schleitheimia* are found very closely related in the equally-weighted topologies, and in 7% of the MPTs in Analysis 2, the two OTUs form a clade (Table 15). The ilium of *Schleitheimia* is represented by the acetabular region and the postacetabular blade (PIMUZ A/III 550, in Rauhut et al. 2020). The outline of the pubic and ischiadic peduncle is similar to that in *Tuebingosaurus*, with a broad and lateromedially twisted pubic peduncle (in lateral view) and a posteriorly projected 'heel' in the ischiadic peduncle (Fig. 6). The postacetabular process in *Schleitheimia* has a triangular outline, whereas in *Tuebingosaurus* the ventral margin of the postacetabular process is ventrally turned (Fig. 6). In *Tuebingosaurus*, the supracetabular crest is accompanied by a medially projected crest of similar size, seen in both ilia (Fig. 7a), whereas in *Schleitheimia*, the ilium only has the supracetabular crest projecting laterally. The partial left femur of *Schleitheimia* (PIMUZ A/III 551, in Rauhut et al. 2020) cannot be accurately compared to that of *Tuebingosaurus* (Fig. 12) because the preserved elements in *Schleitheimia*, i.e., the midshaft and the distal end, correspond to some of the reconstructed parts of the femur in *Tuebingosaurus*. The fourth trochanter of *Tuebingosaurus* has a more pronounced asymmetrical outline, with a curved ventral margin and a straight dorsal margin, whereas in *Schleitheimia*, the fourth trochanter is more symmetrical, but the ventral margin has a slope in the opposite direction to the dorsal margin.

The astragalus recovered from Schleitheim-Santierge (PIMUZ A/III 4391, in Rauhut et al. 2020) was referred to as *Plateosaurus* sp. since it has a similar outline to the one of specimen SMNS 13200; however, the neotype SMNS 13200 does not have an anterior foramen, as is present in PIMUZ A/III 439. Furthermore, the lateral and posterior outlines are similar to the overall astragalar morphology of *Tuebingosaurus*, which suggests that this specimen is more appropriately referred to as cf. *Tuebingosaurus* than to as *Plateosaurus* sp.

Ohmdenosaurus is a sauropodomorph from the Early Jurassic found in the Posidonia Shale at Holzmaden, Germany (Wild 1978). It was considered a member of the 'family' Vulcanodontidae (McIntosh 1990) and has been compared to *Rhoetosaurus*, the earliest sauropods from the Early Jurassic characterised for having slender tibiae (Nair and Salisbury 2012). In our topologies, *Ohmdenosaurus* is consistently (93% of the MPTs) grouped with *Isanosaurus*, *Tazoudasaurus*, *Vulcanodon* and sauropods (iteration 2.1), consistent with previous diagnoses of *Ohmdenosaurus*. The proximal end of the tibia in *Ohmdenosaurus* has a circular outline, as lateromedially wide as it is anterodorsally long, with a cnemial crest oriented anteriorly; in *Tuebingosaurus*, the proximal outline is more elliptical, with a lateromedially width longer than the anteroposterior length, and a cnemial crest oriented anterolaterally. The tallest point of the cnemial crest in *Ohmdenosaurus* is halfway along the length of the crest, whereas in *Tuebingosaurus*, it is closer to the proximal end of the cnemial crest. In *Ohmdenosaurus* and *Tuebingosaurus*, in the proximal articular surface of the tibia, the posterior end of the fibular condyle is anteriorly placed to the posterior margin of the articular surface. Distally, the lateromedial width of the tibia is larger than the anteroposterior length in *Ohmdenosaurus*, but it is subequal in *Tuebingosaurus*. As in other Sauropodiformes, *Ohmdenosaurus* and *Tuebingosaurus* have a posteroventral process set well back from the anterolateral corner of the distal tibia.

Non-sauropod sauropodomorphs have a periodically interrupted growth, which translates into the formation of fibrolamellar bone interrupted by regularly spaced growth marks, unlike in sauropods, where the growth is continuous (Chinsamy 1993; Sander et al. 2004; Sander and Klein 2005; Cerda et al. 2017; Fig. 21). In sauropods, there is an uninterrupted deposition of fibrolamellar bone tissue during the early development, followed by periodical interruptions that form lines of arrested growth, LAGs, after sexual maturity was attained (Sander et al. 2004). The histological configuration of the femur in *Tuebingosaurus* is similar to that found in *Mussaurus* and *Lessemsaurus* (Cerda et al. 2017). In *Mussaurus*, the vascular canals have a plexiform arrangement alternating with regions of longitudinally oriented canals. In one specimen of *Mussaurus* (MLP 61-III-20-22), there is a large proportion of woven fibered bone relative to the parallel fibered bone, whereas another specimen (MPM-PV-1815) has more parallel fibered bone relative to the woven fibered bone. In *Lessesaurus*, however, specimen PVL 4822/64 has a larger proportion of woven fibered bone than parallel fibered bone. In our topologies, *Tuebingosaurus* is placed between the early non-sauropod sauropodomorphs, such as *Riojasaurus* and *Coloradisaurus*, and the more derived non-sauropod sauropodomorphs, such as *Volkheimeria* and *Patagosaurus*. *Riojasaurus* and *Coloradisaurus* have a larger proportion of parallel fibered bone than woven fibered bone; in *Riojasaurus*, there is an abrupt change of vascularisation pattern at the outer cortex (Cerda et al. 2017).

On the other hand, *Volkheimeria* and *Patagosaurus* have a matrix exclusively with woven fibered bone. In lamellar bone, successive thin layers form a plywood structure. Woven fibered bone consists of coarse and loosely packed collagen fibres with no spatial order and a high vascular density. Parallel fibered bone seems to be an intermediate between lamellar and woven fibered bones. Lamellar bone suggests a slow growth rate, whereas woven fibered bone suggests a fast growth. Therefore, animals like *Riojasaurus* and *Coloradisaurus* seem to have had a slower growth through growth cycles (Apaldetti et al. 2018), whereas animals like *Mussaurus*, *Lessemsaurus* (Apaldetti et al. 2018) and *Tuebingosaurus* have a faster growth rate but show growth cycles. Sauropods evolved fast and continuous growth rates.

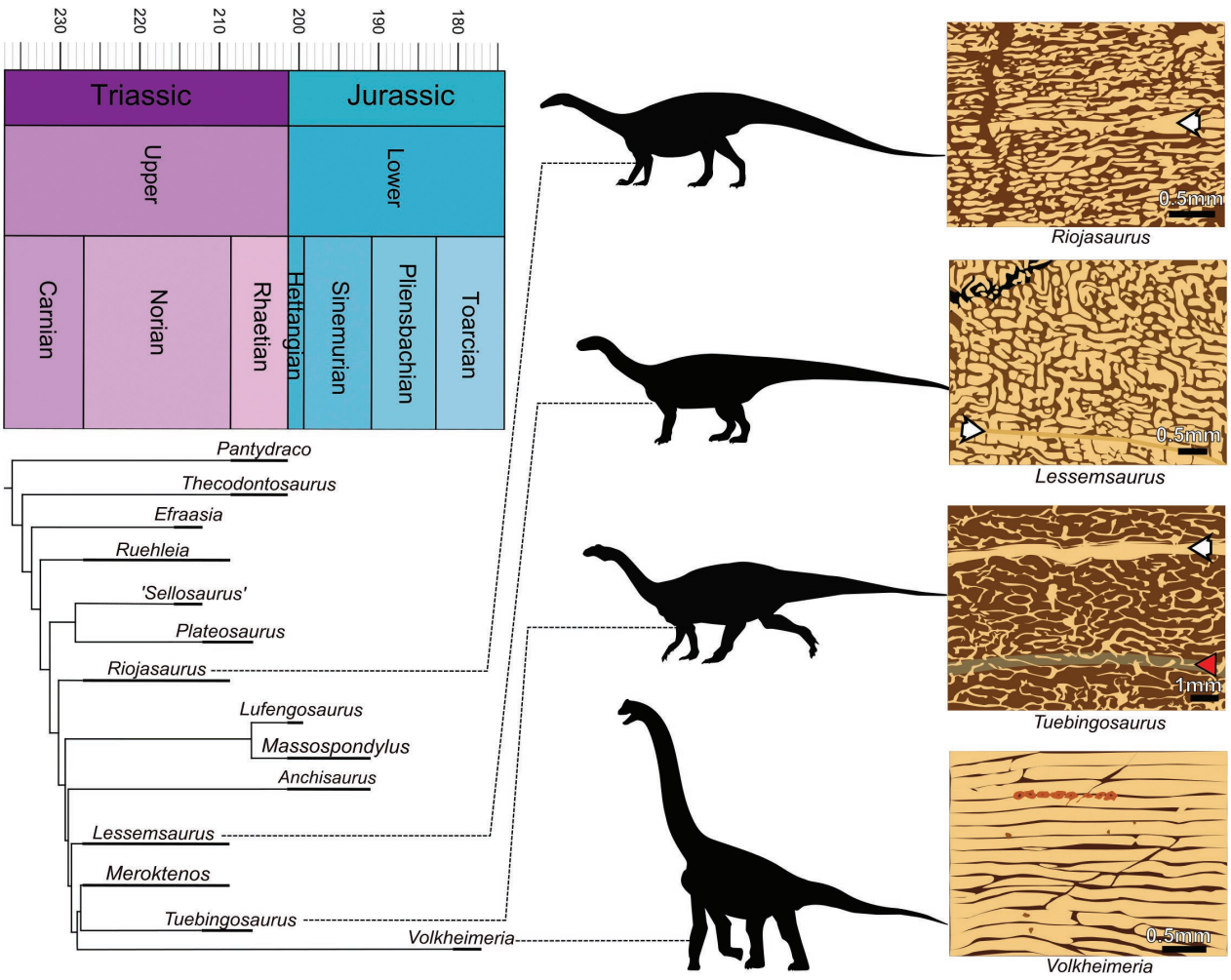

Figure 21. Diagrams showing the histological structure of long bones of four sauropodomorphs: *Riojasaurus*, *Lessemsaurus*, *Tuebingosaurus* and *Volkheimeria*. The phylogenetic relationships are based on the total evidence phylogenetic analyses from iteration 2.1. The white arrows point to lines of arrested growth (LAG) that correspond to a momentary but complete cessation of growth. The red arrow points to an annulus corresponding to periods of slow growth. The histological samples of *Riojasaurus*, *Lessemsaurus* and *Volkheimeria*, were redrawn from the pictures published in Apaldetti et al. (2018, fig. 2b), and the histological sample of *Tuebingosaurus* was redrawn from the photographs published in Klein (2004, fig.3E), interpreted there as a fully grown *Plateosaurus*.

4.2. Plateosaurian and massopodan characters

In Upchurch et al. (2007), Plateosauridae was restricted to *Coloradisaurus*, *Plateosaurus* and *Riojasaurus*, defined by three synapomorphies: 1) a deep, transverse wall of bone between the basipterygoid process, 2) a deltopectoral crest with a sigmoid outline in anterior view, 3) a 'heel'-like projection of the posterior margin of the ischial articulation. Of these three characters, the available material of *Tuebingosaurus* has a 'heel'-like projection in the ilium (3), justifying the referral to Plateosauridae.

Massospondylus and *Lufengosaurus* were included by Upchurch et al. (2007) in the group Plateosauria, supported by six synapomorphies: 1) a triangular outline in the external naris, 2) a shelf-like area lateral to the external naris, 3) a prefrontal ventral process long and extending down the medial surface of the lacrimal, 4) a supratemporal fenestra obscured in lateral view by the supratemporal bar, 5) laterally expanded tables at the mid-length of the distal surface of cervical neural spines, and 6) a second distal carpal not wholly covering the proximal surface of metacarpal II. None of these characters can be traced to *Tuebingosaurus*.

The characters were mapped to compare the synapomorphies with Upchurch et al. (2007) using the character-by-taxon matrix and the topology reported therein. This character mapping was also repeated in all the topologies where these results are not reported in the paper. For example, in Yates (2007b), Massospondylidae was recovered as a group containing *Massospondylus*, *Coloradisaurus* and *Lufengosaurus*. Six synapomorphies supported this node: 1) dorsal profile of the snout with depression behind the naris, 2) the symphyseal end of the dentary is strongly curved ventrally, 3) the length of cervical 4 or 5 exceeds four times the anterior centrum height, 4) manual digit I is greater than the length of manual digit II, 5) a pyramidal dorsal process on the posteromedial corner of the astragalus, 6) the length of the pedal digit II is less than 90% of the length of the ungual of the pedal digit I. Again, none of these characters can be applied to *Tuebingosaurus*.

Regarding Massopoda, the mapping of characters in Yates (2007b) recovers that this node is supported by twelve synapomorphies: 1) a slot-shaped subnarial foramen, 2) an antorbital fossa on the ascending process of the maxilla delimited by a rounded rim or a change in slope, 3) the anterior process of the lacrimal is half or less as long as the ventral process of the lacrimal, 4) the ratio of the minimum depth of the jugal below the orbit to the length between the anterior end of the jugal and the anteroventral corner of the infratemporal fenestra is greater than 0.2 – a character shared with '*Plateosaurus engelhardti*', 5) the dorsal margin of the postorbital in lateral view has a distinct embayment between the anterior and the posterior dorsal processes, 6) the quadratojugal sutures along the ventrolateral margin of the jugal, 7) the teeth have serrations along the mesial and distal carinae restricted to the upper half of the crown – although noting that *Plateosaurus* and *Colorodisaurus* share this character, 8) ventral keels on the anterior cervical vertebrae, but this is reversed later on in more advanced sauropodiformes, 9) the anterior margin of the scapula rises from the blade at an angle equal to or greater than 65° from the scapular axis, 10) metacarpal I has a proximal width that represents 80% to 100% of the metacarpal I length, noting that this character then reverses several times in sauropodiformes, 11) notch separating the posteroventral end of the ischial obturator from the ischial shaft, 12) the position of the proximal tip of the lesser trochanter is levelled with the femoral head. Nevertheless, in *Tuebingosaurus*, the proximal tip of the lesser trochanter is distal to the femoral head.

In McPhee et al. (2015b) and the modification by Wang et al. (2017), in the synapomorphy-based definition of Massopoda, we found that the mapped characters are consistent with the definition of Yates (2007b), except for the synapomorphies of the scapula (9) and the metacarpal (10), and adds a new one, the medial peg of calcaneum fits into the astragalus. On the other hand, Plateosauridae seems to be supported by only four synapomorphies in Yates (2007b) when mapping their characters onto the topologies: 1) the medial margin of the supratemporal fossa bears a projection at the frontal/postorbital-parietal suture producing a scalloped margin, 2) the basipterygoid processes and the parabasisphenoid process are below the level of the basioccipital condyle and the basal tubera, a condition also reported in *Coloradisaurus*, 3) the symphyseal end of the dentary is strongly curved ventrally relative to the long axis of the dentary, a condition shared with *Massospondylus* and *Coloradisaurus*, 4) the lateral margin of the proximal margin in metatarsal II is straight, a character present in *Tuebingosaurus*. In McPhee et al. (2015b) and the modification by Wang et al. (2017), the synapomorphy-based of Plateosauridae is identical but adds the transverse width of the distal humerus is less than 33% of the humeral length.

Although we get a consistent definition of massopodan characters in the matrices derived from Yates (2007b), Massopoda is not recovered as a group in the matrices derived from Upchurch et al. (2007). Furthermore, based on the comparative cladistic analyses performed by Peyre de Fabrègues et al. (2015), only 80% of the characters are shared between Upchurch et al. (2007) and Yates (2007b), suggesting that the only way to obtain a consensus is by merging the two datasets. This was partially attempted by Sekiya et al. (2013), who merged both datasets but only on the taxa that they had in common, namely for a total of 27 sauropodomorphs. Sekiya et al. (2013) recovered the topology of Prosauropoda defined only by two synapomorphies, 1) a maxillary lamina that is twice as longer than it is high, a character found only in the matrix by Upchurch et al. (2007), and 2) a centrally located tubercle in the palatine, a character found only in the matrix by Yates (2007b). Since there are contradictory phylogenetic signals, all the taxa and the characters should be included in a single matrix to discern consistent plateosaurian and massopodan features. Alternatively, a character analysis is required to assess the character delineation, the impact of such delineation in the final topology, and a comparison of the character scores to resolve any disagreement between the authors.

4.3. *Plateosaurus* in comparative anatomy

P. trossingensis specimen "GPIT I" (GPIT-PV-30784) is often employed as the representative of plateosaurian anatomy along with specimen SMNS 13200 in comparisons with other sauropodomorphs (e.g. Galton 1971; Langer 2003; Yates 2004; Galton and Kermack 2010; Langer et al. 2010; Yates et al. 2011; Rauhut et al. 2011; Yates et al. 2012; Bittencourt et al. 2012; Apaldetti et al. 2014; Otero et al. 2015; McPhee et al. 2015a; Otero 2018; Otero et al. 2019; Fig. 3). Specimen "GPIT II" (GPIT-PV-30785) has been less often used as a comparison point (Smith and Pol 2007; Bittencourt et al. 2012), and in one study, the skull specimen "GPIT 18318a" has been used to represent the anatomy of *Plateosaurus* (Cabreira et al. 2016). In a small number of studies, *P. gracilis* has been explicitly used to compare plateosaurian anatomy against other sauropodomorphs (Pol and Powell 2007; Claessens 2004; Otero and Pol 2013; Fechner and Gößling 2014; Bronzati et al. 2017).

A study on the growth rings in long bones from material stored in SMNS, GPIT and MSF considered all individuals to belong to the same species (Klein 2004; Sander and Klein 2005). Klein (2004) included the specimens "GPIT I" (GPIT-PV-30785, the composite, no sample was taken), "GPIT 11921" (which refers to the humerus of GPIT-PV-30788, currently lost), "GPIT 192.1" (currently the femur of *Tuebingosaurus*), "GPIT 163" (currently the tibia of *Tuebingosaurus*), and "GPIT II" (GPIT-PV-30784, no histological sample was taken). The analysis of the medulla of long bones (Sander and Klein 2005) determined three groups of growth: "fast growth" in specimens where the fibrolamellar bone is the last tissue type to have been formed, "slow growth" in specimens in which growth cycles in fibrolamellar bone in the outer cortex become thinner and loses vascularity, and "fully grown" (i.e. "GPIT 163", "GPIT 11921", the

Figure 22. Reconstruction of the last moments in the life of *Tuebingosaurus maierfritzorum* (collection number of the painting: GPIT-PV-41827). The cortical bone on the left side of the fossil is fractured into flakes, which can be explained if the carcass was exposed over a long time on the mud, two to four years, before being buried – in the reconstruction, the animal will fall to its right body side. The reconstruction shows the animal sinking in a mud trap, attacked by a rauisuchian, *Teratosaurus* Meyer, 1861, which has also been found in the Trossingen Formation in Baden-Württemberg (Brusatte et al. 2009). In the background, a herd of *P. trossingensis* runs away from the scene. The flora in the swamp is reconstructed based on fossils from the Germanic basin, with shoots of horsetails and ferns covering the swamp and a forest comprising cycads (*Taeniopteris* Brongniart, 1828), lycophytes (*Lepacyclotes* Emmons, 1856) and coniferous plants (*Brachyphyllum* Brongniart, 1828) (Kustatscher et al., 2018).

femur and tibia of *Tuebingosaurus*), with a lamellar-zonal bone with closely spaced LAGs and poor to absent vascularisation (e.g. "GPIT II"). Sander and Klein (2005) explored three hypotheses to explain the disparity in the growth patterns found in Trossingen. The first hypothesis was that several biological species were represented by the material identified as *P.* '*engelhardti*'. The hypothesis was rejected because, at the time, there was an agreement that there was only evidence for one species of sauropodomorph in the Triassic beds of Central Europe (Moser 2003; Yates 2003a; Galton and Upchurch 2004). Similarly, sexual dimorphism was rejected as an explanation since the body size shows a unimodal distribution (Sander and Klein 2005). Finally, the hypothesis stated that *P.* '*engelhardti*' had strong developmental plasticity. The latter was supported because individuals from the Frick bone bed are smaller on average, whereas the Trossingen bone beds yield larger individuals. The phenotypic plasticity was explained as either a habitat difference with different plants in one region or a product of a change in habitat through time (Sander and Klein 2005). Nevertheless, as outlined in the section above (see section 'Taxonomic composition of *Plateosaurus* in phylogenetic analyses'), after 2007, it became clear that the consensus on *Plateosaurus* as a monospecific genus was disputed, with four potential species being identified and used so far, namely *P.* '*engelhardti*', *P. gracilis*, '*P. erlenbergiensis*' (= *P. longiceps*) and *P. ingens*, with several specimens from Frick belonging to *Gresslyosaurus* and *Schleitheimia* (Rauhut et al. 2020). Then, after revising the taxonomy, the different growth patterns could support separating distinct species in Central Europe.

5. Conclusions

Based on our phylogenetic analysis, the new species *Tuebingosaurus maierfritzorum* is positioned as the earliest massopodan discovered in the Trossingen beds (Fig. 19). It displays some characters traditionally considered plateosaurian, like the heel-like projection in the posterior part of the ischiadic peduncle of the ilium and a straight lateral margin in metatarsal II. The fact that it has been illustrated since the early 20th century as part of *Plateo-*

saurus may suggest that some noise has been introduced into the phylogenetic analyses of the past decade by assuming all the medium to large-sized sauropodomorphs from Germany belonged to the same species. It is also clear that there is no consensus, in phylogenetic terms, on plateosaurian features and massopodan features since, through the literature, two incompatible overall topologies have been produced. Through comparative anatomy and the evidence from our phylogenetic analysis, *Tuebingosaurus* displays several derived features consistent with the position among massopodans and hints to an early diversification of Sauropodomorpha as they occupied the vacant niches in Pangaea left by rhynchosaurs and aetosaurs (Barrett et al. 2010). A rapid disparification event could explain the contradictory phylogenetic signals discussed in the literature. Many cranial characters that support one group could be a product of convergence as the animals adopted similar feeding strategies in different parts of Pangaea.

Furthermore, a thorough revision needs to be done to the material referred to as *P. trossingensis* or *Plateosaurus* that was not obtained from the Obere Mühle outcrop, and the hypothesis that these are different species needs to be tested with morphometric, specimen-level phylogenetic, and stratigraphic analyses. Nevertheless, restricting *P. trossingensis* to SMNS 13200, GPIT-PV-30784, AMNH FARB 6810, and all Seemann's material stored in Stuttgart should remove any noise that may have been added by using the literature in which all specimens were considered *Plateosaurus*. SMNS 13200, GPIT-PV-30784, AMNH FARB 6810, and all Seemann's material specimens come from the lower dinosaur bone bed in Obere Mühle and are likely to represent different individuals that died at different times, but that can be referred to as part of the same chronospecies.

6. Competing interests

The authors have declared no competing interests exist.

7. Author contributions

O.R.R.F and I.W. conceived the idea, analyzed, interpreted, and discussed the data, and contributed to the final version of the manuscript.

8. Competing interests

The authors have declared no competing interests exist.

9. Acknowledgements

We would like to thank Toru Sekiya and Emanuel Tschopp, whose valuable comments and suggestions helped us improve the quality of the manuscript.

We thank Henrik Stöhr for his help tracing the material in the collection and compiling a lot of the information known about the specimens in the collection as well as Agnes Fatz for taking the photographs of the material that help document this work. We also thank Marcus Burkhardt for the painting reconstructing *Tuebingosaurus maierfritzorum*.

Funding. Some of the first-hand data collected for this project was obtained as part of the funding from the Consejo Nacional de Ciencia y Tecnología (CVU 540250/Grant: 384614 granted to ORRF). In addition, IW was supported by DFG-grant WE5440/6-1.

10. References

Allain R, Aquesbi N (2008) Anatomy and phylogenetic relationships of *Tazoudasaurus naimi* (Dinosauria, Sauropoda) from the late Early Jurassic of Morocco. Geodiversitas 30(2): 345–424.

Allain R, Aquesbi N, Dejax J, Meyer CA, Monbaron M, Montenat C, Rechir P, Rochdy M, Russell DA, Taquet P (2004) A basal sauropod dinosaur from the Early Jurassic of Morocco. Comptes Rendus Palevol 3(3): 199–208. https://doi.org/10.1016/j.crpv.2004.03.001

Apaldetti C, Pol D, Yates AM (2013) The postcranial anatomy of *Coloradisaurus brevis* (Dinosauria: Sauropodomorpha) from the Late Triassic and its phylogenetic implications. Palaeontology 56(2): 277–301. https://doi.org/10.1111/j.1475-4983.2012.01198.x

Apaldetti C, Martínez RN, Alcober OA, Pol D (2011) A new basal sauropodomorph (Dinosauria: Saurischia) from Quebrada del Barro formation (Marayes-El Carrizal basin), Northwestern Argentina. PLoS ONE 6(11): e26964. https://doi.org/10.1371/journal.pone.0026964

Apaldetti C, Martínez RN, Pol D, Souter T (2014) Redescription of the sull of *Coloradisaurus brevis* (Dinosauria, Sauropodomorpha) from the Late Triassic Los Colorados Formation of the Ischigualasto-Villa Union Basin, northwestern Argentina. Journal of Vertebrate Paleontology 34: 1113–1132. https://doi.org/10.1080/02724634.2014.859147

Apaldetti C, Martínez RN, Cerda I, Pol D, Alcober OA (2018) An early trend towards gigantism in Triassic sauropodomorph dinosaurs. Nature Ecology & Evolution 2(8): 1227–1232. https://doi.org/10.1038/s41559-018-0599-y

Bandyopadhyay S, Gillette DD, Ray S, Sengupta DP (2010) Osteology of *Barapasaurus tagorei* (Dinosauria: Sauropoda) from the Early Jurassic of India. Palaeontology 53(3): 533–569. http://dx.doi.org/10.1111/j.1475-4983.2010.00933.x

Baron M, Norman D, Barrett PM (2017) A new hypothesis of dinosaur relationships and early dinosaur evolution. Nature 543: 501–506. https://doi.org/10.1038/nature21700

Barrett PM, Butler RJ, Nesbitt S (2010) The roles of herbivory and omnivory in early dinosaur evolution. Earth and Environmental Science Transactions of the Royal Society of Edinburgh 101(3-4): 383–396. http://dx.doi.org/10.1017/S1755691011020111

Beccari V, Mateus O, Wings O, Milàn J, Clemmensen LB (2021) *Issi saaneq* gen. et sp. nov. – A new sauropodomorph dinosaur from the Late Triassic (Norian) of Jameson Land, Central East Greenland. Diversity 13(11): 1–59. https://doi.org/10.3390/d13110561

Bittencourt JS, Leal LA, Langer MC, Azevedo, SAK (2012) An additional sauropodomorph specimen from the Upper Triassic Caturrita Formation, southern Brazil, with comments on the biogeography of plateosaurids. Alcheringa 36(2): 269–278. http://dx.doi.org/10.1080/03115518.2012.634111

Bonaparte JF (1969) Dos nuevas "faunas" de reptiles triásicos de Argentina. Gondwana Stratigraphy (IUGS Symposium, Buenos Aires) 2: 283–306.

Bonaparte JF (1979) Dinosaurs: a Jurassic assemblage from Patagonia. Science 205: 1377–1378. https://doi.org/10.1126/science.205.4413.1377

Bonaparte (1999) Evolución de las vértebras presacras en Sauropodomorpha. Ameghiniana 36(2): 115–187.

Bonaparte JF, Vince M (1979) El hallazgo del primer nido de dinosaurios triásicos, (Saurischia, Prosauropoda), Triásico Superior de Patagonia, Argentina. Ameghiniana 16(1–2): 173–182.

Bonaparte JF, Ferigolo J, Ribeiro M (1999) A new early Late Triassic saurischian dinosaur from Rio Grande do Sol state, Brazil. In: Tomida Y, Rich TH, and Vickers-Rich P (Eds) Proceedings of the Second Gondwanan Dinosaur Symposium, National Science Museum Monographs 15: 89–109.

Broom R (1915) Catalogue of the type and figured specimens of fossil vertebrates in the American Museum of Natural History. III. Permian, Triassic and Jurassic reptiles of South Africa. Bulletin of the American Museum of Natural History 25: 105–164.

Brongniart AT (1828) Prodrome d'une histoire des végétaux fossiles. Paris, F. G. Levrault, 232 pp. https://doi.org/10.5962/bhl.title.62840

Bronzati MF, Rauhut OWM (2017) Braincase redescription of *Efraasia minor* von Huene, 1908 (Dinosauria: Sauropodomorpha) from the Late Triassic of Germany, with comments on the evolution of the sauropodomorph braincase. Zoological Journal of the Linnean Society 1908: 173–224. https://doi.org/10.1093/zoolinnean/zlx029

Bronzati MF, Rauhut OWM, Bittencourt JS, Langer MC (2017) Endocast of the Late Triassic (Carnian) dinosaur *Saturnalia tupiniquim*: implications for the evolution of brain tissue in Sauropodomorpha. Scientific Reports 7: 11931. http://dx.doi.org/10.1038/s41598-017-11737-5

Brusatte SL, Butler RJ, Sulej T, Niedzwiedzki G (2009) The taxonomy and anatomy of rauisuchian archosaurs from the Late Triassic of Germany and Poland. Acta Palaeontologica Polonica 54: 221–230. http://dx.doi.org/10.4202/app.2008.0065

Buffetaut E, Suteethorn V, Cuny G, Tong H, Le Loeuff J, Khansubha S, Jongautchariyakul S (2000) The earliest known sauropod dinosaur. Nature 407: 72–74. https://doi.org/10.1038/35024060

Cabreira A (1947) Un saurópodo nuevo del Jurásico de Patagonia. Instituto del Museo de la Universidad Nacional de La Plata, Notas del Mueso de La Plata, Paleontología 12(95): 1–17.

Cabreira SF, Schultz CL, Bittencourt JS, Soares MB, Fortier DC, Silva LR, Langer MC (2011) New stem-sauropodomorph (Dinosauria, Saurischia) from the Triassic of Brazil. Naturwissenschaften 98(12): 1035–1040. https://doi.org/10.1007/s00114-011-0858-0

Cabreira SF, Kellner AWA, Dias-da-Silva S, Roberto da Silva L, Bronzati MF, Marsola JCA, Müller RT, Bittencourt JS, Batista BJA, Raugust T, Carrilho R, Brodt A, Langer MC (2016) A unique Late Triassic dinosauromorph assemblage reveals dinosaur ancestral anatomy and diet. Current Biology 26: 3090–3095. http://dx.doi.org/10.1016/j.cub.2016.09.040

Carrano MT, Benson RBJ, Sampson SD (2012) The phylogeny of Tetanurae (Dinosauria: Theropoda). Journal of Systematic Palaeontology 10(2): 211–300. http://dx.doi.org/10.1080/14772019.2011.630927

Cerda IA, Chinsamy A, Pol D, Apaldetti C, Otero A, Powell JE, Martínex RN (2017) Novel insight into the origin of the growth dynamics of sauropod dinosaurs. PLoS ONE 12: e0179707. http://dx.doi.org/10.1371/journal.pone.0179707

Chapelle KEJ, Choiniere JN (2018) A revised cranial description of *Massospondylus carinatus* Owen (Dinosauria: Sauropodomorpha) based on computed tomographic scans and a review of cranial characters for basal Sauropodomorpha. PeerJ 6: e4224. https://doi.org/10.7717/peerj.4224

Chapelle KEJ, Barrett PM, Botha J, Choiniere JN (2019) *Ngwevu intloko*: a new early sauropodomorph dinosaur from the Lower Jurassic Elliot Formation of South Africa and comments on cranial ontogeny in Massospondylus carinatus. PeerJ 7: e7240. https://doi.org/10.7717/peerj.7240

Claessens L (2004) Dinosaur gastralia: origin, morphology, and function. Journal of Vertebrate Paleontology 24(1): 89–106. http://dx.doi.org/10.1671/A1116-8

Cooper MR (1984) A reassessment of *Vulcanodon karibaensis* Raath (Dinosauria: Saurischia) and the origin of the Sauropoda. Palaeontologia Africana 25: 203–231.

Cope ED (1877) On a gigantic saurian from the Dakota epoch of Colorado. Paleontological Bulletin 25: 5–10.

Dong Z, Zhou S, Zhang H (1983) [Dinosaurs from the Jurassic of Sichuan]. Palaeontologica Sinica, New Series C 162(23): 1–136

Emmons E (1856) Geological Report of the Midland Counties of North Carolina, 351 pp.

Ezcurra MD (2010) A new early dinosaur (Saurischia: Sauropodomorpha) from the Late Triassic of Argentina: a reassessment of dinosaur origin and phylogeny. Journal of Systematic Palaeontology 8(3): 371–425. https://doi.org/10.1080/14772019.2010.484650

Ezcurra MD, Apaldetti C (2011) A robust sauropodomorph specimen from the Upper Triassic of Argentina and insights on the diversity of the Los Colorados Formation. Proceedings of the Geologists' Association 123(1): 155–164. http://dx.doi.org/10.1016/j.pgeola.2011.05.002

Fechner R, Gößling R (2014) The gastralial apparatus of *Plateosaurus engelhardti* morphological description and soft-tissue reconstruction. Palaeontologia Electronica 17: 1–11. https://doi.org/10.26879/357

Fraas E (1879) Kralle (I. Phalanx) des *Zanclodon laevis* Plien. Neues Jahrbuch für Mineralogie, Geognosie, Geologie und Petrefaktekunde 1879: 863.

Fraas E (1896) Die Schwäbischen Trias-Saurier nach dem Material der Kgl. Naturalien-Sammlung in Stuttgart zusammengestellt. Festgabe des Königlichen Naturalien-Cabinets in Stuttgart zur 42. Versammlung der Deutschen Geologischen Gesellschaft in Stuttgart. Schweizerbart, Stuttgart. http://idb.ub.uni-tuebingen.de/opendigi/LXI38_qt#p=5

Fraas E (1897) Reste von *Zanclodon* aus dem oberen Keuper vom Langenberge bei Wolfenbüttel. Zeitschrift der Deutschen Geologischen Gesellschaft 49(3): 482–485.

Fraas E (1913) Die neuesten Dinosaurierfunde in der schwäbischen Trias. Naturwissenschaften 1913: 1907–1100. https://doi.org/10.1007/BF01493265

Fraas E (1915) *Plateosaurus integer*. Neues Jahrbuch für Geologie und Paläontologie 1915: 3.

Galton PM (1971) The prosauropod dinosaur *Ammosaurus*, the crocodile *Postosuchus*, and their bearing on the age of the Navajo Sandstone of Northeastern Arizona. Journal of Paleontology 45(5): 781–795.

Galton PM (1973) On the anatomy and relationships of *Efraasia diagnostica* (Huene) n. gen., a prosauropod dinosaur (Reptilia: Saurischia) from the Upper Triassic of Germany. Paläontologische Zeitschrift 47(3/4): 229–255. https://doi.org/10.1007/BF02985709

Galton PM (1976) Prosauropod dinosaurs (Reptilia: Saurischia) of North America. Postilla 169: 1–98.

Galton PM (1984) Cranial anatomy of the prosauropod dinosaur *Plateosaurus* from the Knollenmergel (Middle Keuper, Upper Triassic)

of Germany. I. Two complete skulls from Trossingen Württ. with comments on the diet. Geologica et Palaeontologica 18: 139–171.

Galton PM (1985a) The poposaurid thecodontian *Teratosaurus suevicus* v. Meyer, plus referred specimens mostly based on prosauropod dinosaurs, from the Middle Stubensandstein (Upper Triassic) of Nordwürttemberg. Stuttgarter Beiträge zur Naturkunde, Serie B (Geologie und Paläontologie) 116: 1–29.

Galton PM (1985b) Cranial anatomy of the prosauropod dinosaur *Plateosaurus* from the Knollenmergel (Middle Keuper, Upper Triassic) of Germany. II. All the cranial materials and details of soft-part anatomy. Geologica et Palaeontologica 19: 119–159.

Galton PM (1985c) Cranial anatomy of the prosauropod dinosaur '*Sellosaurus gracilis*' from the Middle Stubensandstein (Upper Triassic) of Nordwürttemberg, West Germany. Stuttgarter Beiträge zur Naturkunde, Serie B (Geologie und Paläontologie) 118: 1–39.

Galton PM (1985d) Notes on the Melanorosauridae, a family of large prosauropod Dinosaurs (Saurischia: Sauropodomorpha). Geobios 18(5): 671–676. https://doi.org/10.1016/S0016-6995(85)80065-6

Galton PM (1986) Prosauropod dinosaur *Plateosaurus* (=*Gresslyosaurus*) (Saurischia: Sauropodornorpha) from the Upper Triassic of Switzerland. Geologica et Palaeontologica 20: 167–183.

Galton PM (1990) Basal Sauropodomorpha – Prosauropoda.. In: Weishampel DB, Dodson P, Osmólska H (Eds) The Dinosauria. University of California Press, Berkeley, 320–344.

Galton PM (1999) Sex, sacra and '*Sellosaurus gracilis*' (Saurischia, Sauropodomorpha, Upper Triassic, Germany)—or why the character "two sacral vertebrae" is plesiomorphic for Dinosauria. Neues Jahrbuch für Geologie und Paläontologie – Abhandlungen 213(1): 19. http://dx.doi.org/10.1127/njgpa/213/1999/19

Galton PM (2000) The prosauropod dinosaur *Plateosaurus* Meyer, 1837 (Saurischia: Sauropodomorpha). I. The syntypes of '*P. engelhardti*' Meyer, 1837 (Upper Triassic, Germany), with notes on other European prosauropods with "distally straight" femora. Neues Jahrbuch für Geologie und Paläontologie – Abhandlungen 216(2): 233–275. https://doi.org/10.1127/njgpa/216/2000/233

Galton PM (2001a) Prosauropod dinosaurs from the Upper Triassic of Germany. In: Colectivo Arqueológico-Paleontológico de Salas (Eds) Actas de las I Jornadas Internacionales sobre Paleontología de Dinosaurios y su Entorno (Spain), September 1999. C.A.S, Burgos, 25–92.

Galton PM (2001b) The prosauropod dinosaur *Plateosaurus* Meyer, 1837 (Saurischia: Sauropodomorpha; Upper Triassic). II. Notes on the referred species. Revue de Paleobiologie 20(2): 435–502.

Galton PM (2001c) Prosauropod dinosaur '*Sellosaurus gracilis*' (Upper Triassic, Germany): third sacral vertebra as either a dorsosacral or a caudosacral. Neues Jahrbuch für Geologie und Paläontologie Monatshefte 2001(11): 688–704. http://dx.doi.org/10.1127/njgpm/2001/2001/688

Galton PM (2005) Bones of large dinosaurs (Prosauropoda and Stegosauria) from the Rhaetic Bone Bed (Upper Triassic) of Aust Cliff, southwest England. Revue de Paleobiologie 24(1): 51–74.

Galton PM (2007) Notes on the remains of archosaurian reptiles, mostly basal sauropodomorph dinosaurs, from the 1834 fissure fill (Rhaetian, Upper Triassic) at Clifton in Bristol, southwest England. Revue de Paleobiologie 26(2): 505–591.

Galton PM (2012) Case 3560 *Plateosaurus engelhardti* Meyer, 1837 (Dinosauria, Sauropodomorpha): proposed replacement of unidentifiable name-bearing type by a neotype. Bulletin of Zoological Nomenclature 69(3): 203–212. https://doi.org/10.21805/bzn.v69i3.a15

Galton PM, Cluver MA (1976) *Anchisaurus capensis* (Broom) and a revision of the Anchisauridae (Reptilia, Saurischia). Annals of the South African Museum 69(6): 121–159.

Galton PM, Kermack D (2010) The anatomy of *Pantydraco caducus*, a very basal sauropodomorph dinosaur from the Rhaetian (Upper Triassic) of South Wales, UK. Revue de Paleobiologie 29(2): 341–404. https://doi.org/10.1127/0077-7749/2007/0243-0119

Galton PM, van Heerden J (1985) Partial hind limb of *Blikanasaurus cromptoni* n. gen. and n. sp., representing a new family of prosauropod dinosaurs from the Upper Triassic of South Africa. Géobios 18(4): 509–516. https://doi.org/10.1016/S0016-6995(85)80003-6

Galton PM, Upchurch P (2000) Prosauropod dinosaurs: Homeotic transformations ("frame shifts") with third sacral as a caudosacral or a dorsosacral. Journal of Vertebrate Paleontology 20 (Suppl.): 43A. https://doi.org/10.1371%2Fjournal.pone.0014572

Galton PM, Upchurch P (2004) Prosauropoda. In: Weishampel DB, Dodson P, Osmólska H (Eds) The Dinosauria (second edition). University of California Press, Berkeley, 232–258. http://dx.doi.org/10.1525/california/9780520242098.003.0014

Galton PM, van Heerden J, Yates AM (2005) Postcranial anatomy of referred specimens of the sauropodomorph dinosaur *Melanorosaurus* from the Upper Triassic of South Africa. In: Carpenter K, Tidwell V (Eds) Thunder-Lizards: The Sauropodomorph Dinosaurs. Indiana University Press, Bloomington, 1–37.

Galton PM, Yates AM, Kermack D (2007) *Pantydraco* n. gen. for *Thecodontosaurus caducus* Yates, 2003, a basal sauropodomorph dinosaur from the Upper Triassic or Lower Jurassic of South Wales, UK. Neues Jahrbuch für Geologie und Paläontologie – Abhandlungen 243(1): 119–125. http://dx.doi.org/10.1127/0077-7749/2007/0243-0119

Goloboff PA, Farris JS, Nixon KC (2008) TNT, a free program for phylogenetic analysis. Cladistics 24(5): 774–786. https://doi.org/10.1111/j.1096-0031.2008.00217.x

Haughton SH (1924) The fauna and stratigraphy of the Stromberg Series. Annals of the South African Museum 12(17): 323–497.

He X, Wang C, Liu S, Zhou F, Liu T, Cai K, Dai B (1998) [A new species of sauropod from the Early Jurassic of Gongxian Co., Sichuan]. A new species of sauropod from the Early Jurassic of Gongxian Co., Sichuan 18(1): 1–6

Hitchcock E (1865) Appendix [A]. Bones of *Megadactylus polyzelus*. In: Hitchcock CH (Ed.) Supplement of the Ichnology of New England. A Report to the Government of Massachusetts in 1863. Wright and Potter State Printers, Boston, 39–40.

van Heerden J (1979) The morphology and taxonomy of *Euskelosaurus* (Reptilia: Saurischia; Late Triassic) from South Africa. Navorsinge van die Nasionale Museum, Bloemfontein 4(2): 21–84. https://hdl.handle.net/10520/AJA00679208_660

Hinz JK, Werneburg I (2019) The historical archive of the palaeontological collection of Tübingen, Germany. Palaeontologia Electronica 22.2.26A: 1–94. https://doi.org/10.26879/907

van Hoepen ECN (1920) Contributions to the knowledge of the reptiles of the Karroo Formation. 6. Further dinosaurian material in the Transvaal Museum. Annals of the Transvaal Museum 7(2): 93–141.

Hofmann R, Sander PM (2014) The first juvenile specimens of '*Plateosaurus engelhardti*' from Frick, Switzerland: Isolated neural arches and their implications for developmental plasticity in a basal sauropodomorph. PeerJ 2: e458. https://doi.org/10.7717/peerj.458

von Huene F (1901) Vorläufiger Bericht über die triassischen Dinosaurier des europäischen Continents. Neues Jahrbuch für Mineralogie, Geologie und Paläontologie 1901(2): 89–104

von Huene F (1905a) Über die Nomenklatur von *Zanclodon*. Centralblatt für Mineralogie, Geologie und Paläontologie 1905: 10–12.

von Huene F (1905b) Über die Trias-Dinosaurier Europas. Zeitschrift der Deutschen Geologischen Gesellschaft 57: 345–349.

von Huene F (1907) Die Dinosaurier der europäischen Triasformation mit Berücksichtigung der aussereuropäischen Vorkommnisse. Geologische und Palaeontologische Abhandlungen Suppl. 1(1): 1–419.

von Huene F (1914a) Nachträge zu meinen früheren Beschreibungen triassischer Saurischia. Geologie und Paläontologie Abhandlungen 13(7): 69–82

von Huene F (1914b) Beiträge zur Geschichte der Archosaurier. Geologie und Paläontologie Abhandlungen 13(7): 1–56

von Huene F (1915) Beiträge zur Kenntnis einiger Saurischier der schwäbischen Trias. Neues Jahrbuch für Mineralogie, Geologie und Paläontologie 1915(1): 1–27.

von Huene F (1920) Bemerkungen zur Systematik und Stammesgeschichte einiger Reptilien. Zeitschrift für Induktive Abstammungs und Vererbungslehre 22: 209–212. https://doi.org/10.1007/BF01785394

von Huene F (1921) Coelurosaurier-Reste aus dem obersten Keuper von Halberstadt. Centralblatt für Mineralogie, Geologie und Paläontologie 1921: 315–320.

von Huene F (1926) Vollständige Osteologie eines Plateosauriden aus dem schwäbischen Keuper. Geologische und Palaeontologische Abhandlungen N.F. 15: 139–179.

von Huene F (1928) Lebensbild des Saurischier-Vorkommens im obersten Keuper von Trossingen in Württemberg. Paleobiologica 1: 103–116.

von Huene F (1929) Kurze Übersicht über die Saurischia und ihre natürlichen Zusammenhänge. Paläontologische Zeitschrift 11: 269–273 https://doi.org/10.1007/BF03042732

von Huene F (1932) Die fossile Reptil-Ordnung Saurischia, ihre Entwicklung und Geschichte. Monographien zur Geologie und Palaeontologie (Serie 1) 4: 1–361.

von Huene F (1956) Paläontologie und Phylogenie der Niederen Tetrapoden. Gustav Fischer Verlang, Jena, 716 pp.

von Huene F (1959) Saurians in China and their relations. Vertebrata PalAsiatica 3(3): 119–123.

Hungerbühler A (1998) Taphonomy of the prosauropod dinosaur *Sellosaurus*, and its implications for carnivore faunas and feeding habits in the Late Triassic. Palaeogeography, Palaeoclimatology, Palaeoecology 143: 1–29. https://doi.org/10.1016/S0031-0182(98)00074-1

International Comission on Zoological Nomenclature (2019) Opinion 2435 (Case 3560) *Plateosaurus* Meyer, 1837 (Dinosauria, Sauropodomorpha): new type species designated. Bulletin of Zoological Nomenclature 76: 144–145. http://dx.doi.org/10.21805/bzn.v76.a042

Jaekel O (1911) Die Wirbeltiere. Eine Übersicht über die Fossilen und lebenden Formen. Gebrüder Borntraeger, Berlin, 252 pp. https://doi.org/10.5962/bhl.title.119340

Jaekel O (1913) Über die Wirbeltierfunde in der oberen Trias von Halberstadt. Paläontologische Zeitschrift 1: 155–215. https://doi.org/10.1007/BF03160336

Jain LS, Kutty TS, Roy-Chowdhury T, Chatterjee S (1975) The sauropod dinosaur from the Lower Jurassic Kota Formation of India. Proceedings of the Royal Society of London A 188: 221–228. https://doi.org/10.1098/rspb.1975.0014

Janensch W (1914) Übersicht über der Wirbeltierfauna der Tendaguru-Schichten nebst einer kurzen Charakterisierung der neu aufgeführten Arten von Sauropoden. Archiv für Biontologie 3(1): 81–110.

Klein N (2004) Bone histology and growth of the prosauropod dinosaur *Plateosaurus engelhardti* Meyer, 1937 from the Norian bonebeds of Trossingen (Germany) and Frick (Switzerland). PhD Thesis, Rheinischen Friedrich-Wilhelms-Universität Bonn, Bonn, Germany. https://hdl.handle.net/20.500.11811/2114

Knoll F (2010) A primitive sauropodomorph from the upper Elliot Formation of Lesotho. Geological Magazine 147(6): 814–829. https://doi.org/10.1017/S001675681000018X

Koken E (1900) Review of E. Fraas: Triassaurier. Neues Jahrbuch für Mineralogie, Geologie und Paläontologie 1900(1): 302–303.

Kuhn O (1959) Ein neuer Microsaurier aus dem deutschen Rotliegenden. Neues Jahrbuch für Mineralogie, Geologie und Paläontologie 1900: 303.

Kustatscher E, Ash SR, Karasev E, Pott C, Vajda V, Yu J, McLoughlin S (2018) Chapter 13. Flora of the Late Triassic. In: Tanner LH (Ed.) The Late Triassic World: Earth in a Time of Transition, Springer Cham, 545–622. http://dx.doi.org/10.1007/978-3-319-68009-5_13

Lallensack J, Teschner E, Pabst B, Sander PM (2021) New skulls of the basal sauropodomorph *Plateosaurus trossingensis* from Frick, Switzerland: is there more than one species? Acta Paleontologica Polonica 66(1): 1–28. https://doi.org/10.4202/app.00804.2020

Langer MC, Abdala F, Richter M, Benton MJ (1999) A sauropodomorph dinosaur from the Upper Triassic (Carnian) of southern Brazil. Comptes Rendus de l'Academie des Sciences – Series IIA – Earth and Planetary Science 329(7): 511–517. https://doi.org/10.1016/S1251-8050(00)80025-7

Langer MC (2003) The pelvic and hind limb anatomy of stem-sauropodomorph *Saturnalia tupiniquim* (Late Triassic, Brazil). PaleoBios 23(2): 1–30.

Langer MC, Ezcurra MD, Bittencourt, JS, Novas FE (2010) The origin and early evolution of dinosaurs. Biological Reviews 85(1): 55–110. https://doi.org/10.1111/j.1469-185X.2009.00094.x

Lapparent, AF de (1967) Les dinosaures de France. Sciences 51: 4–19.

Leal LA, Azevedo SAK, Kellner AWA, Da Rosa AAS (2004) A new early dinosaur (Sauropodomorpha) from the Caturrita Formation (Late Triassic), Paraná Basin, Brazil. Zootaxa 690: 1–24. https://doi.org/10.11646/zootaxa.690.1.1

Lefebvre R, Allain R, Houssaye A, Cornette R (2020) Disentangling biological variability and taphonomy: Shape analysis of the limb long bones of the sauropodomorph dinosaur Plateosaurus. PeerJ 8: 1–50 https://doi.org/10.7717/peerj.9359

Lovegrove J, Newell AJ, Whiteside DI, Benton MJ (2021) Testing the relationship between marine transgression and evolving island pa Journal of the Geological Society 178(3): jgs2020-158. https://doi.org/10.1144/jgs2020-158

Lü J, Li T, Zhong S, Azuma Y, Fujita M, Dong Z, Ji Q (2007) New yunnanosaurid dinosaur (Dinosauria, Prosauropoda) From the Middle Jurassic Zhanghe Formation of Yuanmou, Yunnan province of China. Memoir of the Fukui Prefectural Dinosaur Museum 6: 1–15.

Martínez RN, Alcober OA (2009) A basal sauropodomorph (Dinosauria: Saurischia) from the Ischigualasto Formation (Triassic, Carnian) and the early evolution of Sauropodomorpha. PloS ONE 4(2): e4397. https://doi.org/10.1371/journal.pone.0004397

Martínez RN, Haro JA, Apaldetti C (2012) Braincase of *Panphagia protos* (Dinosauria, Sauropodomorpha). Journal of Vertebrate Paleontology 32(Suppl.): 70–82. https://doi.org/10.1080/02724634.2013.819009

Marsh OC (1885) Names of extinct reptiles. American Journal of Science 29: 169.

McIntosh JS (1990) Sauropoda. In: Weishampel DB, Dodson P, Osmólska H (Eds) The Dinosauria. University of California Press, Berkeley, 345–401.

McPhee BW, Bordy E, Sciscio L, Choiniere JN (2017) The sauropodomorph biostratigraphy of the Elliot Formation of southern Africa: Tracking the evolution of Sauropodomorpha across the Triassic – Jurassic boundary. Acta Palaeontologica Polonica 62(3): 441–465. https://doi.org/10.4202/app.00377.2017

McPhee BW, Yates AM, Choiniere JN, Abdala F (2014) The complete anatomy and phylogenetic relationships of *Antetonitrus ingenipes* (Sauropodiformes, Dinosauria): Implications for the origins of Sauropoda. Zoological Journal of the Linnean Society 171(1): 151–205. https://doi.org/10.1111/zoj.12127

McPhee BW, Choiniere JN, Yates AM, Viglietti PA (2015a) A second species of *Eucnemesaurus* Van Hoepen, 1920 (Dinosauria, Sauropodomorpha): new information on the diversity and evolution of the sauropodomorph fauna of South Africa's lower Elliot Formation (latest Triassic). Journal of Vertebrate Paleontology 35(5): e980504. https://doi.org/10.1080/02724634.2015.980504

McPhee BW, Benson RBJ, Botha-Brink J, Bordy EM, Choiniere JN (2018) A giant dinosaur from the earliest Jurassic of South Africa and the transition to quadrupedality in early sauropodomorphs. Current Biology 28(19): 3143-3151.e7. https://doi.org/10.1016/j.cub.2018.07.063

McPhee BW, Bittencourt JS, Langer MC, Apaldetti C, Da Rosa AAS (2019) Reassessment of *Unaysaurus tolentinoi* (Dinosauria: Sauropodomorpha) from the Late Triassic (early Norian) of Brazil, with a consideration of the evidence for monophyly within non-sauropodan sauropodomorphs. Journal of Systematic Palaeontology 28(3): 259–293. https://doi.org/10.1080/14772019.2019.1602856

McPhee BW, Bonnan MF, Yates AM, Neveling J, Choiniere JN (2015b) A new basal sauropod from the pre-Toarcian Jurassic of South Africa: evidence of niche-partitioning at the sauropodomorph–sauropod boundary? Scientific Reports 5: 13224. https://doi.org/10.1038/srep13224

von Meyer H (1861) Reptilien aus dem Stubensandstein des oberen Keupers. Palaeontographica 7: 253–346.

von Meyer H (1837) Mittheilungen, an Professor Bronn gerichtet. Jahrbuch für Mineralogie, Geognosie, Geologie und Petrefaktenkunde 1837: 314–317.

Morris J (1843) A Catalogue of British Fossils. British Museum, London, 222 pp.

Moser M (2003) '*Plateosaurus engelhardti*' Meyer, 1837 (Dinosauria: Sauropodomorpha) from the Feuerletten (Middle Keuper; Upper Triassic) of Bavaria. Zitteliana B 24: 3–186.

Mudroch A, Richter U, Reich M (2006) The dinosaur digs in the Keuper of Halberstadt: a 2nd reconnaissance. In: Barrett PMM, Evans S (Eds) Ninth International Symposium on Mesozoic Terrestrial Ecosystems and Biota, Abstracts and Proceedings. Natural History Museum, London, [no page range given].

Müller RT, Langer MC, Dias-da-Silva S (2018a) An exceptionally preserved association of complete dinosaur skeletons reveals the oldest long-necked sauropodomorphs. Biology Letters 14: 1–5. https://doi.org/10.1098/rsbl.2018.0633

Müller RT, Langer MC, Bronzati MF, Pacheco CP, Cabreira SF, Dias-da-Silva S (2018b) Early evolution of sauropodomorphs: anatomy and phylogenetic relationships of a remarkably well-preserved dinosaur from the Upper Triassic of southern Brazil. Zoological Journal of the Linnean Society 184(4): 1187–1248. https://doi.org/10.1093/zoolinnean/zly009

Neenan JM, Chapelle KEJ, Fernandez V, Choiniere JN (2018) Ontogeny of the *Massospondylus* labyrinth: implications for locomotory shifts in a basal sauropodomorph dinosaur. Palaeontology 62(2): 255–265. https://doi.org/10.1111/pala.12400

Nesbitt SJ, Barrett PM, Werning S, Sidor CA, Charig AJ (2013) The oldest dinosaur? A Middle Triassic dinosauriform from Tanzania. Biology Letters 9(1): 1–5. https://doi.org/10.1098/rsbl.2012.0949

Novas FE, Ezcurra MD, Chatterjee S, Kutty TS (2011) New dinosaur species from the Upper Triassic Upper Maleri and Lower Dharmaram formations of Central India. Earth and Environmental Science Transactions of the Royal Society of Edinburgh 101(3–4): 333–349. http://dx.doi.org/10.1017/S1755691011020093

Olsen PE, Kent DV, Whiteside JH (2011) Implications of the Newark Supergroup-based astrochronology and geomagnetic polarity time scale (Newark-APTS) for the tempo and mode of the early diversification of the Dinosauria. Earth and Environmental Science Transactions of the Royal Society of Edinburgh 101(3–4): 201–229. http://dx.doi.org/10.1017/S1755691011020032

Osborn HF (1905) *Tyrannosaurus* and other Cretaceous carnivorous dinosaurs. Bulletin of the American Museum of Natural History 21(14): 259–265

Otero A (2018) Forelimb musculature and osteological correlates in Sauropodomorpha (Dinosauria, Saurischia). PLoS ONE 13(7): e0198988. http://dx.doi.org/10.1371/journal.pone.0198988

Otero A, Pol D (2013) Postcranial anatomy and phylogenetic relationships of *Mussaurus patagonicus* (Dinosauria, Sauropodomorpha). Journal of Vertebrate Paleontology 33(5): 1138–1168. http://dx.doi.org/10.1080/02724634.2013.769444

Otero A, Krupandan E, Pol D, Chinsamy A, Choiniere JN (2015) A new basal sauropodiform from South Africa and the phylogenetic relationships of basal sauropodomorphs. Zoological Journal of the Linnean Society 174(3): 589–634. http://dx.doi.org/10.1111/zoj.12247

Otero A, Cuff AR, Allen V, Sumner-Rooney L, Pol D, Hutchinson JR (2019) Ontogenetic changes in the body plan of the sauropodomorph dinosaur *Mussaurus patagonicus* reveal shifts of locomotor stance during growth. Scientific Reports 9: 7614. https://doi.org/10.1038/s41598-019-44037-1

Owen R (1842) Report on British fossil reptiles, part II. Report of the British Association for the Advancement of Science 11: 60–204.

Owen R (1854) Descriptive catalogue of the fossil organic remains of Reptilia and Pisces contained in the Museum of the Royal College of Surgeons of England. Taylor and Francis, London, 184 pp.

Pol D, Powell JE (2007) Skull anatomy of *Mussaurus patagonicus* (Dinosauria: Sauropodomorpha) from the Late Triassic of Patagonia. Historical Biology 19: 125–144. https://doi.org/10.1080/08912960601140085

Pol D, Escapa I (2009) Unstable taxa in cladistic analysis: identification and the assessment of relevant characters. Cladistics 25(5): 515–527. http://dx.doi.org/10.1111/j.1096-0031.2009.00258.x

Pol D, Garrido A, Cerda IA (2011) A new sauropodomorph dinosaur from the Early Jurassic of Patagonia and the origin and evolution of the sauropod-type sacrum. PLoS ONE 6(1): e14572. https://doi.org/10.1371/journal.pone.0014572

Peyre de Fabrègues C, Allain R (2016) New material and revision of *Melanorosaurus thabanensis*, a basal sauropodomorph from the Upper Triassic of Lesotho. PeerJ 4: e1639. https://doi.org/10.7717/peerj.1639

Pidancet J, Chopard S (1862) Note sur un saurien gigantesque aux Marnes irisées. Comptes Rendus de l'Académie des Sciences 54: 1259–1262.

Plieninger T (1846) Über ein neues Sauriergenus und die Einreihung der Saurier mit flachen, schneidenden Zähnen in eine Familie. Jahreshefte des Vereins für vaterländische Naturkunde in Württemberg 2: 148–154.

Plieninger T (1847) Verzeichnis der Reptilien Württembergs. Jahreshefte des Vereins für vaterländische Naturkunde in Württemberg 3: 194–208.

Prieto-Márquez A, Norell, MA (2011) Redescription of a nearly complete skull of *Plateosaurus* (Dinosauria: Sauropodomorpha) from the Late Triassic of Trossingen (Germany). American Museum Novitates 3727: 1–58. https://doi.org/http://dx.doi.org/10.1206/3727.2

Quenstedt FA (1882–85) Handbuch der Petrefactenkunde, Laupp, Tübingen, 1289 pp.

Quenstedt FA (1864) Geologische Ausflüge in Schwaben. H. Laupp'schen Buchhandlung, Tübingen. https://www.digitale-sammlungen.de/de/view/bsb10284415

Quenstedt FA (1867) Handbuch der Petrefactenkunde. H. Laupp'schen Buchhandlung, Tübingen. https://www.digitale-sammlungen.de/de/view/bsb10284411

Raath MA (1972) Fossil vertebrate studies in Rhodesia: a new dinosaur (Reptilia: Saurischia) from near the Tria-Jurassic boundary. Arnoldia 5(31): 1–37.

Rauhut OWM, Holwerda F, Furrer H (2020) A derived sauropodiform dinosaur and other sauropodomorph material from the Late Triassic of Canton Schaffhausen, Switzerland. Swiss Journal of Geosciences 113(1): 1–54. https://doi.org/10.1186/s00015-020-00360-8

Rauhut OWM, Fechner R, Remes K, Reis K (2011) How to get big in the Mesozoic: the evolution of the sauropodomorph body plan. In: Klein N, Remes K, Gee CT, Sander PM (Eds) Biology of the Sauropod Dinosaurs: Understanding the life of giants. Indiana University Press, Blumington and Indianapolis, 119–149.

Ray S, Mukherjee D, Bandyopadhyay S (2009) Growth patterns of fossil vertebrates as deduced from bone microstructure: case studies from India. Journal of Biosciences 34(5): 661–672. http://doi.org/10.1007/s12038-009-0055-x

Regalado Fernández OR (2020) Reassessment of the evolutionary history of the late Triassic and early Jurassic sauropodomorph dinosaurs through comparative cladistics and the supermatrix approach. PhD Thesis, UCL (University College London), London, United Kingdom. https://discovery.ucl.ac.uk/id/eprint/10093308

Reig OA (1963) La presencia de dinosaurios saurisquios en los "Estratos de Ischigualasto" (Mesotriasico Superior) de las provincias de San Juan y La Rioja (República Argentina). Ameghiniana 3(1): 3–20.

Reinacher S-J (2021) *Plateosaurus engelhardti* – zwei schwäbische Lindwürmer. In: Seidl E, Bierende E, Werneburg I (Eds) Aus der Tiefenzeit. Die Paläontologische Sammlung der Universität Tübingen. Museum der Universität Tübingen, 394–411.

Remes K (2007) Evolution of the pectoral girdle and forelimb in Sauropodomorpha (Dinosauria, Saurischia): Osteology, myology and function. PhD thesis. Fakultät für Geowissenschaften der Ludwig-Maximilians-Universität, München, Germany. https://doi.org/10.5282/edoc.8395

Remes K, Ortega F, Fierro I, Joger U, Kosma R, Ferrer JMM, Ide OA, Maga A (2009) A new basal sauropod dinosaur from the Middle Jurassic of Niger and the early evolution of Sauropoda. PLoS ONE 4(9): e6924. https://doi.org/10.1371/journal.pone.0006924

Rieß-Stumm S (2021) Dokumentation zur Dinosauriergrabung in Trossingen. Chelyops, Berichte aus der Paläontologischen Sammlung in Tübingen 1: 116–118.

Riley H, Stutchbury S (1836) A description of various fossil remains of three distinct saurian animals discovered in the autumn of 1834, in the Magnesian Conglomerate on Durdham Down, near Bristol. Proceedings of the Geological Society of London 2: 397–399

Rowe TB, Sues H-D, Reisz RR (2011) Dispersal and diversity in the earliest North American sauropodomorph dinosaurs, with a description of a new taxon. Proceedings of the Royal Society B 278(1708): 1044–1053. https://doi.org/10.1098/rspb.2010.1867

Rühle von Lilienstern H (1952) Die Saurier Thüringens. Fischer, Jena, 42 pp.

Rütimeyer L (1856) Fossile Reptilienknochen aus dem Keuper. Verhandlungen der Schweizerischen Naturforschenden Gesellschaft 41: 62–64.

Sander PM (1992) The Norian *Plateosaurus* bonebeds of Central-Europe and their Taphonomy. Palaeogeography, Palaeoclimatology, Palaeoecology 93: 255–299. https://doi.org/10.1016/0031-0182(92)90100-J

Sander PM, Klein N (2005) Developmental plasticity in the life history of a prosauropod dinosaur. Science 310: 1800-1802. http://dx.doi.org/10.1126/science.1120125

Sander PM, Christian A, Clauss M, Fechner R, Gee CT, Griebeler E-M, Gunga H-C, Hummel J, Mallison H, Perry SF, Preuschoft H, Rauhut OWM, Remes K, Tütken T, Wings O, Witzel U (2009) Biology of the sauropod dinosaurs: The evolution of gigantism. Biological Reviews 86(1): 117–155. http://dx.doi.org/10.1111/j.1469-185X.2010.00137.x

Sauvage HE (1907) Vértebrés. In: Thiery P, Sauvage HE, Cosmann M (Eds) Note sur l'infralias de Provenchères-sur-Meuse. Imprimerie Novelle, Chaumont 6–17.

Sereno PC (2007) Basal Sauropodomorpha: Historical and recent phylogenetic hypotheses, with comments on Ammosaurus major (Marsh, 1889). Special Papers in Palaeontology 77: 261–289.

Sereno PC, Forster CA, Rogers RR, Monetta AR (1993) Primitive dinosaur skeleton from Argentina and the early evolution of Dinosauria. Nature 361(6407): 64–66. http://dx.doi.org/10.1038/361064a0

Sereno PC, Martínez RN, Alcober OA (2012) Osteology of *Eoraptor lunensis* (Dinosauria, Sauropodomorpha). Journal of Vertebrate Paleontology 32 (Suppl.): 83–179. https://doi.org/10.1080/02724634.2013.820113

Schoch RR (2011) Tracing Seemann's dinosaur excavation in the Upper Triassic of Trossingen: his field notes and the present status of the material. Palaeodiversity 4: 245–282.

Schoch RR, Seegis D (2014) Taphonomy, deposition and pedogenesis in the Upper Triassic dinosaur beds of Trossingen. Palaeobiodiversity and Palaeoenvironments, 94(4): 571–593. https://doi.org/10.1007/s12549-014-0166-8

Sekiya T, Jin X, Zheng W, Shibata M, Azuma Y (2013) A new juvenile specimen of *Yunnanosaurus robustus* (Dinosauria: Sauropodomorpha) from Early to Middle Jurassic of Chuxiong Autonomous Prefecture, Yunnan Province, China. Historical Biology, August, 37–41. https://doi.org/10.1080/08912963.2013.821702

Sertich JJW, Loewen MA (2010) A new basal sauropodomorph dinosaur from the lower Jurassic Navajo sandstone of southern Utah. PLoS ONE 5(3): e9789. https://doi.org/10.1371/journal.pone.0009789

Smith ND, Pol D (2007) Anatomy of a basal sauropodomorph dinosaur from the Early Jurassic Hanson Formation of Antarctica. Acta Palaeontologica Polonica 52(4): 657–674. https://www.app.pan.pl/article/item/app52-657.html

Steel R (1970) Part 14. Saurischia. Handbuch der Paläoherpetologie. Gustav Fischer Verlag, Stuttgart, 87 pp.

Upchurch P, Barrett PM, Galton PM (2007) A phylogenetic analysis of basal sauropodomorph relationships: Implications for the origin of sauropod dinosaurs. In: Barrett PM, Batten DJ (Eds) Evolution and Palaeobiology of Early Sauropodomorph Dinosaurs. Special Papers in Palaeontology 77: 57–90.

Wang Y, You H, Wang T (2017) A new basal sauropodiform dinosaur from the Lower Jurassic of Yunnan Province, China. Scientific Reports 7: 41881. https://doi.org/10.1038/srep41881

Weishampel DB, Westphal F (1986) Die Plateosaurier von Trossingen im Geologischen Institut der Eberhard-Karls-Universität Tübingen. Attempto Verlag, Tübingen, 27 pp.

Weishampel DB, Chapman R (1990) 3. Morphometric study of *Plateosaurus* from Trossingen (Baden-Württemberg, Federal Republic of Germany). In: Carpenter K, Currie P (Eds) Dinosaur Systematics. Cambridge University Press, Cambridge, 43–52. http://dx.doi.org/10.1017/CBO9780511608377.006

Wellnhofer P (1993) Prosauropod dinosaurs from the Feuerletten (Middle Norian) of Ellingen near Weissenburg in Bavaria. Revue de Paleobiologie 7: 265–271.

Wild R (1978) Ein Sauropoden-Rest (Reptilia, Saurischia) aus dem Posidonienschiefer (Lias, Toarcium) von Holzmaden. Stuttgarter Beiträge zur Naturkunde 41(27): 1–15.

Wilson JA (1999) A nomenclature for vertebral laminae in Sauropods and other Saurischian Dinosaurs. Journal of Vertebrate Paleontology 19(4): 639–653. http://dx.doi.org/10.1080/02724634.1999.10011178

Wilson JA (2011) Anatomical terminology for the sacrum of sauropod dinosaurs. Contribution from the Museum of Paleontology, University of Michigan 32(5): 59–69. http://hdl.handle.net/2027.42/89589

Wilson JA, D'Emic MD, Ikejiri T, Moacdieh EM, Whitlock JA (2011) A nomenclature for vertebral fossae in sauropods and other saurischian dinosaurs. PLoS ONE 6(2): e17114. http://dx.doi.org/10.1371/journal.pone.0017114

Yates AM (2003a) The species taxonomy of the sauropodomorph dinosaurs from the Löwenstein Formation. Palaeontology 46(2): 317–337. https://doi.org/10.1111/j.0031-0239.2003.00301.x

Yates AM (2003b) A new species of the primitive dinosaur *Theocodontosaurus* (Saurischia: Sauropodomorpha) and d its implications for the systematics of early dinosaurs. Journal of Systematic Palaeontology 2003(1): 1–42. https://doi.org/10.1017/S1477201903001007

Yates AM (2004) *Anchisaurus polyzelus* (Hitchcock): The Smallest known sauropod dinosaur and the evolution of gigantism among sauropodomorph dinosaur. Postilla 230: 1–58. https://biostor.org/reference/118461

Yates AM (2007a) Solving a dinosaurian puzzle: the identity of *Aliwalia rex* Galton. Historical Biology 19(1): 93-123. https://doi.org/10.1080/08912960600866953

Yates AM (2007b) The first complete skull of the Triassic dinosaur *Melanorosaurus* Haughton (Sauropodomorpha: Anchisauria). In: Barrett PM, Batten, DJ (Eds) Evolution and Palaeobiology of Early Sauropodomorph Dinosaurs. Special Papers in Palaeontology 77: 57–90.

Yates AM, Kitching W (2003) The earliest known sauropod dinosaur and the first steps towards sauropod locomotion. Proceedings of the Royal Society of London B 270(1525): 1753–1758. https://doi.org/10.1098/rspb.2003.2417

Yates AM, Bonnan MF, Neveling J (2011) A new basal sauropodomorph dinosaur from the Early Jurassic of South Africa. Journal of Vertebrate Paleontology 31(3): 610–625. http://dx.doi.org/10.1080/02724634.2011.560626

Yates AM, Wedel M, Bonnan M (2012) The early evolution of postcranial skeletal pneumaticity in sauropodomorph dinosaurs. Acta Palaeontologia Polonica 57(1): 85–100. https://doi.org/10.4202/app.2010.0075

Yates AM, Bonnan MF, Neveling J, Chinsamy A, Blackbeard M G (2010) A new transitional sauropodomorph dinosaur from the Early Jurassic of South Africa and the evolution of sauropod feeding and quadrupedalism. Proceedings of the Royal Society B 277(1682): 787–794. http://dx.doi.org/10.1098/rspb.2009.1440

Young C-C (1940) Preliminary notes on the Lufeng vertebrate fossils. Bulletin of the Geological Society of China 20(3–4): 235–239. https://doi.org/10.1111/j.1755-6724.1940.mp203-4003.x

Young C-C (1941) A complete osteology of *Lufengosaurus huenei* Young (gen. et sp. nov) from Lufeng, Yunnan, China. Palaeontologia Sinica, New Series C 7: 1–59164.

Zhang Y, Yang Z (1995) A new complete osteology of Prosauropoda in Lufeng Basin, Yunnan, China. Yunnan Publishing House of Science and Technology, Kunming, 100 pp.

Zhang Q-N, Wang T, Yang Z-W, You H-L (2019) Redescription of the cranium of *Jingshanosaurus xinwaensis* (Dinosauria: Sauropodomorpha) from the Lower Jurassic Lufeng Formation of Yunnan Province, China. The Anatomical Record 303(4): 759–771. https://doi.org/10.1002/ar.24113

Appendix 1

Summary of changes

Ch. 318 (Rauhut et al. 2020) has been removed, so all characters from Ch. 318 in this matrix are shifted one to the left relative to Rauhut et al. (2020). Characters are shaded in grey.

Ch. 380 (Rauhut et al. 2020) has been removed, so all characters from Ch. 380 in this matrix are shifted one to the left relative to Rauhut et al. (2020). Characters are shaded in grey.

Rauhut et al. (2020) also had some typos in the columns, and some derived characters were replaced by a generic "State" label. The characters corrected are Ch. 8, Ch. 108, Ch. 166, Ch. 212, Ch. 225, and Ch. 360 (Ch. 359 in this matrix).

Appendix 2

Character scorings of the OTUs added to the character-by-taxon matrix of Rauhut et al. (2020) in Analysis 2.

Table A1. *Tuebingosaurus maierfritzorum*

1									10										20										30
?	?	?	?	?	?	?	?	?	?	?	?	?	?	?	?	?	?	?	?	?	?	?	?	?	?	?	?	?	?
?	?	?	?	?	?	?	?	?	?	?	?	?	?	?	?	?	?	?	?	?	?	?	?	?	?	?	?	?	?
?	?	?	?	?	?	?	?	?	?	?	?	?	?	?	?	?	?	?	?	?	?	?	?	?	?	?	?	?	?
?	?	?	?	?	?	?	?	?	?	?	?	?	?	?	?	?	?	?	?	?	?	?	?	?	?	?	?	?	?
?	?	?	?	?	?	?	?	?	?	?	?	?	?	?	?	?	?	?	?	?	?	?	?	?	?	?	?	?	?
?	?	?	?	?	?	?	?	?	?	?	?	?	?	?	?	?	?	?	?	?	?	?	?	?	?	1	0	1	1
0	1	1	1	0	0	1	0	1	1	?	0	1	?	?	?	?	0	0	?	?	?	?	?	?	?	?	?	?	?
?	?	?	?	?	?	?	?	?	?	?	?	?	?	?	?	?	?	?	?	?	?	?	?	?	?	?	?	?	?
?	?	?	?	?	?	?	?	?	?	?	?	?	?	?	?	0	0	1	0	0	1	2	1	0	1	1	1	0	1
0	2	0	0	1	0	0	0	0	0	0	1	0	0	1	1	0	0	1	0	1	1	0	?	0	0	1	0	1	1
1	1	0	0	0	0	0	0	1	1	1	?	0	?	0	1	0	0	0	0	2	1	1	0	1	0	1	?	1	1
1	1	0	0	?	1	1	0	1	1	1	1	0	0	1	1	?	?	?	?	?	?	?	?	?	?	?	?	?	?
?	0	0	?	1	?	0	?	?	?	0	0	0	?	0	?	?	0	0	1										

Table A2. *Plateosaurus trossingensis* – only specimen SMNS 13200

1									10										20										30
1	0	0	1	1	0	0	1	1	0	1	0	2	0	1	1	0	1	1	1	1	1	2	1	1	1	1	0	0	1
0	1	1	0	0	0	0	1	0	0	1	0	1	0	1	0	1	1	0	0	1	1	0	0	1	1	0	0	0	1
1	0	0	1	0	0	1	1	0	1	1	0	1	1	0	1	1	0	1	?	1	1	?	1	1	0	0	0	1	0
1	1	1	1	0	0	1	0	1	1	0	1	0	1	1	1	1	1	1	0	0	1	0	1	0	1	0	0	0	0
1	1	0	0	1	1	1	1	0	0	0	1	1	0	1	0	0	1	0	1	1	0	1	1	0	1	0	0	0	2
0	0	1	1	1	0	0	1	1	0	0	0	0	0	0	0	0	0	0	0	0	0	0	1	0	1	1	0	1	0
0	0	1	0	0	0	0	0	0	0	0	0	0	1	0	0	0	0	0	0	0	0	0	1	0	0	0	1	1	1
1	1	2	0	0	0	0	1	1	1	0	0	0	0	0	1	1	0	1	1	1	1	0	1	0	1	1	0	1	0
0	1	0	0	2	0	1	0	0	0	0	0	0	1	0	0	0	0	1	0	0	0	3	1	1	0	1	0	0	1
0	2	0	0	1	0	1	0	0	0	0	1	1	1	1	1	0	0	1	0	1	1	1	1	0	0	0	0	1	1
1	1	0	0	0	0	0	0	1	1	0	0	0	1	0	1	0	0	0	1	1	1	1	1	1	1	0	0	1	0
0	1	1	0	1	0	1	0	0	1	1	0	0	1	0	1	1	1	0	0	1	0	1	1	1	0	0	0	0	0
0	1	0	1	1	0	0	1	0	0	0	0	0	1	0	0	0	0	0	?										

Table A3. *'Sellosaurus'* complex

1									10										20										30
?	?	?	?	?	?	?	?	?	?	?	?	?	?	?	?	?	?	?	?	?	?	?	?	?	?	?	?	?	?
?	?	?	?	?	?	?	?	?	?	?	?	?	?	?	?	?	?	?	?	?	?	?	?	?	?	?	?	?	?
?	?	?	?	?	?	?	?	?	?	?	?	?	?	?	?	?	?	?	?	?	?	?	?	?	?	?	?	?	?
?	?	?	?	?	?	?	?	?	?	?	?	?	?	?	?	?	?	?	?	?	?	?	?	?	?	?	?	?	?
?	?	0	0	1	1	1	1	0	0	0	1	1	0	1	0	0	1	0	1	1	0	1	1	0	1	0	0	0	2
0	0	1	1	1	0	0	1	1	0	0	0	0	0	0	0	0	0	0	0	0	0	0	1	0	1	1	0	1	0
0	0	1	0	0	0	0	0	0	0	0	0	0	1	0	0	0	0	0	0	0	0	0	1	0	0	0	1	1	1
1	1	2	0	0	0	0	1	1	1	0	0	0	0	0	1	1	0	1	1	1	1	0	1	0	1	1	0	1	0
0	1	0	0	2	0	1	0	0	0	0	0	0	1	0	0	0	0	1	0	0	0	3	1	1	0	1	0	0	1
0	2	0	0	1	0	1	0	0	0	0	1	1	1	1	1	0	0	1	0	1	1	1	1	0	0	0	0	1	1
1	1	0	0	0	0	0	0	1	1	0	0	0	1	0	1	0	0	0	1	1	1	1	1	1	1	0	0	1	0
0	1	1	0	1	0	1	0	0	1	1	0	0	1	0	1	1	1	0	0	1	0	1	1	1	0	0	0	0	0
0	1	0	1	1	0	0	1	0	0	0	0	0	1	0	0	0	0	0	?										

Appendix 3

Ward clustering analyses

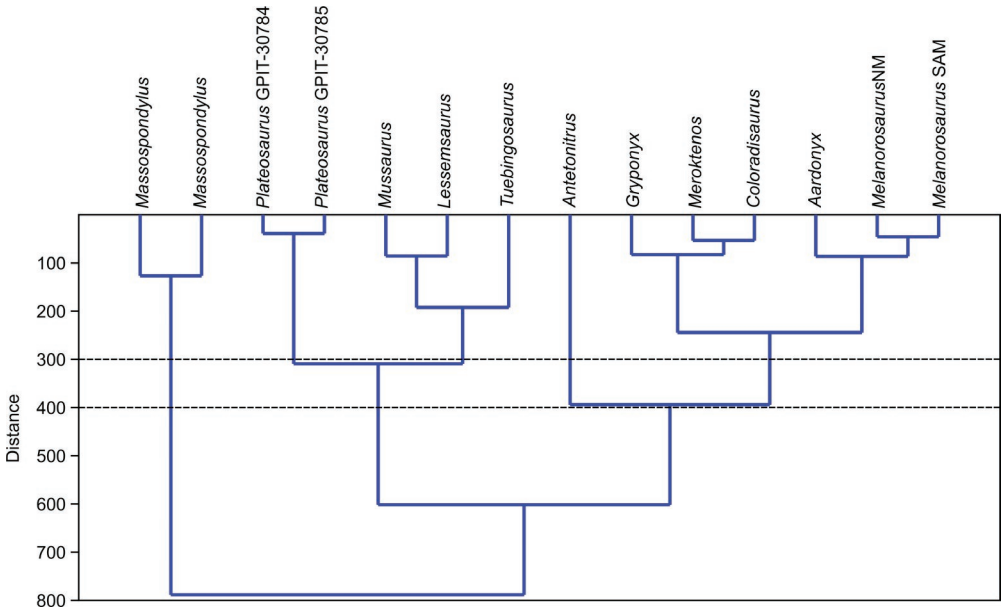

Figure A1. Ward clustering of the sauropodomorph femora in Table 10, showing the clusters of *Massospondylus*, *Plateosaurus* and *Melanorosaurus*. *Tuebingosaurus* is placed in a cluster with *Mussaurus* and *Lessemsaurus*. Analysis was performed in PAST 2.03 (Hammer et al. 2001). Cophenetic correlation coefficient: 0.5822.

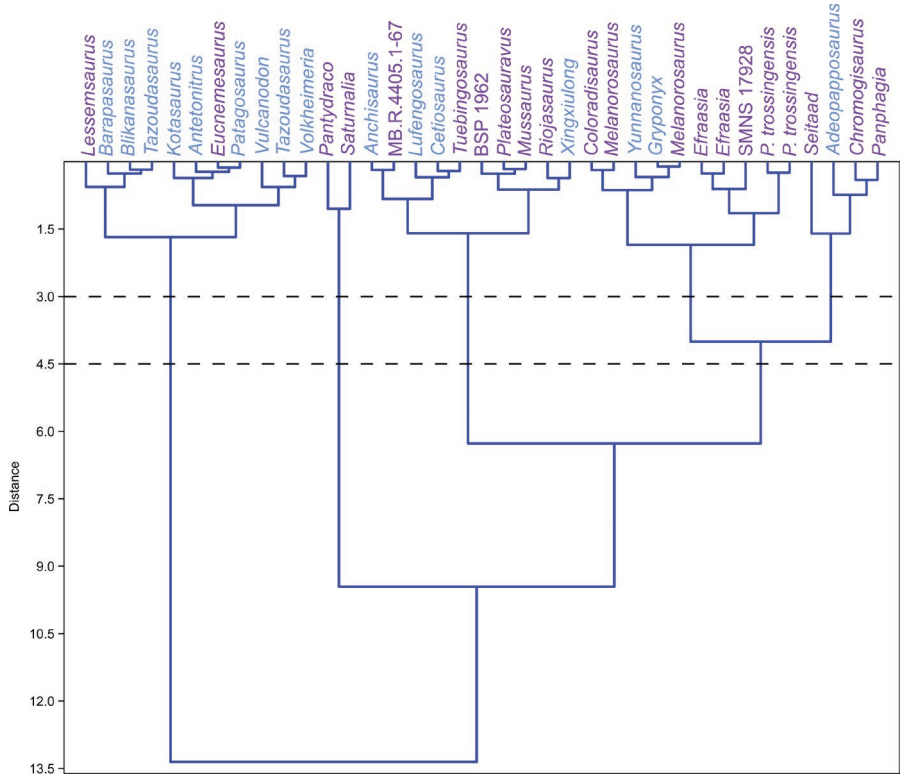

Figure A2. Ward clustering of two variables: the ratio between the total length and anteroposterior depth of the proximal end of tibia (L/Pw), and the ratio total length and anteroposterior depth at mid-length of tibia (L/Mw). *Efraasia* and *Plateosaurus* (neotype, SMNS 13200, and referred specimen GPIT-PV-30784) are in the same clusters. The other specimens referred to as *Plateosaurus*, i.e., MB.R.4405.1-67 and BSP 1962, and *Tuebingosaurus* are clustered with other massopodans such as *Mussaurus*, *Riojasaurus*, and *Anchisaurus*. The two larger clusters (at distance = 12) almost clearly separates the morphology of the tibiae into Late Triassic (purple) and Early Jurassic (light blue) specimens, which is consistent with separating sauropodan morphotypes from early-sauropodomorph ones. Analysis was performed in PAST 2.03 (Hammer et al. 2001). Cophenetic correlation coefficient: 0.5611.

Supplementary material 1

Iteration 1: Character-by-taxon matrix

Authors: Regalado Fernández OR, Werneburg I (2022)
Data type: .nex
Explanation note: In a first round of analysis (Figure 4), five iterations were run using TNT 1.1 (Goloboff et al. 2008), employing the new searching techniques, with the sectorial, ratchet, drift and tree fusing algorithms run through 1.000 random addition sequences. Iteration 1.1 included all taxa; in iteration 1.2 the two *Plateosaurus* OTUs were removed and were then alternatively removed in iterations 1.3 and 1.4 (see Figure 4). Finally, specimen GPTI-PV-30787 was constrained to form a clade with Plateosaurus and a Templeton Test was performed to contrast the trees obtained in Iteration 1.5 against Iteration 1.1.

Link: https://doi.org/10.3897/vz.72.e86348.suppl1

Supplementary material 2

Iteration 2: Character-by-taxon matrix

Authors: Regalado Fernández OR, Werneburg I (2022)
Data type: .nex
Explanation note: In a second round of analysis (Figure 4), five iterations were run using TNT 1.1 (Goloboff et al. 2008), employing the new searching techniques, with the sectorial, ratchet, drift and tree fusing algorithms run through 1.000 random addition sequences. Iteration 2.1 included all taxa; in iteration 2.2 the two *Plateosaurus* OTUs were removed and were then alternatively removed in iterations 2.3 and 2.4 (see Figure 4). Finally, specimen GPTI-PV-30787 was constrained to form a clade with *Plateosaurus* and a Templeton Test was performed to contrast the trees obtained in Iteration 2.5 against Iteration 2.1.

Link: https://doi.org/10.3897/vz.72.e86348.suppl2